

Supporting Information

A Strategy to Improve the Performance of Cerium(III) Photocatalysts

Yusen Qiao, Thibault Cheisson, Brian C. Manor, Patrick J. Carroll, and Eric J. Schelter*

P. Roy and Diana T. Vagelos Laboratories, Department of Chemistry, University of Pennsylvania, 231 S. 34th Street, Philadelphia, PA 19104, United States

*Corresponding authors. E-mail: schelter@sas.upenn.edu

Table of Contents

1. Materials and Methods	S2–S3
2. Synthetic Details and Characterizations	S4
3. NMR Spectra	S5–S6
4. X-ray Diffraction Studies	S7–S11
5. Steady State Absorption and Emission Spectra	S12–S17
6. Lifetime Data	S18–S19
7. Summary of Spectroscopy Data	S20
8. Electrochemistry	S21–S25
9. Computational Details	S26–S55
10. Determination of Structural Metrics	S56–S59
11. Stern-Volmer Experiments	S60–S61
12. Procedure for Ce-catalyzed phenylation reaction	S62–S65
13. References	S66–S67

1. Materials and Methods

General Methods. All reactions and manipulations were performed under an inert atmosphere (N_2) using standard Schlenk techniques or in a Vacuum Atmospheres, Inc. Nexus II drybox equipped with a molecular sieves 13X / Q5 Cu–0226S catalyst purifier system. Glassware was oven-dried for 3 hours at 150 °C prior to use. 1H NMR spectra were obtained on a Bruker DMX–300 Fourier transform NMR spectrometer at 300 MHz. Chemical shifts were recorded in units of parts per million referenced to residual solvent peaks (1H). Elemental analyses were performed using a Costech ECS 4010 analyzer at the Earth & Environmental Science Department of the University of Pennsylvania.

Materials. Toluene, THF, CH_2Cl_2 , hexanes, and *n*-pentane were purchased from Fisher Scientific. The solvents were sparged for 20 min with dry N_2 and dried using a commercial two column solvent purification system comprising columns packed with Q5 reactant and neutral alumina respectively (for hexanes and *n*-pentane), or two columns of neutral alumina (for toluene, THF and CH_2Cl_2). Benzene- d_6 was purchased from Cambridge Isotopes Laboratories, Inc., and dried over potassium mirror for 24 hours before use. Cel_3 was purchased from Alfa Aesar and used as received. $KN(SiMe_3)_2$ was purchased from Sigma-Aldrich and used as received. $NaN(SiMe_3)_2$ were purchased from Acros Organics and used as received. Ferrocene (Fc) was purchased from Acros Organics and purified by sublimation before use. $KN(SiMe_3)_2^{t}Bu$ and $KN(SiMe_3)_2^{t}Pr$,¹ $\{[(Me_3Si)_2NC(N^{t}Pr)_2]_2Ce\}_2(\mu^2-I)_2$,² $[(Me_3Si)_2NC(N^{t}Pr)_2]_2Ce[N(SiMe_3)_2]$ (**1**),² and $[^nPr_4N][BAr^F_4]$ ³ were prepared according to literature procedures. $KNPh_2$ and $KNPh^{t}Pr$ were prepared by deprotonation of $HNPh_2$ or $HNPh^{t}Pr$, respectively, with $KN(SiMe_3)_2$ in diethyl ether and were used without further purification.

Absorption and Emission Spectroscopy. 10 mm path length quartz cells fused with a J-Young valve (Figure S1) were used for UV-vis and luminescence studies of air and moisture sensitive compounds.



Figure S1. 10 mm pathlength quartz cell fused with a J-Young valve used for luminescence data collection of air sensitive compounds.

Electronic absorption spectra (UV-Vis) were collected on a Perkin Elmer 950 UV-Vis/NIR spectrophotometer. Emission and excitation spectra were collected on Fluorolog®-3 spectrofluorometer (HORIBA Jobin Yvon, Inc.) using an R928 PMT detector. Deconvolution of the spectra was accomplished with Gaussian functions using fityk program.⁴ Lifetime measurements were performed on a PTI PicoMaster TCSPC lifetime fluorometer with a 380 nm wavelength source. Quantum yields of samples (Φ_x) were measured using a comparative method^{5,6} and calculated against 9,10-diphenylanthracene ($\Phi_{ST} = 0.97$ in cyclohexane)⁷ with the following equation:

$$\Phi_x = \Phi_{ST} \left(\frac{\text{Grad}_x}{\text{Grad}_{ST}} \right) \left(\frac{\eta_x^2}{\eta_{ST}^2} \right)$$

where subscripts ST and x denote the standard (9,10-diphenylanthracene) and a sample, respectively. Grad is the gradient obtained from the plot of integrated emission intensity versus absorbance. η is the diffraction index of the solvent.

2. Synthetic Details and Characterizations

General Synthesis of $\{[(\text{Me}_3\text{Si})_2\text{NC}(\text{N}^{\text{i}}\text{Pr})_2]_2\text{Ce}(\text{NR}_1\text{R}_2)\}$ (2–5). To a vial containing $\{[(\text{Me}_3\text{Si})_2\text{NC}(\text{N}^{\text{i}}\text{Pr})_2]_2\text{Ce}\}_2(\mu^2-\text{I})_2$ (0.084 g, 0.050 mmol, 0.50 equiv) suspended in 4 mL toluene, an excess amount of KNR_1R_2 (0.150 mmol, 1.50 equiv) was added. After stirring for 12 h, all volatiles were removed under reduced pressure. The resulting mixture was extracted into 15 mL *n*-pentane and filtered through Celite packed on a coarse porosity fritted filter. The filtrate was concentrated to 1 mL and stored at –25 °C for 12 h to yield yellow crystalline product. The product was collected by filtration on a medium porosity fritted filter and dried under reduced pressure for 1 h. Single crystals suitable for X-ray analysis were obtained by storing *n*-pentane solutions of **2–5** at –25 °C.

For **2**, $\text{R}_1 = \text{TMS}$, $\text{R}_2 = \text{tBu}$, Yield: 0.048 g, 0.056 mmol, 56%. ^1H NMR (C_6D_6 , 300 MHz, 300 K): δ 14.47 (br, 4H, $-\text{CH}^{\text{iPr}}$), 4.64 (br, 36H, $-\text{CH}_3^{\text{SiMe}^3}$), -4.71 (br, 9H, $-\text{CH}_3^{\text{tBu}}$), -5.51 (br, 24H, $-\text{CH}_3^{\text{iPr}}$), -11.79 (br, 9H, $-\text{CH}_3^{\text{SiMe}^3}$). Elemental analysis found (calculated) for $\text{C}_{33}\text{H}_{82}\text{CeN}_7\text{Si}_5$: C, 46.45 (46.22), H, 9.89 (9.64), N, 11.41 (11.43).

For **3**, $\text{R}_1 = \text{TMS}$, $\text{R}_2 = \text{iPr}$, Yield: 0.036 g, 0.043 mmol, 43%. ^1H NMR (C_6D_6 , 300 MHz, 300 K): δ 14.66 (br, 4H, $-\text{CH}^{\text{iPr}}$), 4.92 (br, 36H, $-\text{CH}_3^{\text{SiMe}^3}$), -1.14 (br, 9H, $-\text{CH}_3^{\text{SiMe}^3}$), -6.73 – -6.83 (br, 30H, $-\text{CH}_3^{\text{iPr}}$), -9.95 (br, 1H, $-\text{CH}^{\text{iPr}}$). Elemental analysis found (calculated) for $\text{C}_{32}\text{H}_{80}\text{CeN}_7\text{Si}_5$: C, 45.70 (45.56), H, 9.79 (9.56), N, 11.58 (11.62).

For **4**, $\text{R}_1 = \text{Ph}$, $\text{R}_2 = \text{iPr}$, Yield: 0.041 g, 0.048 mmol, 48%. ^1H NMR (C_6D_6 , 300 MHz, 300 K): δ 17.32 (br, 4H, $-\text{CH}^{\text{iPr}}$), 12.27 (br, 1H, $-\text{CH}^{\text{iPr}}$), 5.46 (br, 36H, $-\text{CH}_3^{\text{SiMe}^3}$), 3.17 (s, 1H, $-\text{CH}^{\text{Ph}}$), 1.37 (s, 2H, $-\text{CH}^{\text{Ph}}$), -0.11 (s, 2H, $-\text{CH}^{\text{Ph}}$), -6.48 (br, 24H, $-\text{CH}_3^{\text{iPr}}$), -8.28 (br, 6H, $-\text{CH}_3^{\text{iPr}}$). Elemental analysis found (calculated) for $\text{C}_{35}\text{H}_{76}\text{CeN}_7\text{Si}_4$: C, 49.83 (49.60), H, 8.82 (9.04), N, 11.44 (11.57).

For **5**, $\text{R}_1 = \text{R}_2 = \text{Ph}$, Yield: 0.050 g, 0.057 mmol, 57%. ^1H NMR (C_6D_6 , 300 MHz, 300 K): δ 18.52 (br, 4H, $-\text{CH}^{\text{iPr}}$), 5.74 (br, 36H, $-\text{CH}_3^{\text{SiMe}^3}$), 2.98 (s, 2H, $-\text{CH}^{\text{Ph}}$), 2.10 (s, 4H, $-\text{CH}^{\text{Ph}}$), -3.60 (br, 4H, $-\text{CH}^{\text{Ph}}$), -6.79 (br, 24H, $-\text{CH}_3^{\text{iPr}}$). Elemental analysis found (calculated) for $\text{C}_{38}\text{H}_{74}\text{CeN}_7\text{Si}_4$: C, 51.60 (51.78), H, 8.59 (8.46), N, 11.44 (11.12).

3. NMR Spectra

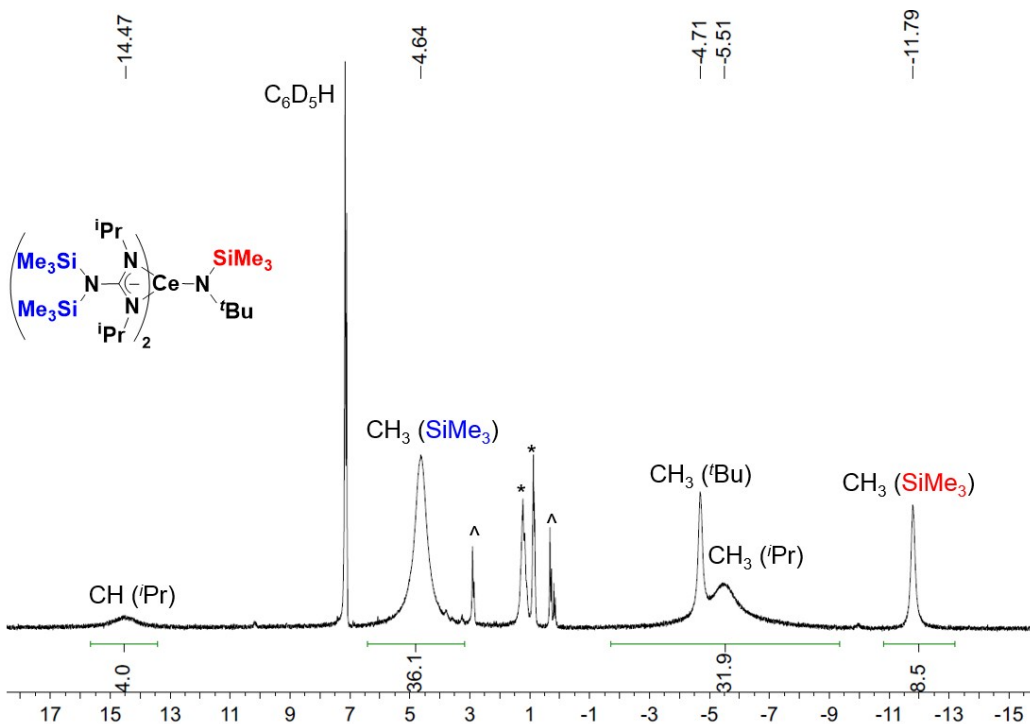


Figure S2. ¹H NMR of **2** in C₆D₆. Signals of *n*-pentane were noted by *. Protonated ligand impurity resonance is marked as ^.

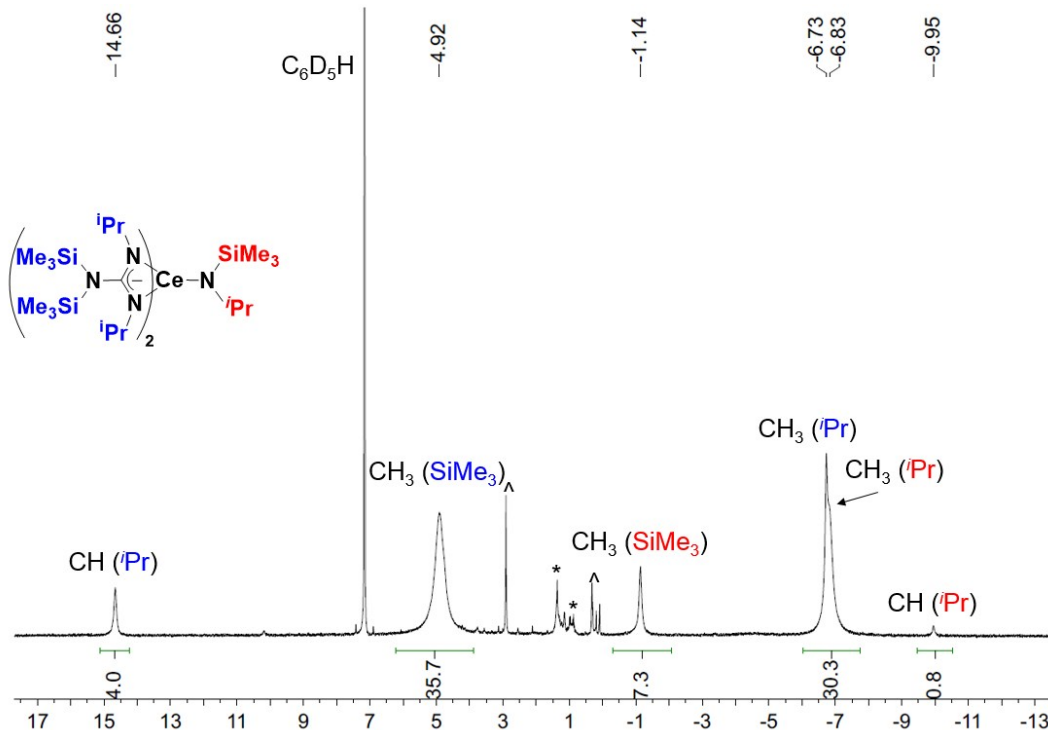


Figure S3. ¹H NMR of **3** in C₆D₆. Signals of *n*-pentane were noted by *. Protonated ligand impurity resonance is marked as ^.

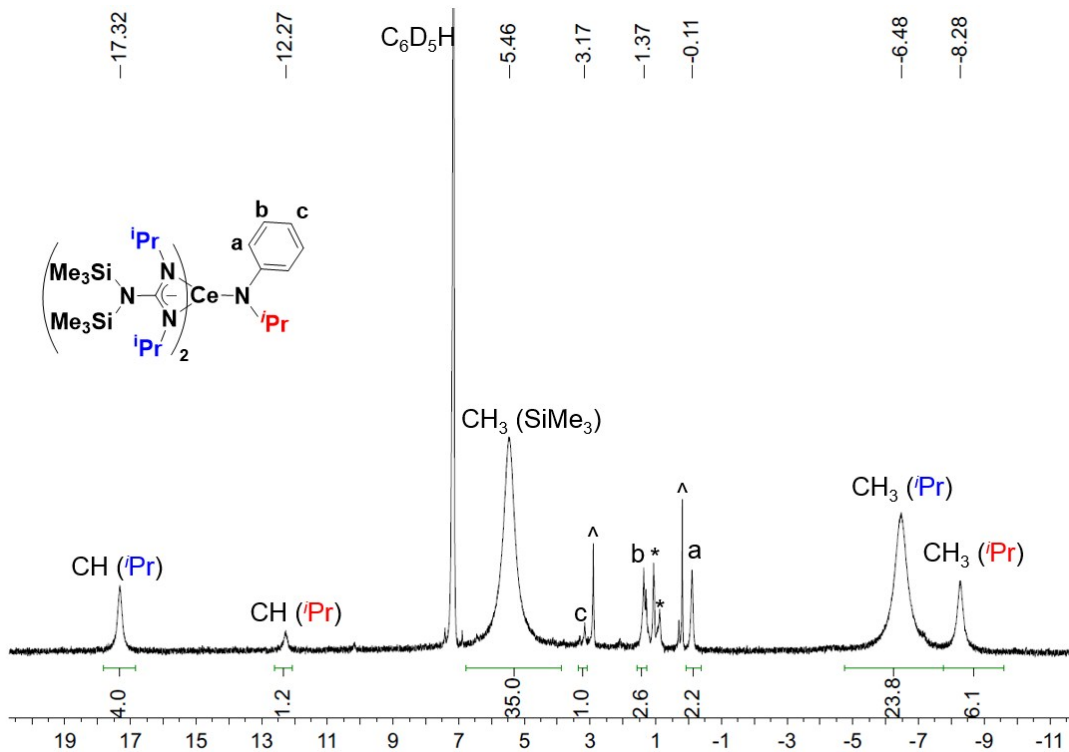


Figure S4. ^1H NMR of **4** in C_6D_6 . Signals of n -pentane were noted by *. Protonated ligand impurity resonance is marked as \wedge .

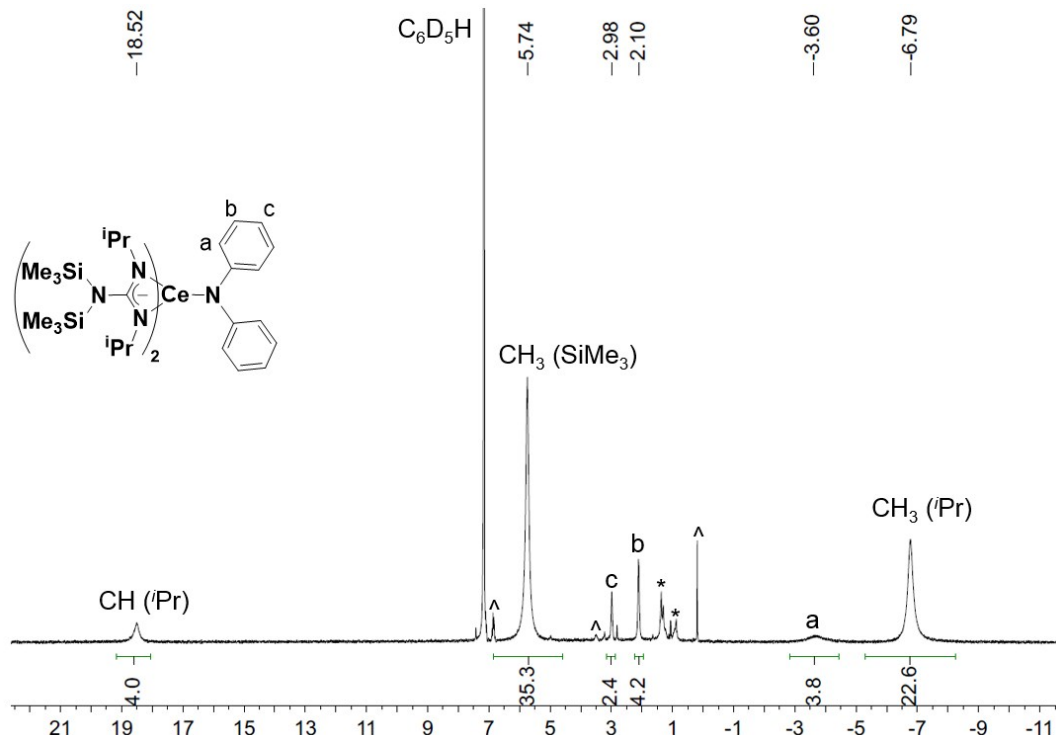


Figure S5. ^1H NMR of **5** in C_6D_6 . Signals of n -pentane were noted by *. Protonated ligand impurity resonance is marked as \wedge .

4. X-ray Diffraction Studies

X-ray intensity data were collected on a Bruker APEXII CCD area detector employing graphite-monochromated Mo-K α radiation ($\lambda=0.71073\text{ \AA}$) at a temperature of 100(1) K or 143(1) K. Preliminary indexing was performed from a series of thirty-six 0.5° rotation frames with exposures of 10 seconds. Following full data collection, rotation frames were integrated using SAINT,⁸ producing a listing of unaveraged F^2 and $\sigma(F^2)$ values which were then passed to the SHELXTL⁹ program package for further processing and structure solution. The intensity data were corrected for Lorentz and polarization effects and for absorption using SADABS¹⁰ or TWINABS¹¹. The structure was solved by direct methods (SHELXS-97¹²). Refinement was by full-matrix least squares based on F^2 using SHELXL-2014.¹³ All reflections were used during refinement. Non-hydrogen atoms were refined anisotropically and hydrogen atoms were refined using a riding model.

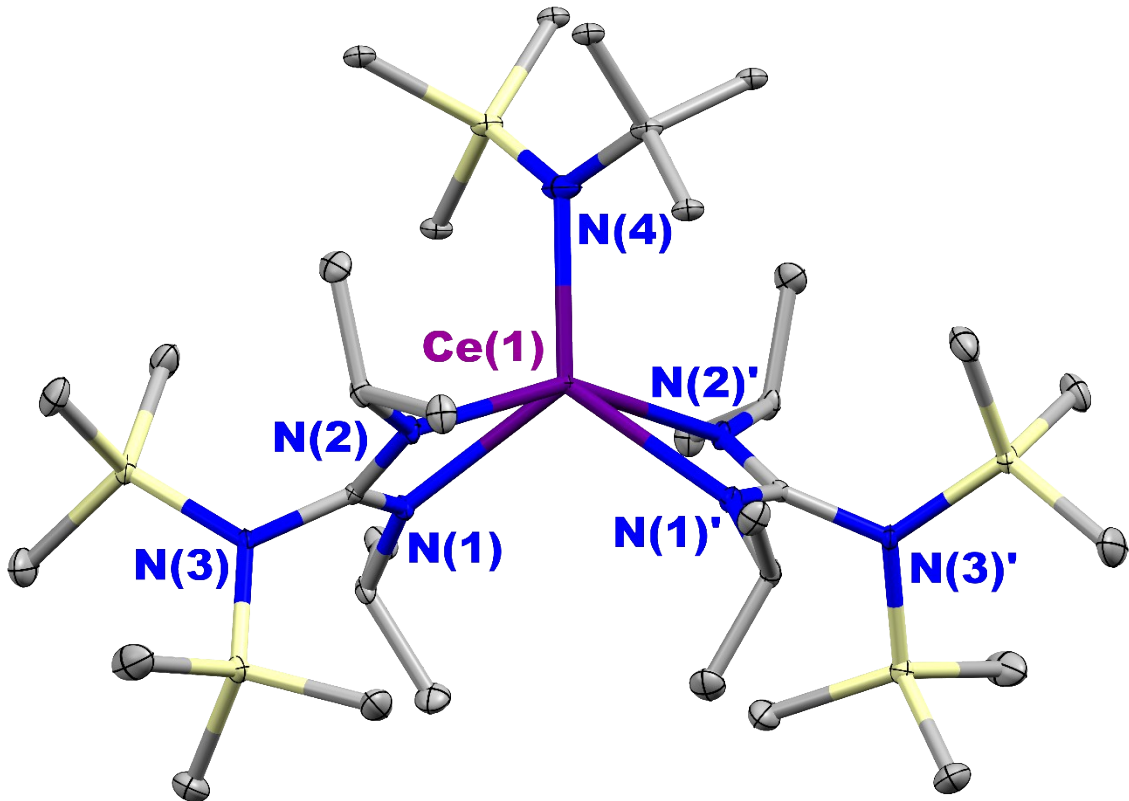


Figure S6. Thermal ellipsoid plot of **2** at 30% probability level. Selected bond length (Å) and angles (deg): Ce(1)–N(1) 2.4646(15), Ce(1)–N(2) 2.5465(14), Ce(1)–N(4) 2.337(2); N(1)–Ce(1)–N(2) 53.23(5).

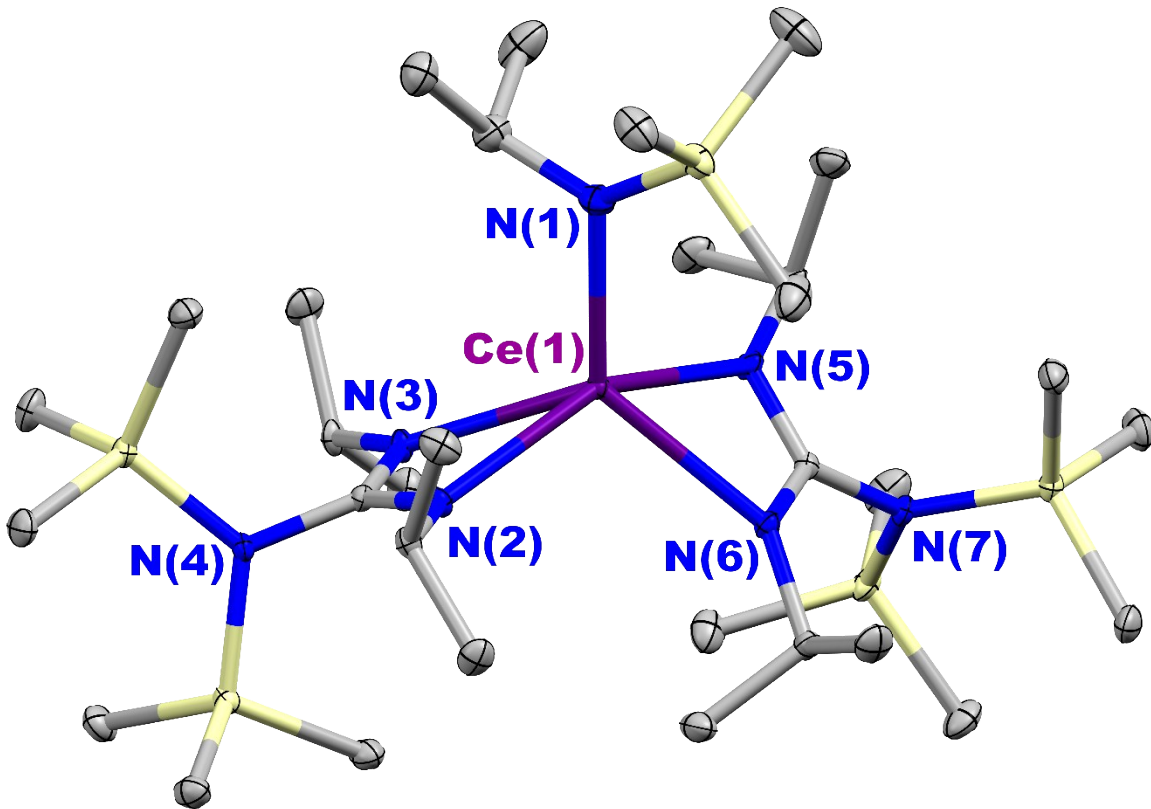


Figure S7. Thermal ellipsoid plot of **3** at 30% probability level. Selected bond length (\AA) and angles (deg): Ce(1)–N(1) 2.296(2), Ce(1)–N(2) 2.526(2), Ce(1)–N(3) 2.450(2), Ce(1)–N(5) 2.515(2), Ce(1)–N(6) 2.499(2); N(2)–Ce(1)–N(3) 53.70(6), N(5)–Ce(1)–N(6) 53.43(6).

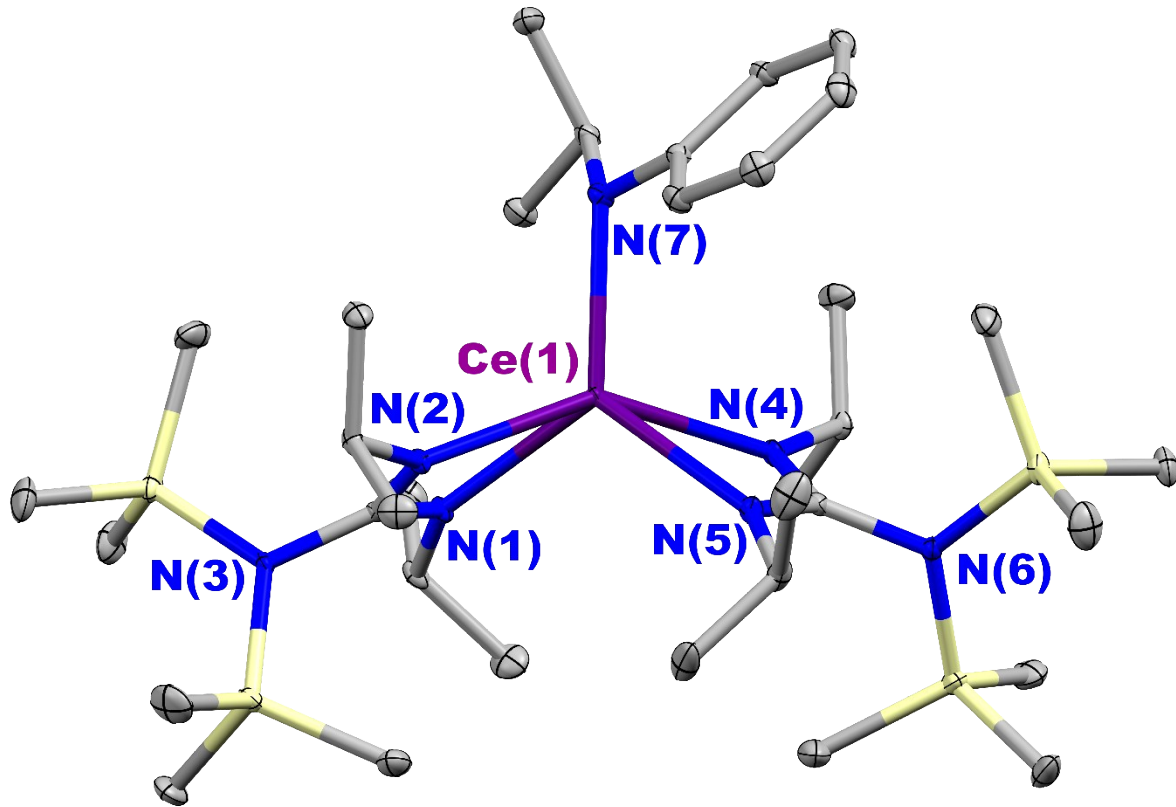


Figure S8. Thermal ellipsoid plot of **4** at 30% probability level. Selected bond length (\AA) and angles (deg): Ce(1)–N(1) 2.4483(14), Ce(1)–N(2) 2.5190(13), Ce(1)–N(4) 2.5090(14), Ce(1)–N(5) 2.4483(14), Ce(1)–N(7) 2.3677(14); N(1)–Ce(1)–N(2) 53.86(4), N(4)–Ce(1)–N(5) 54.04(4).

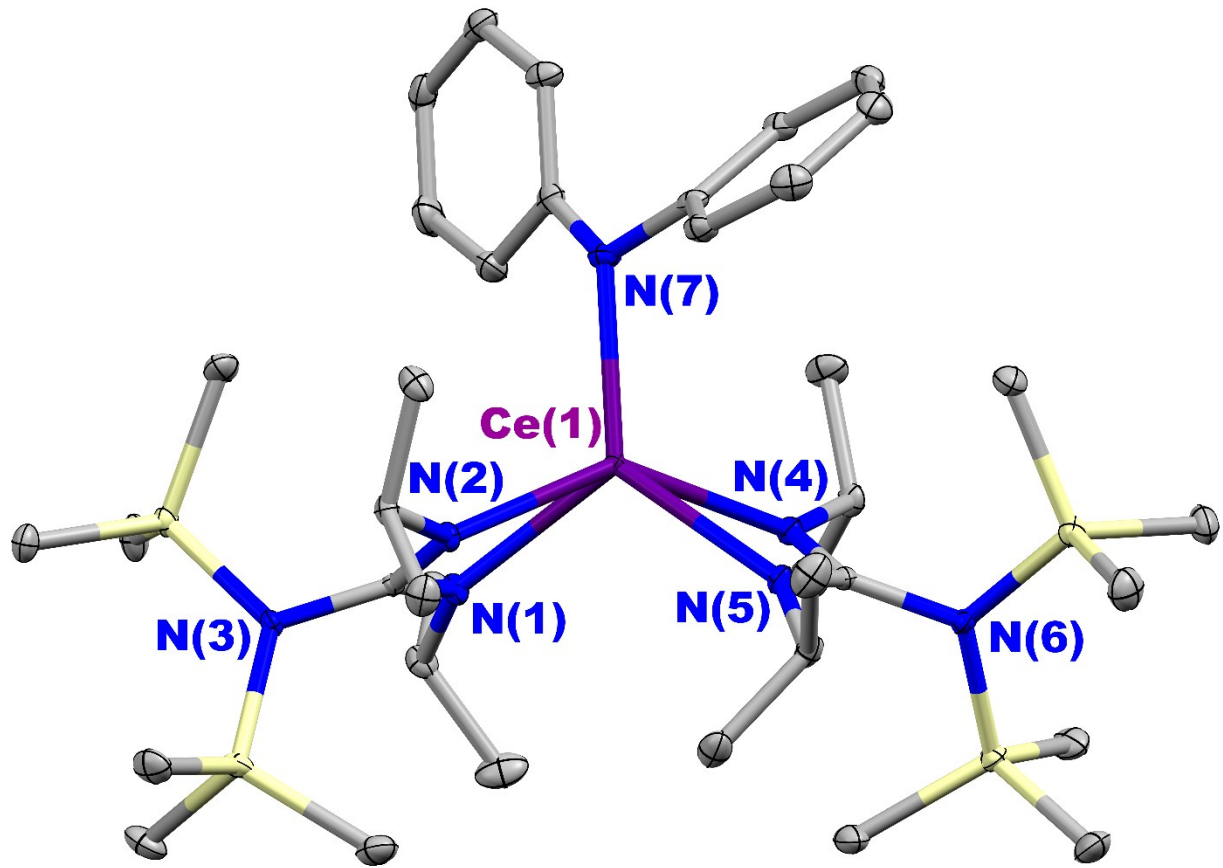


Figure S9. Thermal ellipsoid plot of **5** at 30% probability level. Selected bond length (\AA) and angles (deg): Ce(1)–N(1) 2.4091(15), Ce(1)–N(2) 2.5149(14), Ce(1)–N(4) 2.4889(15), Ce(1)–N(5) 2.4318(15), Ce(1)–N(7) 2.3975(15); N(1)–Ce(1)–N(2) 54.44(5), N(4)–Ce(1)–N(5) 54.22(5).

5. Steady State Absorption and Emission Spectra

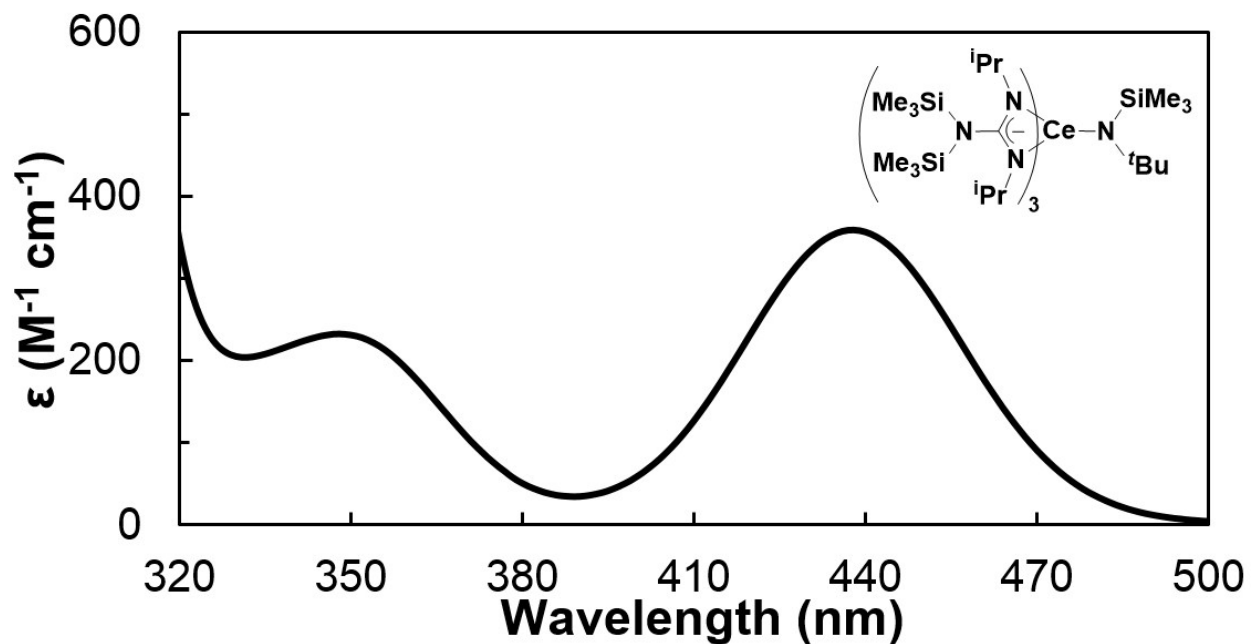


Figure S10. UV-vis spectrum of **2** recorded in toluene.

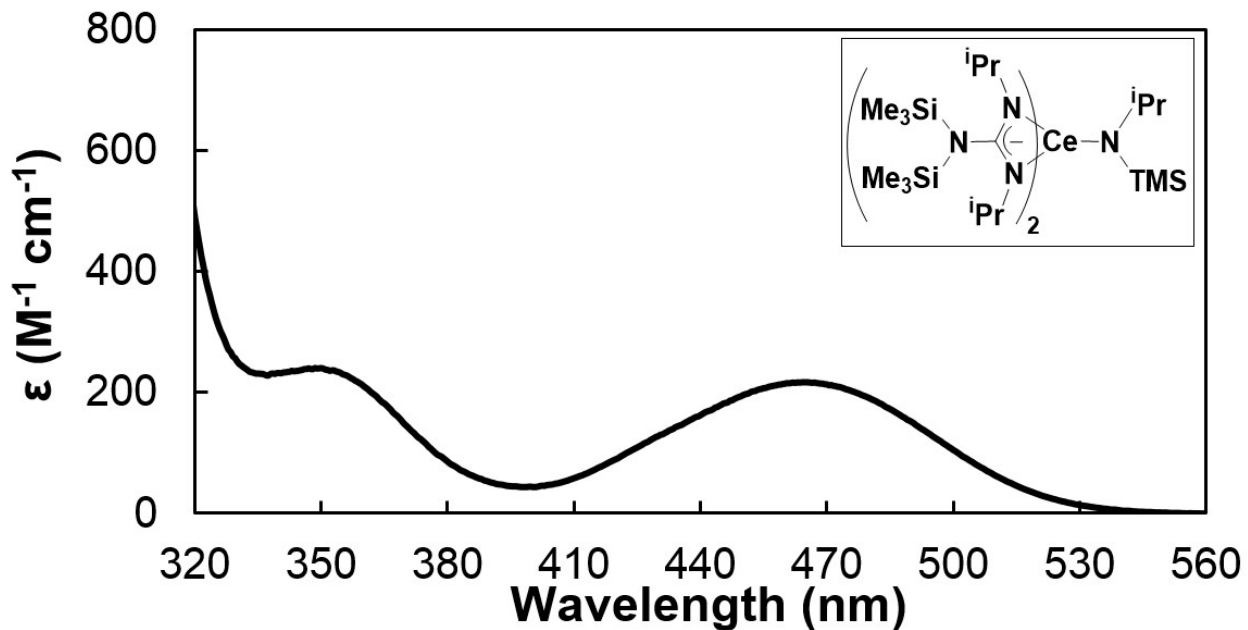


Figure S11. UV-vis spectrum of **3** recorded in toluene.

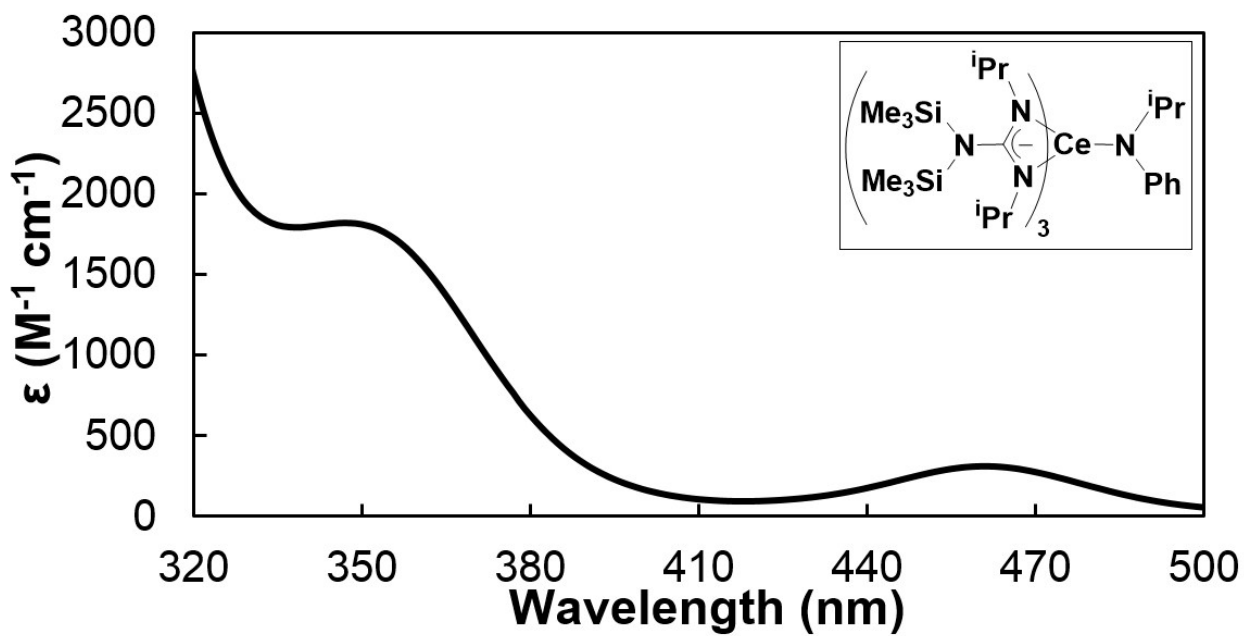


Figure S12. UV-vis spectrum of **4** recorded in toluene.

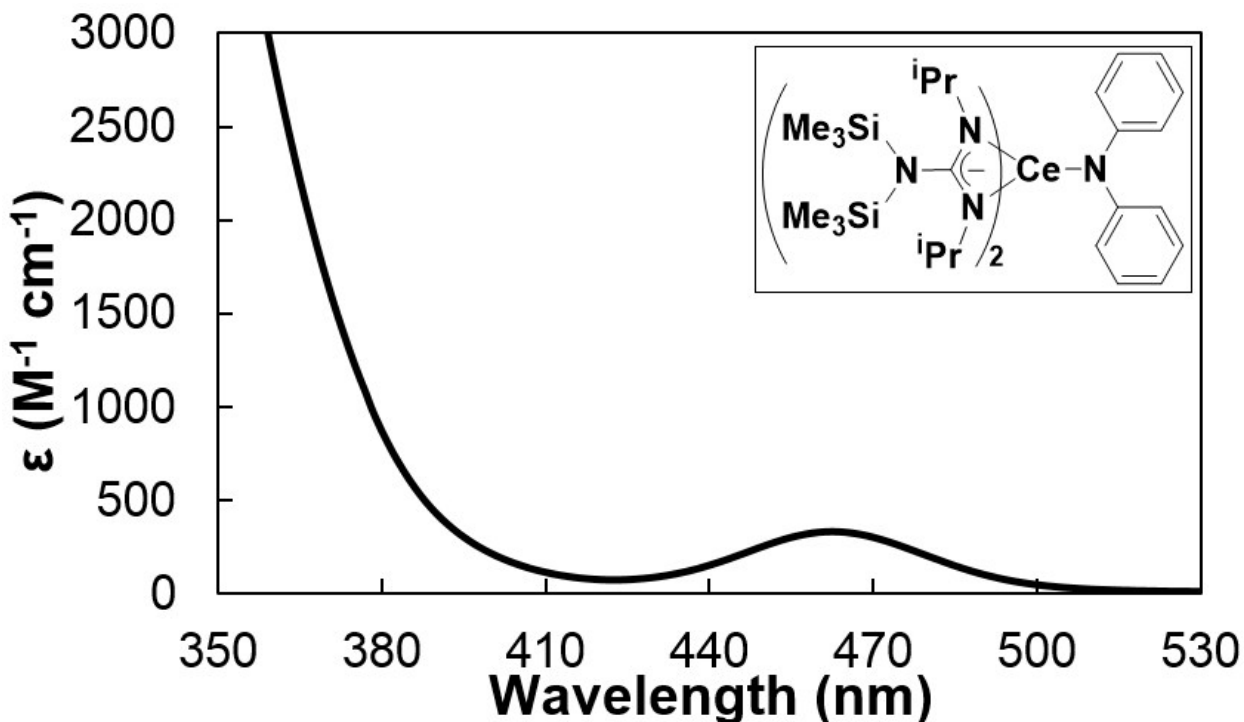


Figure S13. UV-vis spectrum of **5** recorded in toluene.

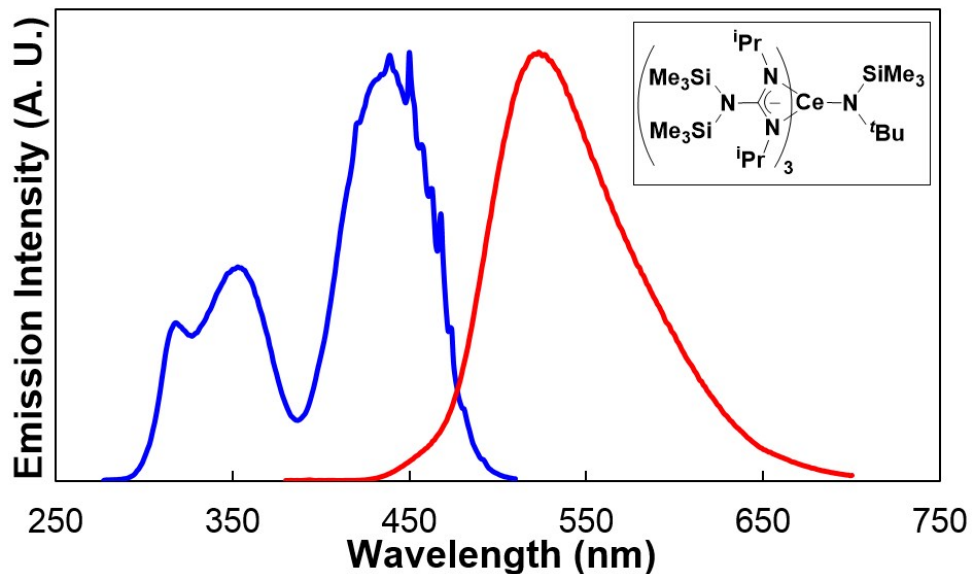


Figure S14. Normalized emission (red) and excitation (blue, uncorrected to lamp emission profile) spectra of **2** recorded in toluene.

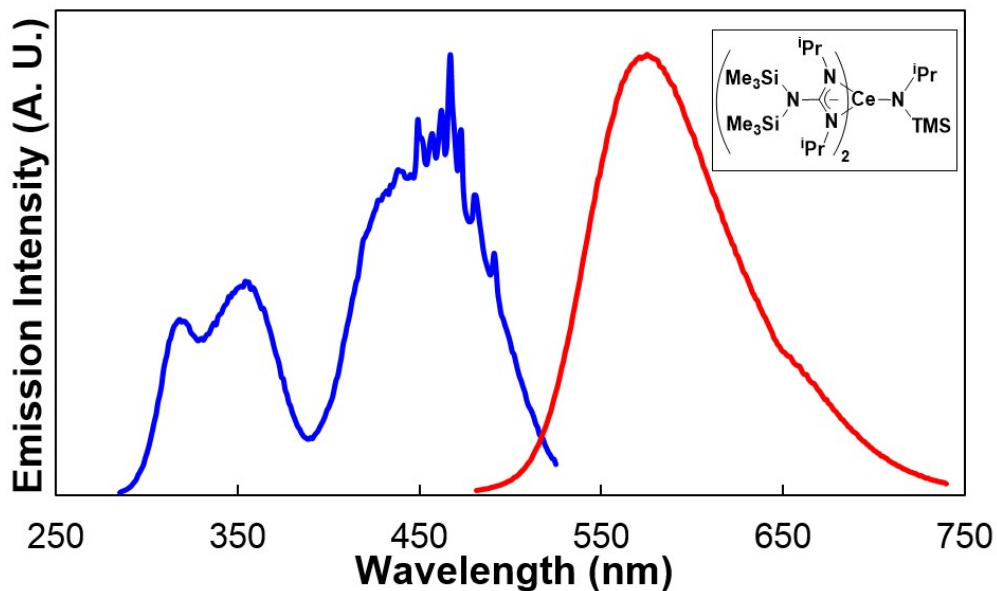


Figure S15. Normalized emission (red) and excitation (blue, uncorrected to lamp emission profile) spectra of **3** recorded in toluene.

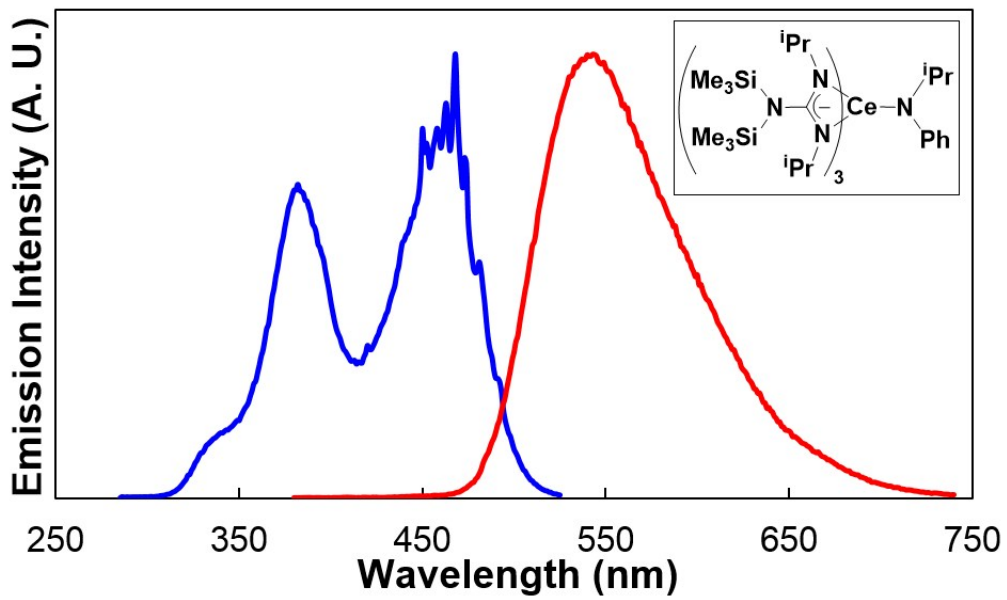


Figure S16. Normalized emission (red) and excitation (blue, uncorrected to lamp emission profile) spectra of **4** recorded in toluene.

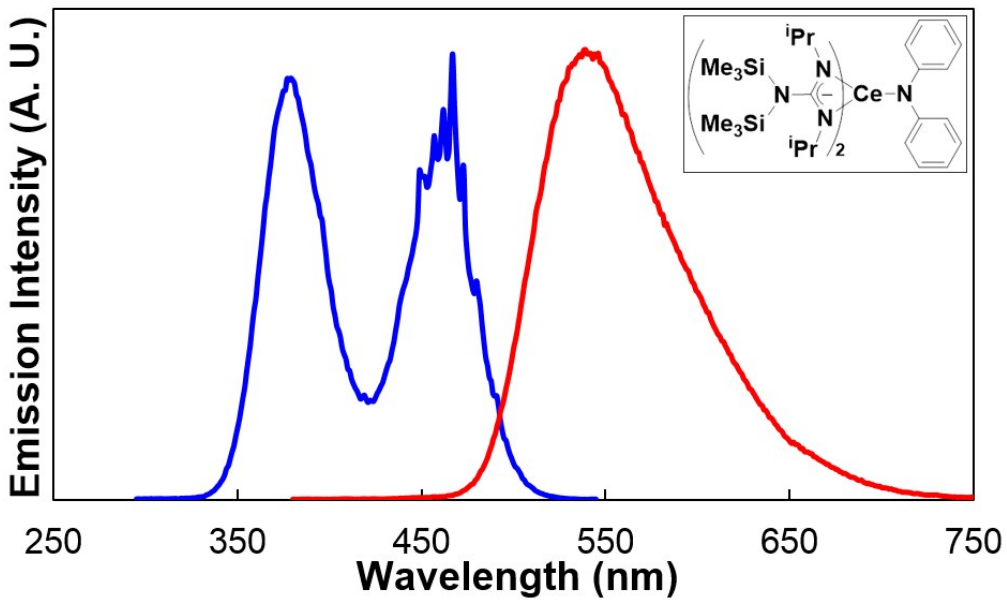


Figure S17. Normalized emission (red) and excitation (blue, uncorrected to lamp emission profile) spectra of **5** recorded in toluene.

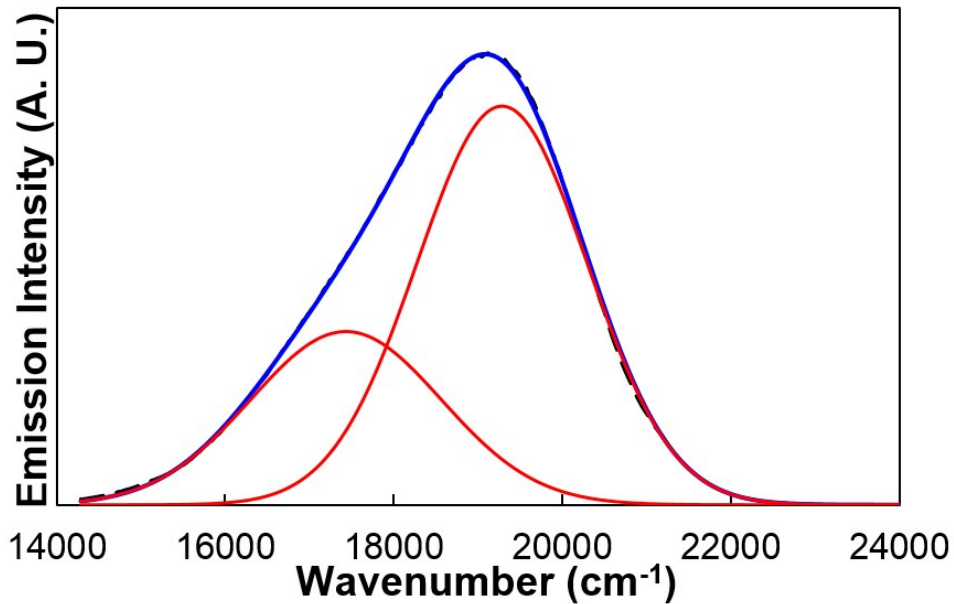


Figure S18. Fitting of emission spectrum of **2** plotted in wavenumbers. Two Gaussian bands (red solid lines) were applied for each fitting, featuring transitions to ${}^2\text{F}_{5/2}$ and ${}^2\text{F}_{7/2}$. Sum of the fit (blue solid lines) is in good agreement with experimental spectra (black dashed lines).

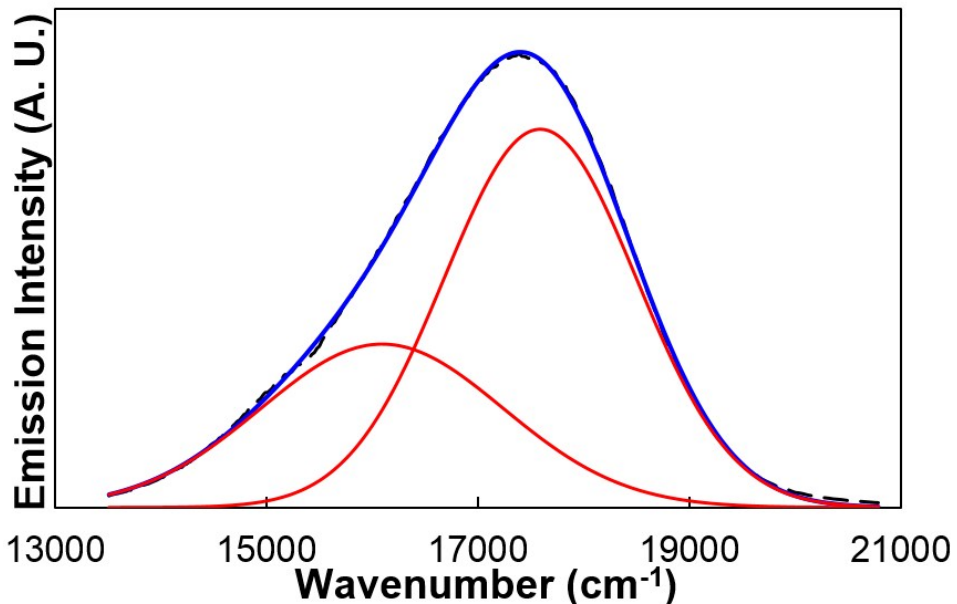


Figure S19. Fitting of emission spectrum of **3** plotted in wavenumbers. Two Gaussian bands (red solid lines) were applied for each fitting, featuring transitions to ${}^2\text{F}_{5/2}$ and ${}^2\text{F}_{7/2}$. Sum of the fit (blue solid lines) is in good agreement with experimental spectra (black dashed lines).

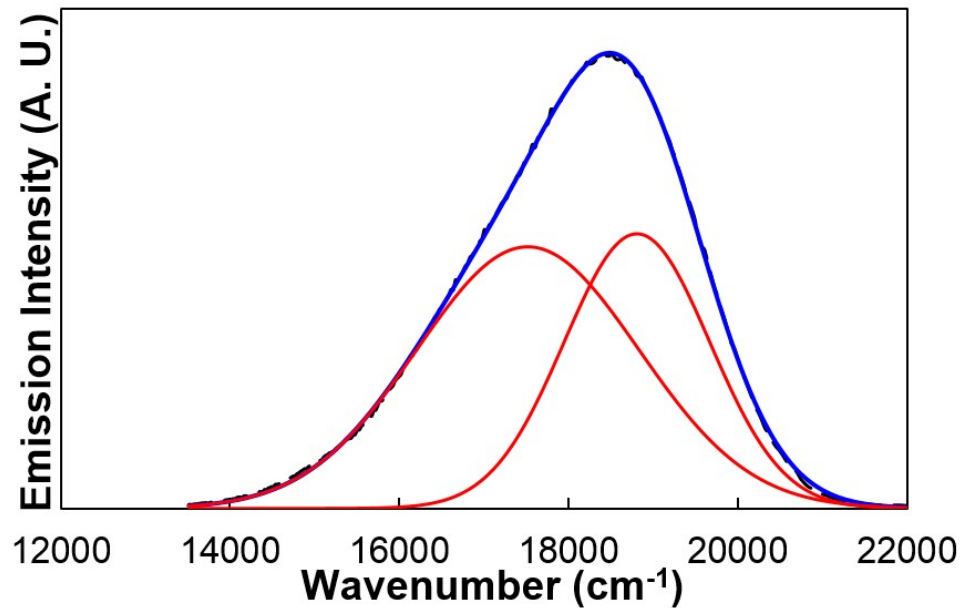


Figure S20. Fitting of emission spectrum of **4** plotted in wavenumbers. Two Gaussian bands (red solid lines) were applied for each fitting, featuring transitions to $^2\text{F}_{5/2}$ and $^2\text{F}_{7/2}$. Sum of the fit (blue solid lines) is in good agreement with experimental spectra (black dashed lines).

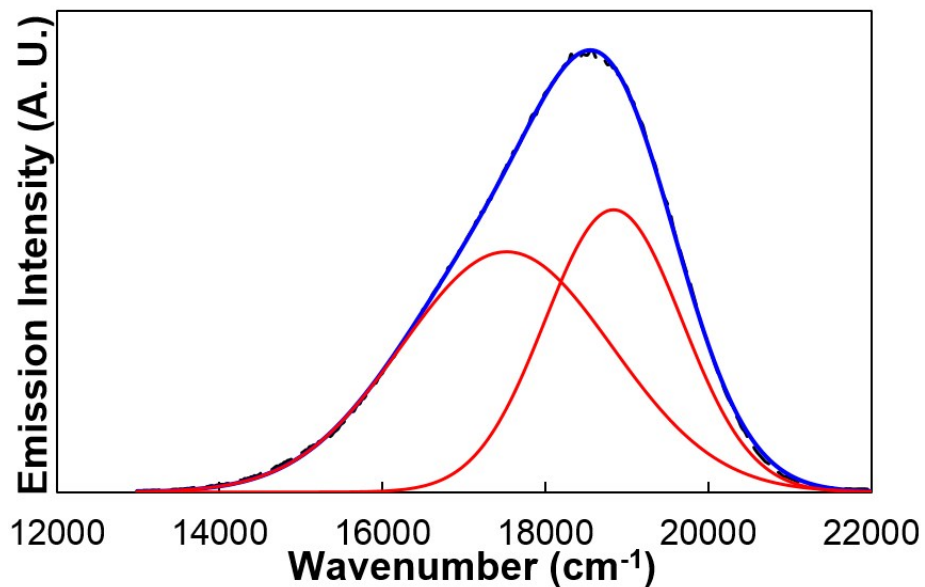


Figure S21. Fitting of emission spectrum of **5** plotted in wavenumbers. Two Gaussian bands (red solid lines) were applied for each fitting, featuring transitions to $^2\text{F}_{5/2}$ and $^2\text{F}_{7/2}$. Sum of the fit (blue solid lines) is in good agreement with experimental spectra (black dashed lines).

6. Lifetime Data

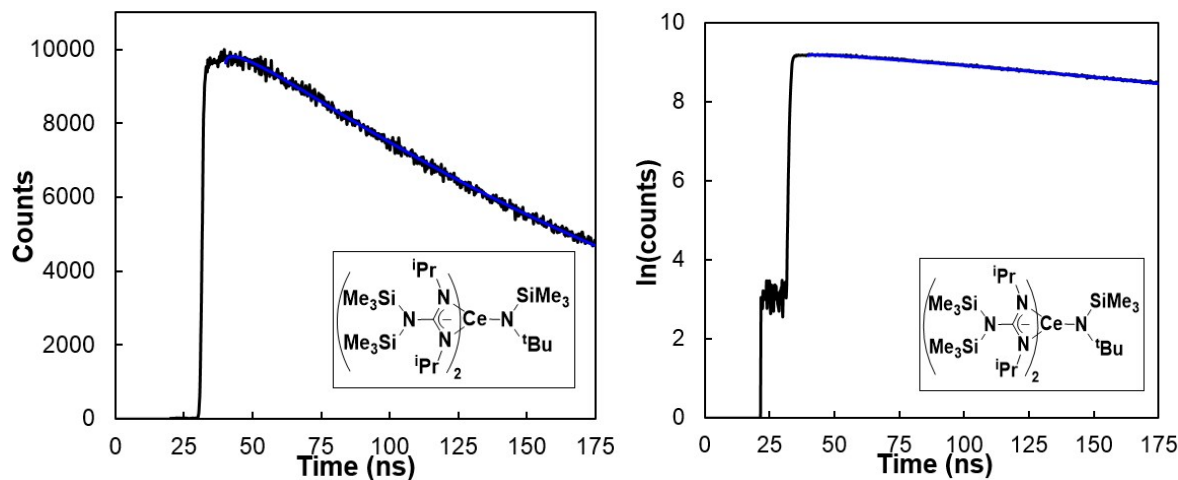


Figure S22. (left) Time-resolved emission intensity decay of **2** in toluene shown in black trace. The decay data was collected at 520 nm upon 380 nm excitation. A single exponential fit from 40 ns to 175 ns is given as blue lines, affording $\tau = 221.3 \pm 3.8$ ns. (right) The $\ln(\text{counts})$ versus time plot of time-resolved emission intensity decay for **2** in toluene is shown in the black trace with the model shown as the blue solid line ($R^2 = 0.9982$).

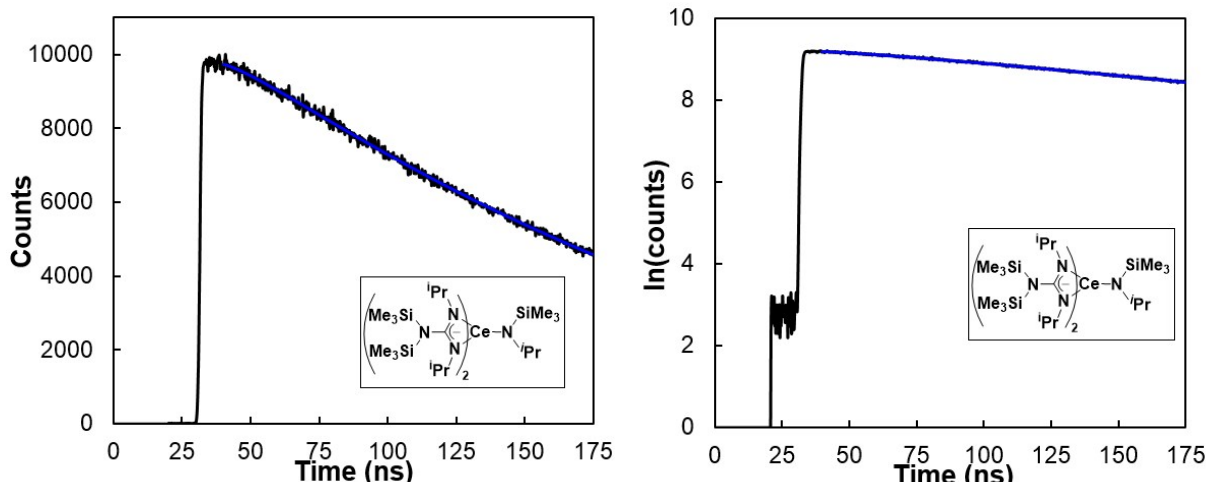


Figure S23. (left) Time-resolved emission intensity decay of **3** in toluene shown in black trace. The decay data was collected at 570 nm upon 380 nm excitation. A single exponential fit from 40 ns to 175 ns is given as blue lines, affording $\tau = 158.2 \pm 3.1$ ns. (right) The $\ln(\text{counts})$ versus time plot of time-resolved emission intensity decay for **3** in toluene is shown in the black trace with the model shown as the blue solid line ($R^2 = 0.9980$).

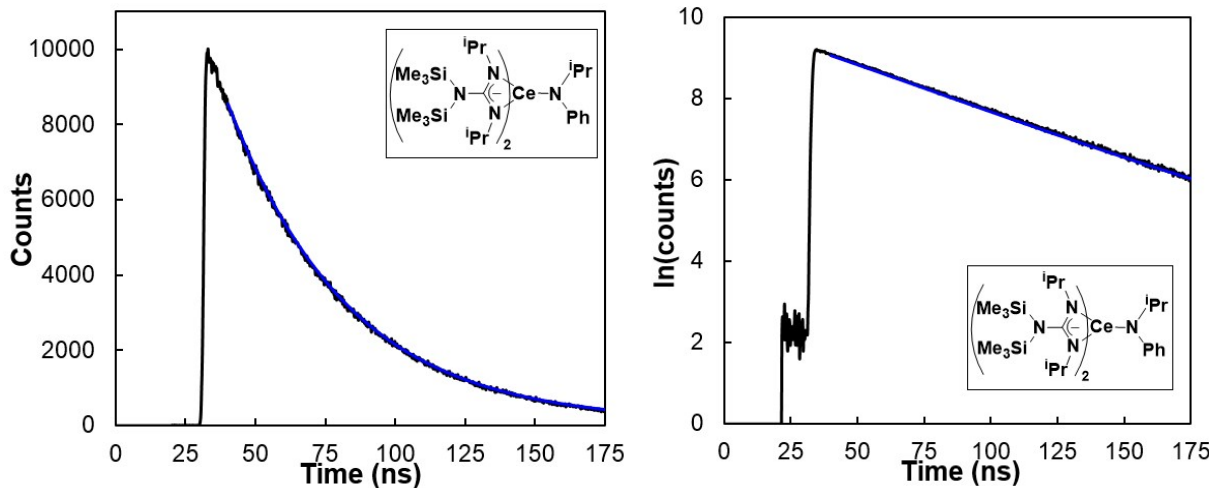


Figure S24. (left) Time-resolved emission intensity decay of **4** in toluene shown in black trace. The decay data was collected at 540 nm upon 380 nm excitation. A single exponential fit from 40 ns to 175 ns is given as blue lines, affording $\tau = 41.01 \pm 0.07$ ns. (right) The ln(counts) versus time plot of time-resolved emission intensity decay for **4** in toluene is shown in the black trace with the model shown as the blue solid line ($R^2 = 0.9988$).

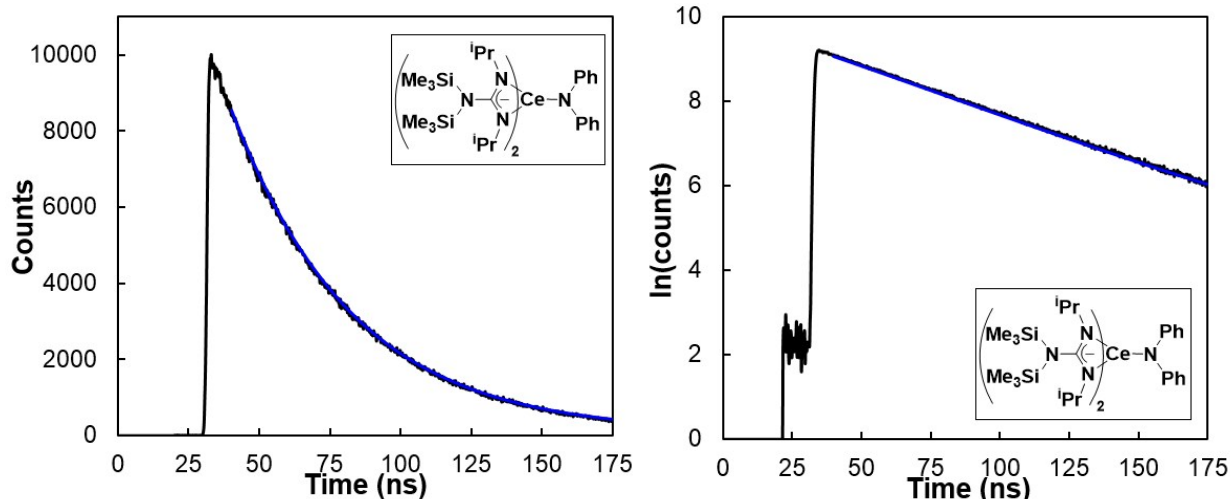


Figure S25. (left) Time-resolved emission intensity decay of **5** in toluene shown in black trace. The decay data was collected at 540 nm upon 380 nm excitation. A single exponential fit from 40 ns to 175 ns is given as blue lines, affording $\tau = 43.3 \pm 0.2$ ns. (right) The ln(counts) versus time plot of time-resolved emission intensity decay for **5** in toluene is shown in the black trace with the model shown as the blue solid line ($R^2 = 0.9982$).

7. Summary of Spectroscopy Data

Table S1. Summary of spectroscopy data for **1**, **2**, **3**, **4** and **5** in toluene.

		1	2	3	4	5
Spectra data	λ_{abs} /nm (ϵ M ⁻¹ cm ⁻¹) (FWHM cm ⁻¹)	429 (402) 352 (235) (2238)	438 (359) 348 (232) (2041)	463 (217) 350 (241) (3143)	461 (310) (2222)	463 (328) (2109)
	λ_{emi} /nm	508	522	575	540	540
	Stokes shift /nm	79	84	112	79	77
Fit of Emission data	$\rightarrow^2F_{5/2}$ /cm ⁻¹ (HWHM cm ⁻¹)	19978 (992)	19285 (1189)	17593 (1069)	18809 (1012)	18837 (992)
	$\rightarrow^2F_{7/2}$ /cm ⁻¹ (HWHM cm ⁻¹)	18683 (1666)	19919 (1334)	16097 (1350)	17520 (1547)	17525 (1523)
Φ^a		0.79	0.75	0.23	0.136	0.104
τ /ns		117	221	158	41	43
k_r ^b/×10⁶ s⁻¹		6.8	3.4	1.5	3.3	2.3
k_{nr} ^b/×10⁶ s⁻¹		1.8	1.1	4.9	21.1	20.9

a. Referenced to 9,10-diphenylanthracene (absolute quantum yield $\Phi = 0.97$)⁴ b. $\Phi = k_r/(k_r + k_{nr})$,

$$\tau = 1/(k_r + k_{nr})$$

8. Electrochemistry

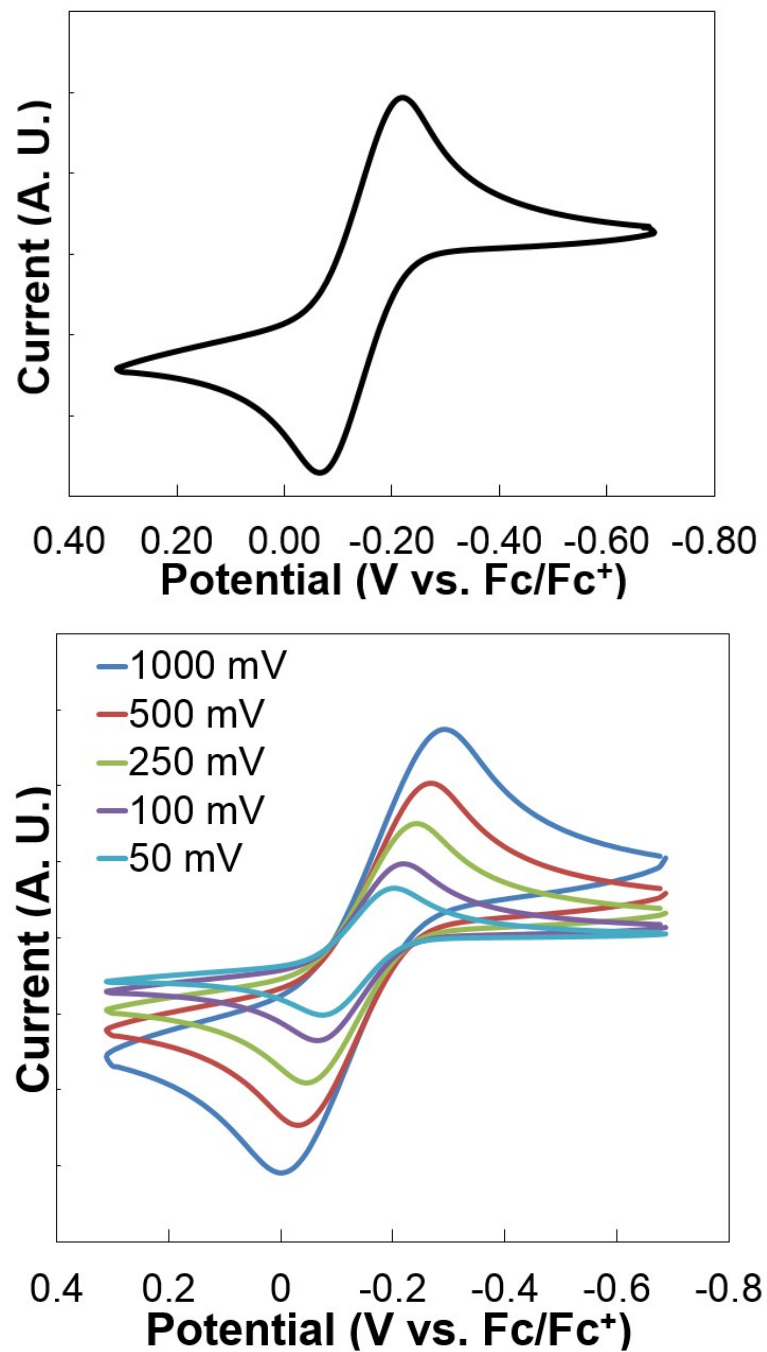


Figure S26. (Top) Full scan cyclic voltammetry of **1** in DCM with 0.1 M $[n\text{Pr}_4\text{N}][\text{BAr}^{\text{F}}_4]$; [analyte] = ca. 1 mM; $v = 0.1$ V/sec. $E_{1/2}$ of $\text{Ce}^{\text{III}}/\text{Ce}^{\text{IV}}$ couple was determined to be -0.14 V vs. Fc/Fc^+ . (Bottom) Isolated cerium(III/IV) redox couple at varying scan rates of **1**.

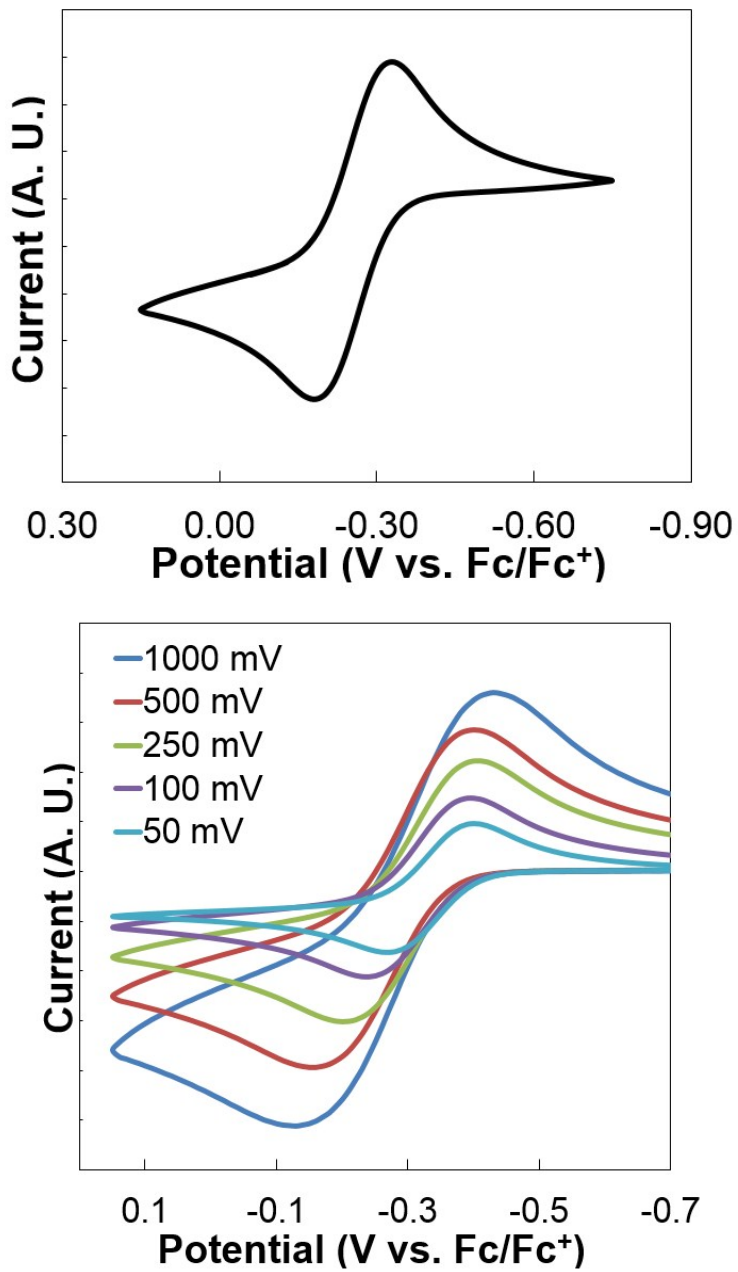


Figure S27. (Top) Full scan cyclic voltammetry of **2** in DCM with 0.1 M [Pr_4N^+][BAr_4^-]; [analyte] = ca. 1 mM; $v = 0.1$ V/sec. $E_{1/2}$ of $\text{Ce}^{\text{III}}/\text{Ce}^{\text{IV}}$ couple was determined to be -0.26 V vs. Fc/Fc^+ . (Bottom) Isolated cerium(III/IV) redox couple at varying scan rates of **2**.

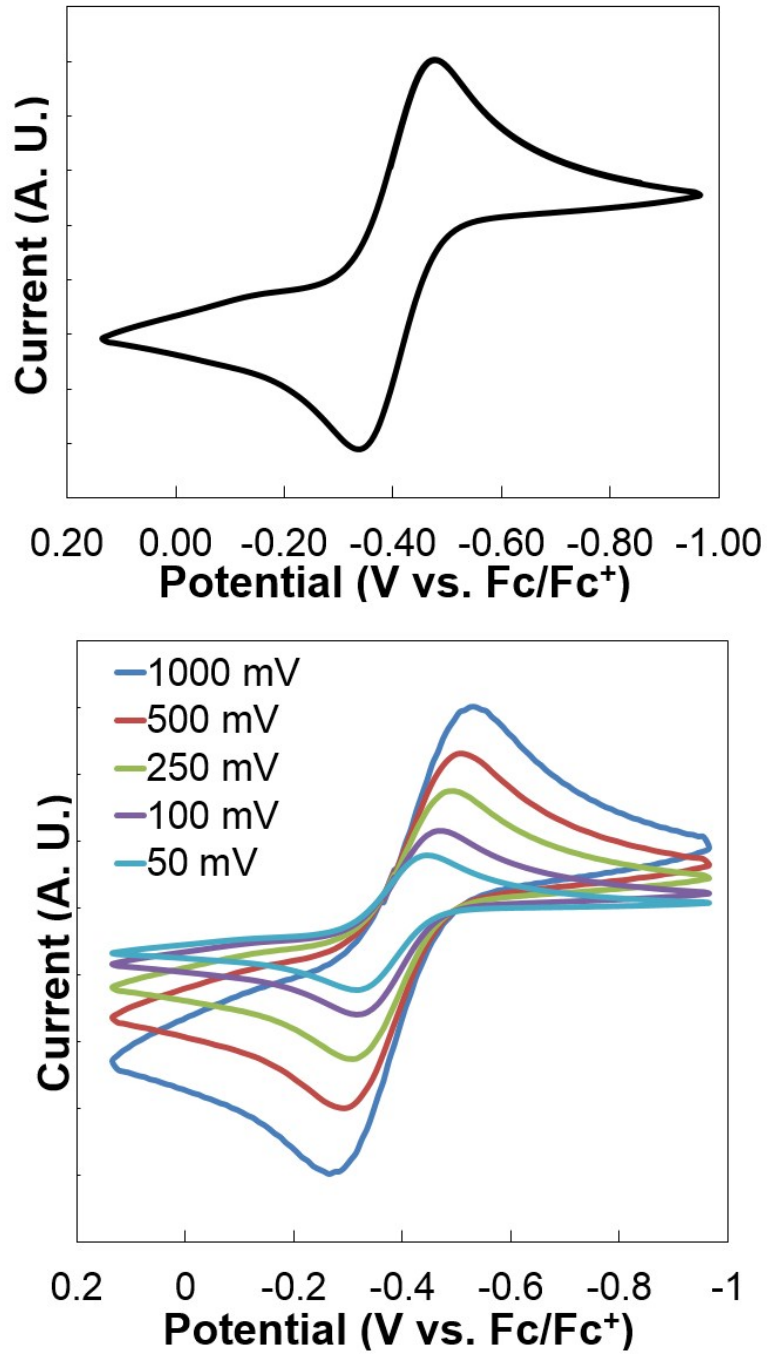


Figure S28. (Top) Full scan cyclic voltammetry of **3** in DCM with 0.1 M [$^n\text{Pr}_4\text{N}][\text{BAr}^{\text{F}}_4]$; [analyte] = ca. 1 mM; $v = 0.1$ V/sec. $E_{1/2}$ of $\text{Ce}^{\text{III}}/\text{Ce}^{\text{IV}}$ couple was determined to be -0.41 V vs. Fc/Fc^+ . (Bottom) Isolated cerium(III/IV) redox couple at varying scan rates of **3**.

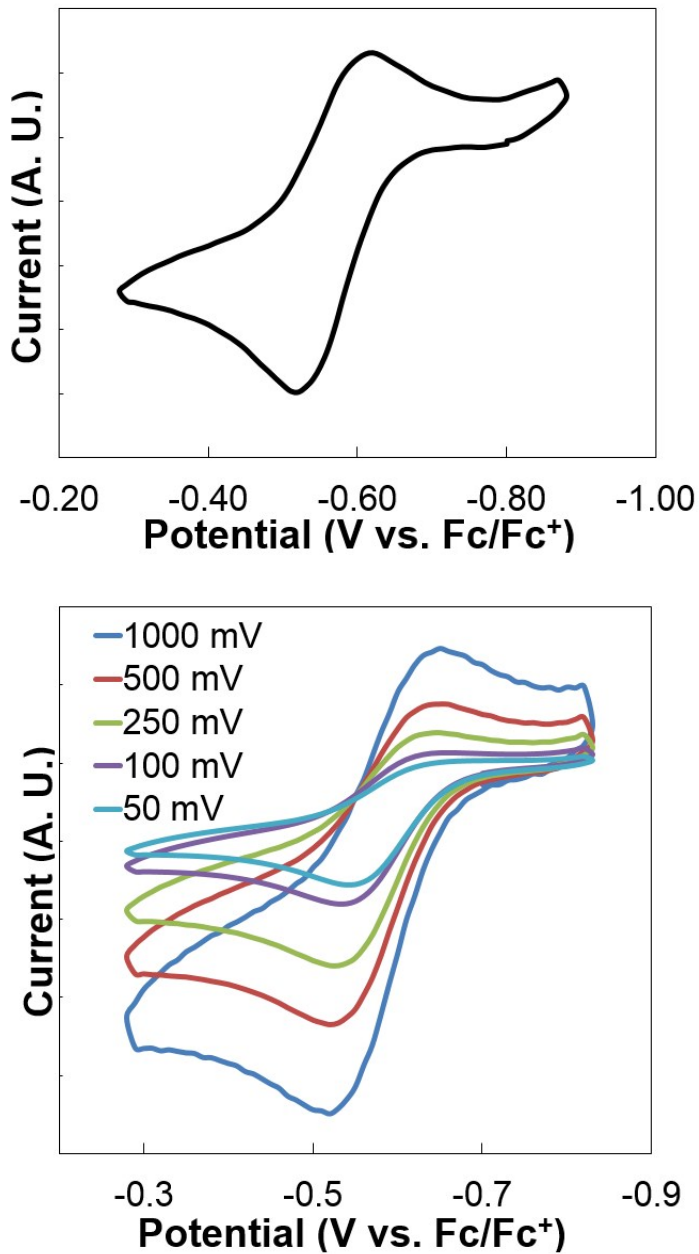


Figure S29. (Top) Full scan cyclic voltammetry of **4** in DCM with 0.1 M [*n*Pr₄N][BAr^F₄]; [analyte] = ca. 1 mM; v = 0.1 V/sec. E_{1/2} of Ce^{III}/Ce^{IV} couple was determined to be -0.57 V vs. Fc/Fc⁺. (Bottom) Isolated cerium(III/IV) redox couple at varying scan rates of **4**.

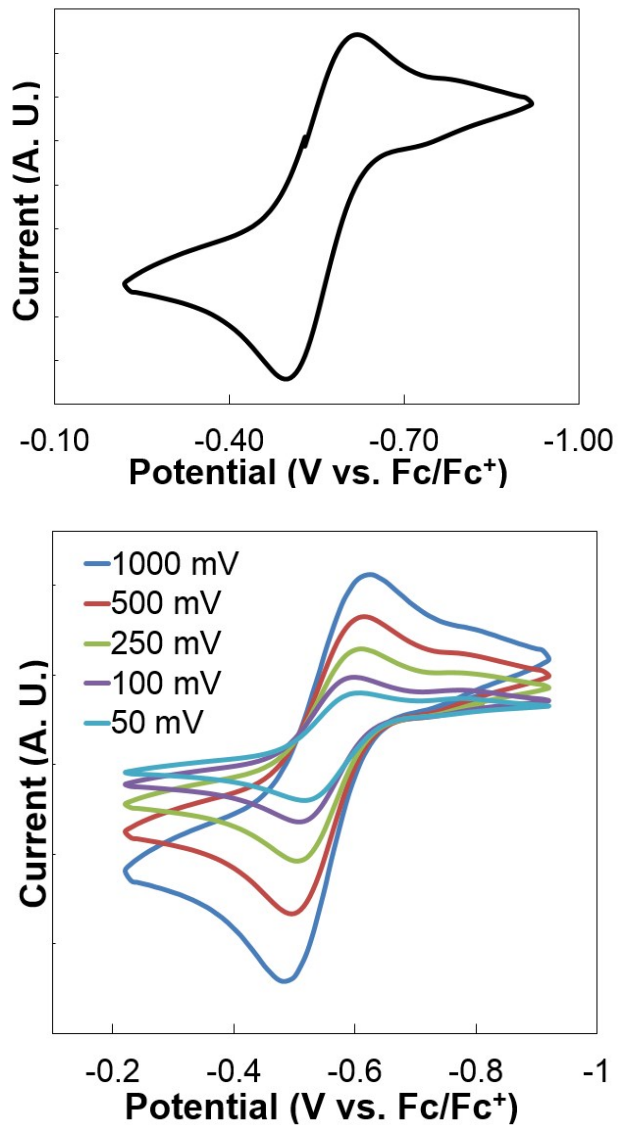


Figure S30. (Top) Full scan cyclic voltammetry of **5** in DCM with 0.1 M [ⁿPr₄N][BAr₄]; [analyte] = ca. 1 mM; v = 0.1 V/sec. E_{1/2} of Ce^{III}/Ce^{IV} couple was determined to be -0.56 V vs. Fc/Fc⁺. (Bottom) Isolated cerium(III/IV) redox couple at varying scan rates of **5**.

Table S2. Summary of electrochemical data for **1**, **2**, **3**, **4** and **5** in DCM.

	1	2	3	4	5
E _{pa} / V	-0.07	-0.19	-0.34	-0.52	-0.50
E _{pc} / V	-0.22	-0.33	-0.48	-0.62	-0.62
E _{1/2} / V	-0.14	-0.26	-0.41	-0.57	-0.56
ΔE / V	0.15	0.14	0.14	0.10	0.12

9. Computation Details

Gaussian 09 Rev. A.02 was used for all electronic structure calculations.¹⁴ The B3LYP hybrid DFT method was employed, with a 28-electron small core pseudopotential on cerium with published segmented natural orbital basis set incorporating quasi-relativistic effects,¹⁵ and the 6-31G* basis set for all other atoms. Gas phase ground-state geometry optimization for **2–5** were carried out starting from the coordinates of the crystal structure. The only constraint was the spin state (doublet). The frequency calculation was performed to indicate that the geometry was the minimum (no imaginary frequencies). Calculated metal-ligand bond lengths were within 0.04 Å of the crystal structures in all cases. TD-DFT calculation was carried out for **2–5** in gas phase. Molecular orbitals were rendered with the program Chemcraft v1.6.¹⁶ Natural Transition Orbitals (NTOs)¹⁷ were calculated using keyword pop=NTO. Corresponding donor and acceptor orbitals from NTOs calculation were rendered with the program Chemcraft v1.6.¹⁶ DFT and TD-DFT calculations on **1** was previously reported by us.² For predicting the reduction potential of **5-F** and **5-OMe**, the geometry optimizations and frequency calculations of **5-F**, **[5-F]⁺**, **5-OMe**, and **[5-OMe]⁺** were performed with the conductor-like polarizable continuum model (CPCM) with the Gaussian-defined solvent parameters for dichloromethane.¹⁸ $\Delta G^\circ(\text{Ce}^{\text{IV}}/\text{Ce}^{\text{III}})$ was determined for **5-F** and **5-OMe**, and the reduction potentials were predicted by an experimental $E_{1/2}$ -computed $E_{1/2}$ correlation previously reported by our group.¹⁸

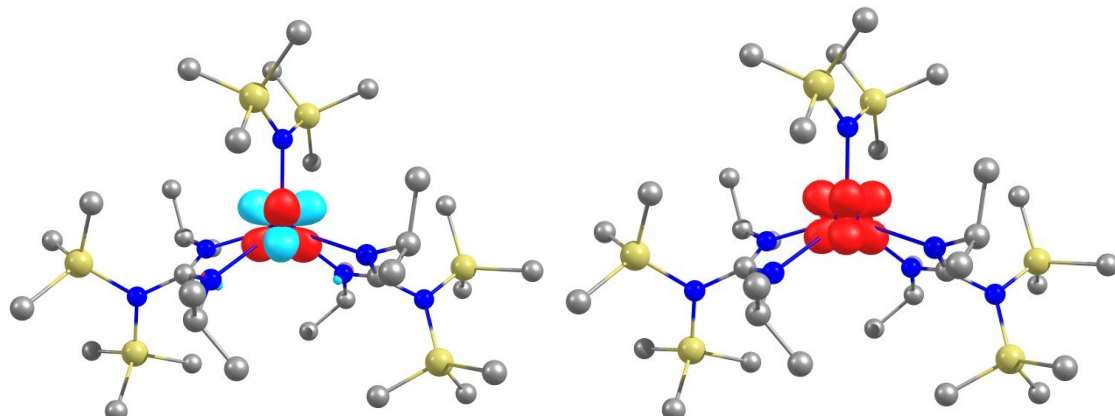


Figure S31. HOMO (left) and spin density plot (right) of **1**.

Table S3. Cartesian coordinates of optimized gas phase structure for **2**

Ce	0.011563	0.740126	0.042021	H	-1.665	1.866405	-2.1422
Si	-5.34384	-0.38456	-0.55047	Si	5.398862	-0.27515	0.540989
Si	-4.05413	-3.01889	0.511241	Si	4.154236	-2.88052	-0.63366

N	-1.82172	-0.63876	-1.04702	N	1.861815	-0.65444	1.032642
N	-2.16116	-0.0222	1.10877	N	2.201536	0.108059	-1.07372
N	-3.92205	-1.31137	0.009998	N	3.988549	-1.20317	-0.04423
N	0.032212	3.089479	0.251855	C	2.68039	-0.58291	-0.03135
C	-2.62911	-0.65884	0.025943	C	2.995823	0.412894	-2.25977
C	-2.96672	0.201729	2.305816	H	3.919179	-0.17967	-2.24793
H	-3.86949	-0.42028	2.2647	C	2.220909	0.05458	-3.5381
C	-2.1821	-0.19009	3.56811	H	1.922391	-0.99814	-3.54382
H	-1.84522	-1.23019	3.52283	H	2.832278	0.243366	-4.42891
H	-2.80233	-0.06781	4.464422	H	1.311128	0.661223	-3.6266
H	-1.2956	0.444346	3.691061	C	3.383911	1.902943	-2.29197
C	-3.4073	1.67378	2.406469	H	2.487761	2.534891	-2.2992
H	-2.53413	2.335859	2.434006	H	3.973319	2.136829	-3.1877
H	-3.99786	1.847188	3.315137	H	3.974044	2.180702	-1.41325
H	-4.01388	1.968388	1.544695	C	2.148471	-1.49364	2.194674
C	-2.07493	-1.45734	-2.23245	H	3.17401	-1.87465	2.123912
H	-3.08772	-1.87335	-2.17781	C	2.034833	-0.70102	3.507015
C	-1.97994	-0.63541	-3.52724	H	2.722182	0.149777	3.526234
H	-2.69843	0.189294	-3.53831	H	2.267672	-1.34583	4.363245
H	-2.18213	-1.27327	-4.3964	H	1.018159	-0.31624	3.649054
H	-0.978	-0.20974	-3.65353	C	1.190065	-2.69641	2.240413
C	-1.07773	-2.62755	-2.29881	H	0.153075	-2.35211	2.32138
H	-0.05264	-2.24815	-2.37227	H	1.40266	-3.3392	3.104145
H	-1.26816	-3.26126	-3.17445	H	1.269548	-3.3054	1.334029
H	-1.1373	-3.25546	-1.40368	C	4.829114	1.252796	1.492405
C	-4.78978	1.204327	-1.40677	H	4.092224	1.844092	0.940747
H	-4.08216	1.785185	-0.80725	H	5.696671	1.898545	1.678509
H	-5.66788	1.838019	-1.58509	H	4.393638	0.996687	2.462775
H	-4.32166	1.008766	-2.37602	C	6.450066	-1.33359	1.710422
C	-6.35542	-1.40304	-1.78897	H	5.863849	-1.70917	2.556758
H	-5.75299	-1.71252	-2.65051	H	7.262537	-0.71775	2.117621
H	-7.18421	-0.79034	-2.16704	H	6.915558	-2.19325	1.215773
H	-6.79726	-2.30279	-1.34618	C	6.536939	0.306411	-0.8607

C	-6.51334	0.090525	0.86476	H	6.966583	-0.52561	-1.42762
H	-6.94867	-0.78224	1.361863	H	7.372654	0.875549	-0.4321
H	-7.34406	0.685773	0.462918	H	6.023716	0.962983	-1.5709
H	-6.01648	0.695556	1.629901	C	2.608703	-3.38946	-1.58659
C	-2.51835	-3.53542	1.477362	H	1.692974	-3.23261	-1.00898
H	-1.59159	-3.30742	0.942458	H	2.67099	-4.45886	-1.82469
H	-2.5473	-4.6201	1.641443	H	2.506776	-2.84418	-2.52943
H	-2.46614	-3.05256	2.457755	C	5.644696	-3.03333	-1.79446
C	-5.56745	-3.27189	1.623993	H	5.589053	-2.32535	-2.62886
H	-5.54577	-2.61462	2.500183	H	5.661694	-4.04569	-2.21866
H	-5.57208	-4.30814	1.986302	H	6.604327	-2.88271	-1.28758
H	-6.51823	-3.11	1.104193	C	4.406729	-4.14384	0.759729
C	-4.23764	-4.21455	-0.95126	H	5.28788	-3.93149	1.373897
H	-5.09927	-3.98088	-1.58519	H	4.549053	-5.13913	0.317545
H	-4.38081	-5.23329	-0.56661	H	3.541938	-4.20493	1.428747
H	-3.34856	-4.2284	-1.59002	C	0.667925	3.732341	1.426744
Si	-0.74729	3.982795	-1.0192	C	2.026808	4.373136	1.057543
C	0.250668	5.402555	-1.80771	H	2.685363	3.630675	0.594625
H	0.38942	6.251041	-1.12707	H	2.532741	4.77585	1.945289
H	-0.28278	5.782017	-2.68973	H	1.897714	5.193636	0.346145
H	1.244215	5.074778	-2.13626	C	-0.22396	4.815318	2.075133
C	-2.45517	4.71657	-0.5935	H	-0.38513	5.658931	1.394905
H	-3.10625	3.968405	-0.12581	H	0.243038	5.214646	2.98488
H	-2.95838	5.07371	-1.50205	H	-1.20398	4.406078	2.344252
H	-2.3872	5.565272	0.09631	C	0.93401	2.650651	2.4949
C	-1.05061	2.730513	-2.42498	H	-0.00483	2.178511	2.816376
H	-0.11411	2.358959	-2.86284	H	1.404399	3.073339	3.390394
H	-1.59565	3.227729	-3.23744	H	1.617224	1.87321	2.127581

Table S4. Comparison of parameters between X-ray structure and optimized gas phase model for 2

	X-ray structure	Optimized model
Average Ce–N _{guanidine} (Å)	2.5056(14)	2.5337

Ce–N _{amide} (Å)	2.337(8)	2.359
Average N _{guanidine} –Ce–N _{guanidine} (°)	53.23(5)	53.14

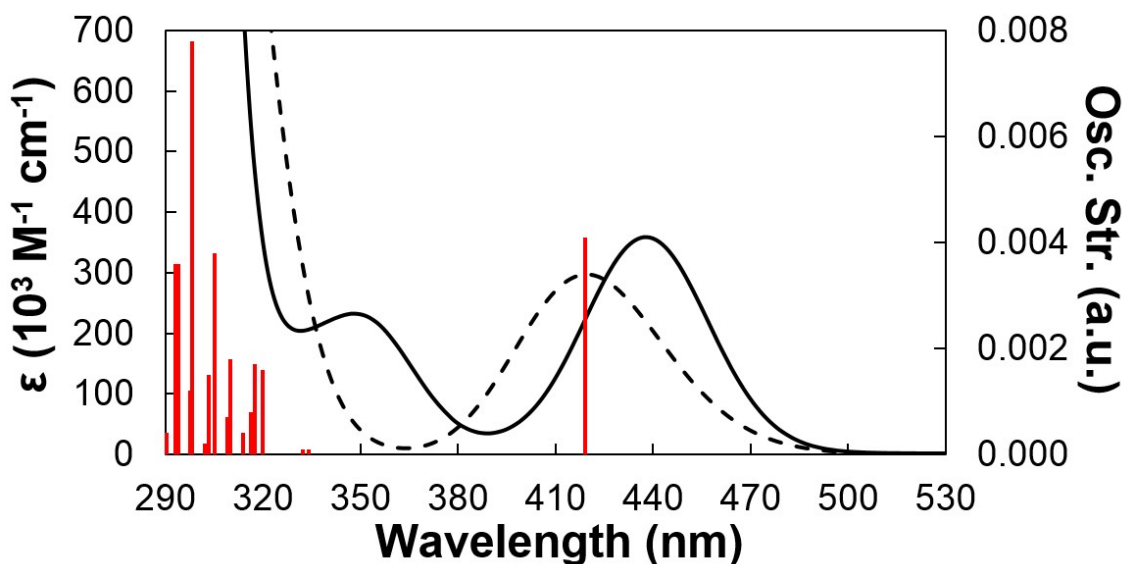


Figure S32. Experimental (black solid line) and TD-DFT predicted (black dashed line) absorption spectrum of **2**. The predicted spectra were rendered as Gaussian line shapes having a fwhm of 3000 cm^{-1} . Oscillator strengths for the electronic transitions are shown as red vertical lines.

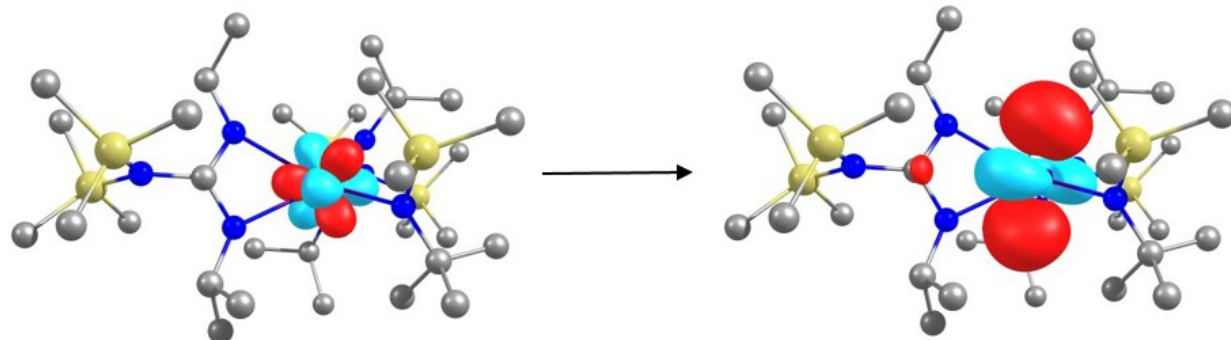


Figure S33. Calculated Natural Transition Orbitals (NTO) of $\lambda_{\text{abs}}^{-1}$ of **2** in gas phase with contour value of 0.05. The calculated transition shown is centered at 419 nm (oscillator strength 0.0041).

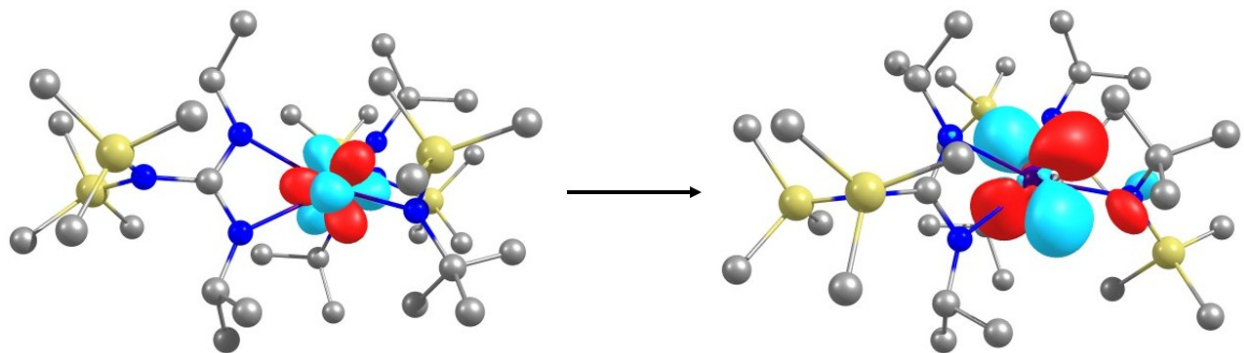


Figure S34. Calculated Natural Transition Orbitals (NTO) of λ_{abs}^2 of **2** in gas phase with contour value of 0.05. The calculated transition shown is centered at 320 nm (oscillator strength 0.0016).

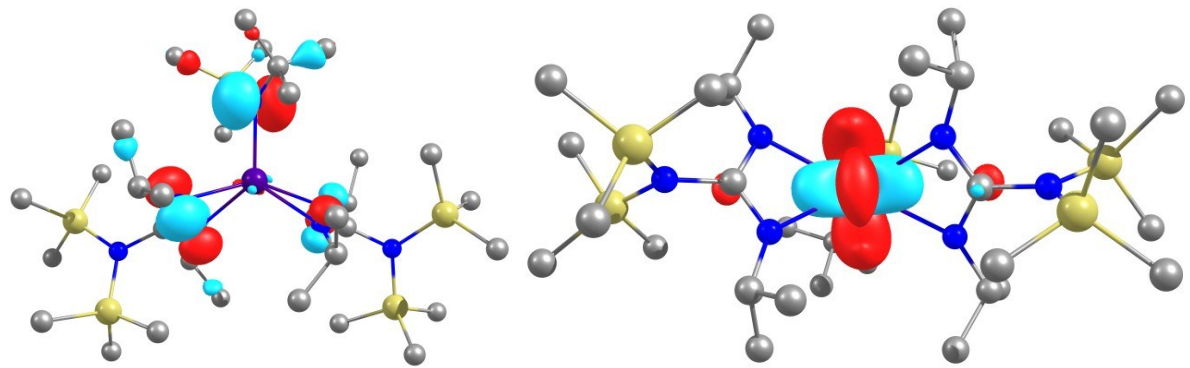


Figure S35. Calculated donor (left) and acceptor (right) orbitals for the LMCT transition of **2** at 317 nm (oscillator strength 0.0017).

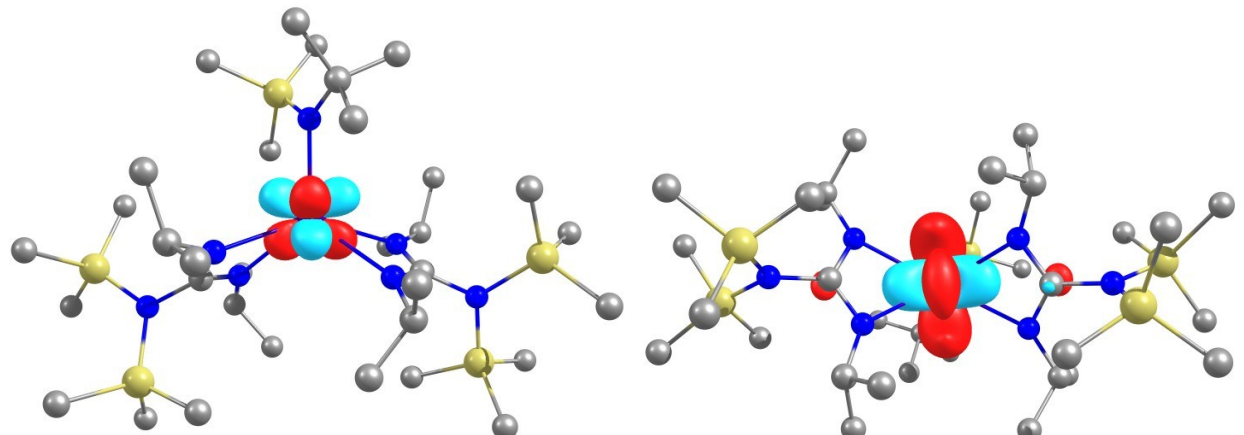


Figure S36. HOMO (left) and LUMO (right) of **2**.

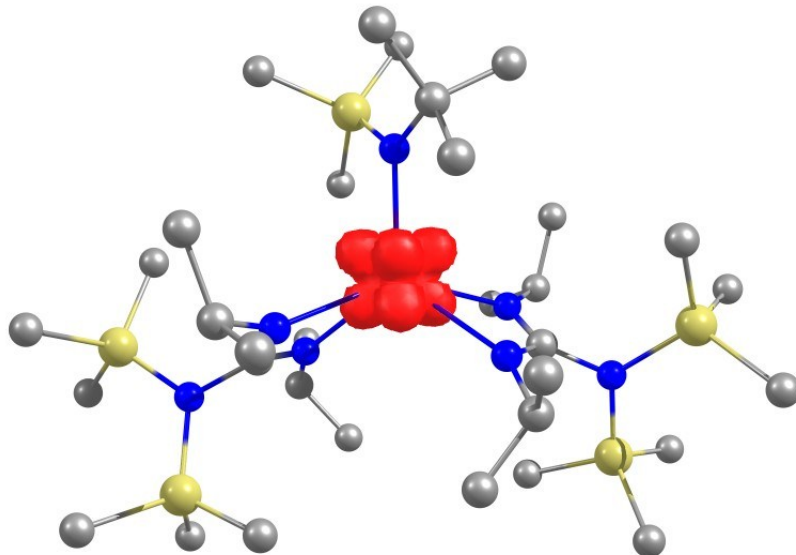


Figure S37. Spin density plot of **2**.

Table S5. Cartesian coordinates of optimized gas phase structure for **3**

Ce	0.011862	0.772564	0.071757	H	4.916023	2.070971	0.031358
Si	-0.79224	4.217248	-0.72375	H	5.770549	1.97835	1.576175
Si	4.179069	-2.72712	-0.85253	H	4.03373	1.650088	1.505339
Si	5.393834	-0.30196	0.690654	C	5.924421	-1.04058	2.356014
Si	-5.29971	-0.41823	-0.69901	H	5.15771	-0.92412	3.128751
Si	-4.04926	-2.95382	0.637463	H	6.82355	-0.51557	2.705545
N	0.028261	3.072011	0.288694	H	6.17351	-2.10456	2.289584
N	2.175107	0.120544	-1.09663	C	2.947843	0.45093	-2.29102
N	1.917089	-0.53045	1.056368	H	3.967689	0.05871	-2.1929
N	4.003091	-1.1328	-0.06293	C	2.314814	-0.17329	-3.54584
N	-2.13054	-0.08226	1.157909	H	2.239767	-1.26175	-3.45971
N	-1.83875	-0.51256	-1.05064	H	2.906801	0.059942	-4.43956
N	-3.90256	-1.29475	-0.00709	H	1.302677	0.219654	-3.70516
C	0.820407	3.383342	1.478937	C	3.045788	1.976204	-2.47326
H	1.080413	2.40997	1.965294	H	2.048933	2.420747	-2.58344
C	2.172417	4.057527	1.170764	H	3.627046	2.225079	-3.37003
H	2.722569	3.495402	0.41186	H	3.524814	2.451504	-1.61226
H	2.79565	4.125038	2.072065	C	-2.9287	0.070993	2.372745

H	2.019525	5.073603	0.791906	H	-3.92364	-0.36163	2.21536
C	0.072529	4.194655	2.555345	C	-3.11448	1.554669	2.731501
H	-0.11092	5.218235	2.20594	H	-2.14996	2.021296	2.961366
H	0.661049	4.261365	3.479395	H	-3.75718	1.662598	3.614278
H	-0.8953	3.743666	2.791451	H	-3.56597	2.114371	1.907451
C	0.236677	5.726008	-1.26304	C	-2.27355	-0.65892	3.557023
H	0.452963	6.402393	-0.4271	H	-2.14498	-1.72594	3.351541
H	-0.31464	6.307234	-2.0143	H	-2.88185	-0.55566	4.464211
H	1.193882	5.42967	-1.70785	H	-1.28318	-0.2373	3.77078
C	-1.25046	3.269181	-2.30905	C	-2.61948	-0.63048	0.037009
H	-0.36316	3.027058	-2.90874	C	-2.09013	-1.24555	-2.29011
H	-1.91063	3.875487	-2.94234	H	-3.02922	-1.80412	-2.20174
H	-1.78627	2.331778	-2.11065	C	-0.96304	-2.25679	-2.55835
C	-2.41226	4.904625	0.004636	H	-0.00488	-1.73891	-2.67553
H	-3.11012	4.096645	0.255628	H	-1.1547	-2.82521	-3.47728
H	-2.91484	5.565608	-0.71427	H	-0.86168	-2.96547	-1.73117
H	-2.2396	5.484689	0.918766	C	-2.21704	-0.28443	-3.48345
C	2.697736	-0.51119	-0.03596	H	-3.02294	0.440676	-3.33255
C	2.225088	-1.30901	2.251401	H	-2.42187	-0.83733	-4.40855
H	3.191032	-1.81108	2.124134	H	-1.28754	0.279131	-3.63096
C	2.318351	-0.39065	3.482367	C	-4.91137	1.42689	-0.79947
H	3.088146	0.376814	3.352112	H	-4.86448	1.889085	0.191595
H	2.55558	-0.96574	4.385945	H	-5.70496	1.933337	-1.36311
H	1.362916	0.121861	3.655267	H	-3.96365	1.627248	-1.30835
C	1.158981	-2.39191	2.487399	C	-5.79236	-1.01384	-2.43065
H	0.1762	-1.93611	2.64947	H	-5.01834	-0.8143	-3.17841
H	1.401093	-2.99553	3.371219	H	-6.69983	-0.4828	-2.74786
H	1.079602	-3.06132	1.625723	H	-6.01483	-2.08542	-2.4589
C	5.012411	-2.64987	-2.55417	C	-6.81783	-0.63878	0.4148
H	4.424551	-2.08659	-3.28558	H	-7.18022	-1.672	0.45731
H	5.127725	-3.67067	-2.94256	H	-7.63954	-0.02624	0.021516
H	6.010698	-2.20228	-2.51302	H	-6.62193	-0.3085	1.441116
C	5.238894	-3.87001	0.22677	C	-4.91649	-3.05041	2.322365

H	6.274518	-3.52987	0.335778	H	-4.34604	-2.56267	3.119052
H	5.274688	-4.86392	-0.23815	H	-5.03345	-4.106	2.602238
H	4.815765	-3.99013	1.230538	H	-5.91659	-2.60504	2.307844
C	2.487118	-3.53783	-1.06174	C	-2.33905	-3.73666	0.814435
H	2.077327	-3.87944	-0.10571	H	-1.91321	-4.00813	-0.15691
H	2.58832	-4.41765	-1.70986	H	-2.42646	-4.65731	1.405203
H	1.754322	-2.86917	-1.52198	H	-1.6257	-3.08185	1.323585
C	6.90029	-0.39107	-0.45713	C	-5.05758	-4.02259	-0.56034
H	7.276769	-1.40972	-0.60199	H	-6.10512	-3.71203	-0.64286
H	7.718096	0.193912	-0.01658	H	-5.05735	-5.05938	-0.19949
H	6.685631	0.033432	-1.44439	H	-4.6256	-4.02295	-1.56743
C	4.979528	1.51585	0.972461				

Table S6. Comparison of parameters between X-ray structure and optimized gas phase model for **3**

	X-ray structure	Optimized model
Average Ce–N _{guanidine} (Å)	2.498(2)	2.5300
Ce–N _{amide} (Å)	2.296(2)	2.3097
Average N _{guanidine} –Ce–N _{guanidine} (°)	53.56(6)	53.22

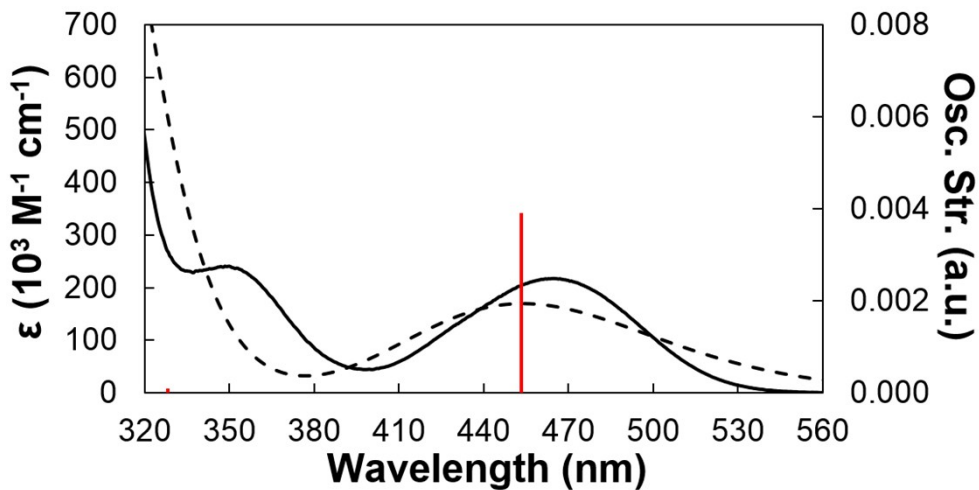


Figure S38. Experimental (black solid line) and TD-DFT predicted (black dashed line) absorption spectrum of **3**. The predicted spectra were rendered as Gaussian line shapes having a fwhm of 3000 cm⁻¹. Oscillator strengths for the electronic transitions are shown as red vertical lines.

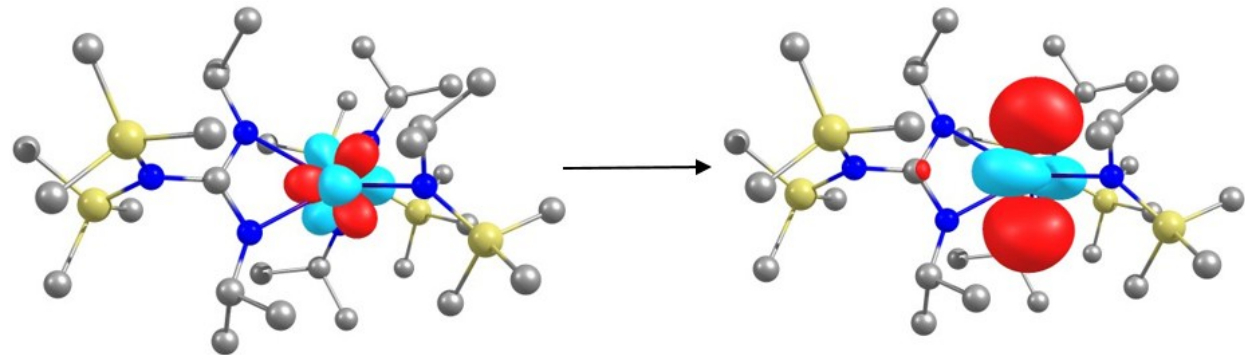


Figure S39. Calculated Natural Transition Orbitals (NTO) of $\lambda_{\text{abs}}^{-1}$ of **3** in gas phase with contour value of 0.05. The calculated transition shown is centered at 454 nm (oscillator strength 0.0039).

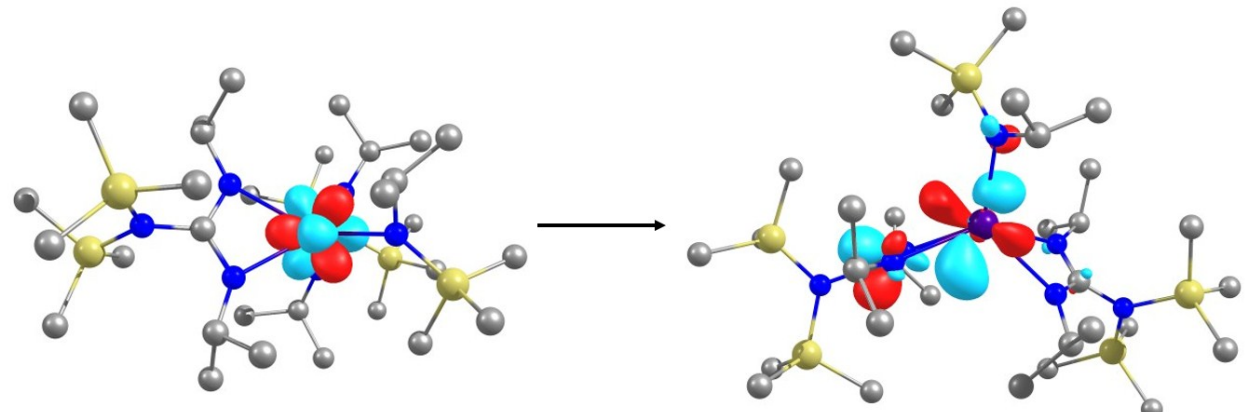


Figure S40. Calculated Natural Transition Orbitals (NTO) of λ_{abs}^2 of **3** in gas phase with contour value of 0.05. The calculated transition shown is centered at 313 nm (oscillator strength 0.0013).

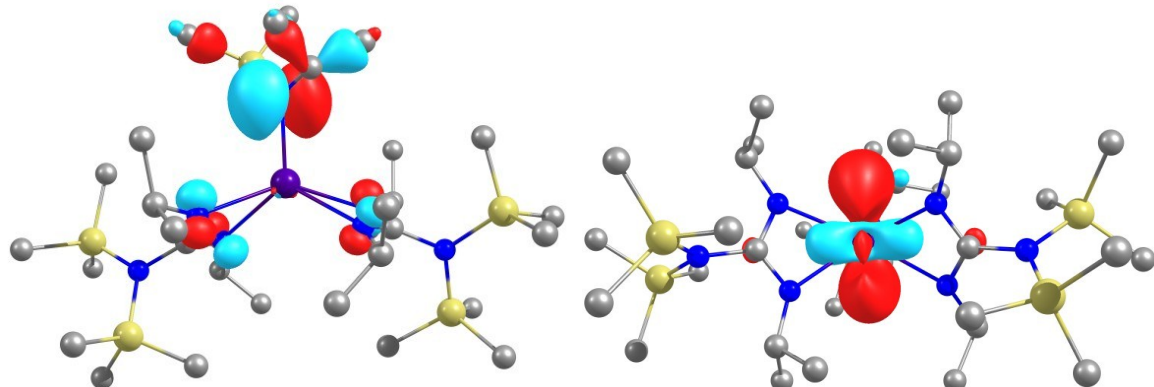


Figure S41. Calculated donor (left) and acceptor (right) orbitals for the LMCT transition of **3** at 307 nm (oscillator strength 0.0018).

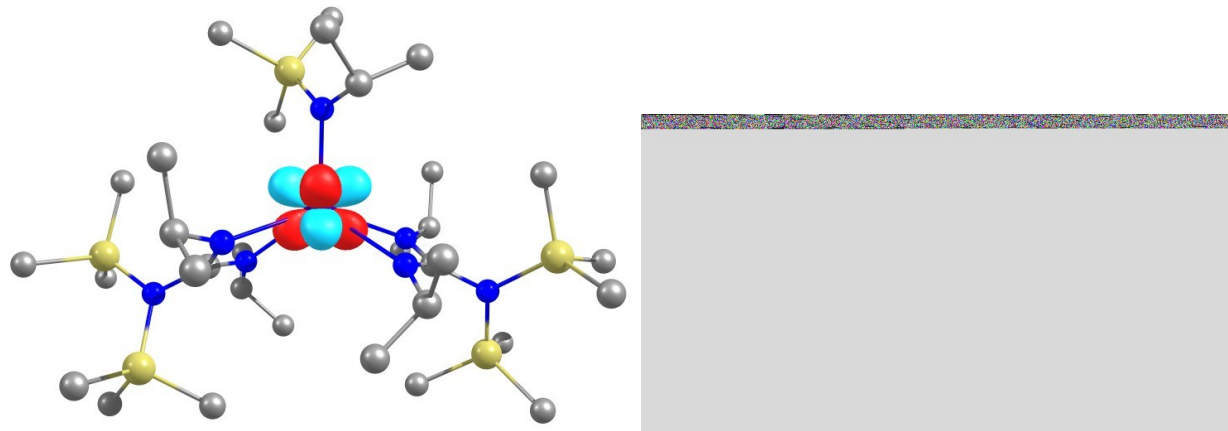


Figure S42. HOMO (left) and LUMO (right) of **3**.

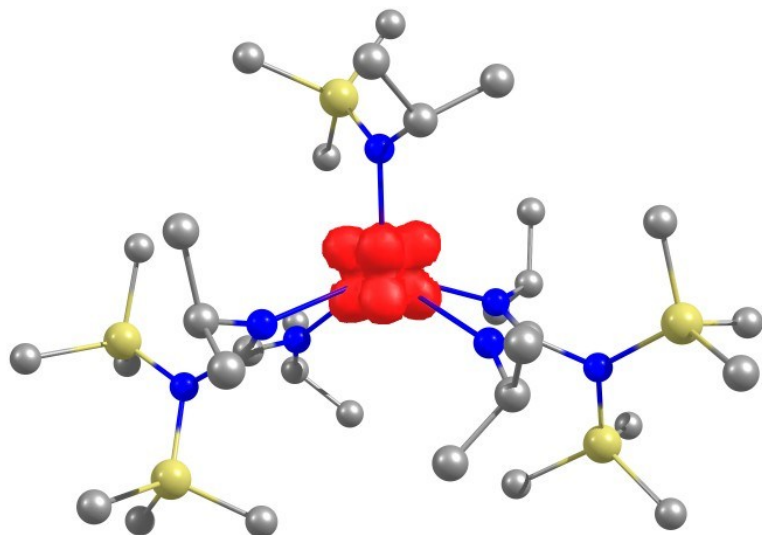


Figure S43. Spin density plot of **3**.

Table S7. Cartesian coordinates of optimized gas phase structure for **4**

Ce	0.060003	0.681688	0.205117	H	-2.75088	-1.01454	4.515993
Si	5.493166	0.026922	0.705432	H	-1.14546	-0.70483	3.83265
Si	4.529026	-2.23169	-1.22818	C	-2.90955	1.233251	2.934661
Si	-3.93971	-3.15009	0.492086	H	-3.31652	1.867828	2.142276
Si	-5.17873	-0.48894	-0.5949	H	-1.92971	1.639204	3.215437
N	2.066779	-0.58846	0.982076	H	-3.56293	1.310852	3.812725
N	2.25785	0.41321	-1.03592	C	-1.96859	-1.226	-2.2794
N	4.196193	-0.81431	-0.19117	H	-2.90159	-1.80057	-2.23377
N	-2.00007	-0.32809	1.249647	C	-0.83898	-2.18526	-2.69153

N	-1.69348	-0.64314	-0.96989	H	-0.7034	-2.98252	-1.95437
N	-3.78437	-1.43914	0.004699	H	0.110669	-1.64421	-2.77964
N	-0.11827	2.999031	0.67928	H	-1.0531	-2.64736	-3.66338
C	2.840281	-0.32929	-0.08538	C	-2.13143	-0.12959	-3.34574
C	2.419289	-1.5563	2.016753	H	-2.38497	-0.56745	-4.31926
H	3.404026	-1.98715	1.797848	H	-1.19739	0.433241	-3.46729
C	2.486902	-0.88081	3.397143	H	-2.91272	0.58444	-3.07041
H	1.512427	-0.45418	3.666854	C	-4.794	-3.39529	2.16766
H	3.220705	-0.06901	3.412317	H	-5.8012	-2.96682	2.194224
H	2.759793	-1.60494	4.17472	H	-4.22532	-2.96063	2.995703
C	1.396279	-2.70525	2.052287	H	-4.89057	-4.47135	2.365219
H	1.335628	-3.21172	1.084269	C	-2.22922	-3.94622	0.585769
H	0.396952	-2.32424	2.294632	H	-2.31873	-4.93864	1.045371
H	1.666701	-3.44807	2.813222	H	-1.528	-3.36221	1.189723
C	2.98681	0.987744	-2.16336	H	-1.78645	-4.08012	-0.40643
H	4.028784	0.646366	-2.14328	C	-4.96238	-4.10039	-0.79059
C	2.998892	2.525249	-2.0894	H	-4.96582	-5.16582	-0.52594
H	3.578782	2.94833	-2.91926	H	-4.53954	-4.01067	-1.79759
H	3.438922	2.872764	-1.15039	H	-6.00849	-3.77729	-0.83475
H	1.983798	2.934118	-2.14622	C	-6.69157	-0.81752	0.500026
C	2.362301	0.534643	-3.4936	H	-7.0568	-1.84881	0.439336
H	2.348639	-0.55698	-3.57769	H	-7.51319	-0.16585	0.175412
H	2.91994	0.939136	-4.34731	H	-6.48906	-0.59308	1.553411
H	1.326288	0.887946	-3.57637	C	-4.78728	1.353461	-0.51878
C	6.121985	-0.93028	2.217794	H	-3.8272	1.616375	-0.97326
H	5.346016	-1.07175	2.976962	H	-4.78227	1.726236	0.510505
H	6.938033	-0.36253	2.684439	H	-5.56459	1.906428	-1.06127
H	6.518362	-1.91665	1.957228	C	-5.68195	-0.9255	-2.37106
C	4.878742	1.708884	1.304054	H	-4.90829	-0.66977	-3.10191
H	4.740328	2.417022	0.481253	H	-6.58316	-0.35656	-2.63628
H	5.618474	2.139347	1.990662	H	-5.91872	-1.98754	-2.49282
H	3.930546	1.630543	1.844123	C	0.171811	3.684264	1.939897
C	6.981534	0.311431	-0.43267	H	-0.76042	3.917042	2.4834

H	7.466014	-0.61711	-0.755	C	0.988768	2.758679	2.849176
H	7.737609	0.898525	0.104536	H	0.43958	1.839169	3.097309
H	6.701336	0.875051	-1.32966	H	1.22859	3.25061	3.798447
C	5.727182	-3.40831	-0.34867	H	1.935068	2.477154	2.371839
H	5.350572	-3.71539	0.633431	C	0.928448	5.005666	1.71272
H	6.728556	-2.98614	-0.20962	H	1.897642	4.806908	1.239952
H	5.84279	-4.31479	-0.95705	H	1.105095	5.529298	2.660934
C	2.927437	-3.176	-1.55994	H	0.363322	5.67303	1.054596
H	3.105308	-3.91902	-2.34762	C	-1.04521	3.572069	-0.17847
H	2.117459	-2.52255	-1.89739	C	-2.05486	4.500514	0.196764
H	2.578621	-3.7137	-0.67209	H	-2.10553	4.857231	1.219924
C	5.314008	-1.79488	-2.89804	C	-2.98745	4.967801	-0.72447
H	5.569011	-2.72275	-3.4274	H	-3.73952	5.681415	-0.394
H	6.237663	-1.21679	-2.78987	C	-2.97715	4.539716	-2.05661
H	4.638117	-1.22557	-3.54393	H	-3.70834	4.914465	-2.76675
C	-2.49302	-0.80507	0.095803	C	-1.98656	3.642373	-2.45672
C	-2.78707	-0.23104	2.475745	H	-1.92872	3.318451	-3.49329
H	-3.79931	-0.61309	2.294948	C	-1.03343	3.184733	-1.54697
C	-2.15311	-1.07127	3.597714	H	-0.2057	2.580341	-1.91894
H	-2.06492	-2.12365	3.310302				

Table S8. Comparison of parameters between X-ray structure and optimized gas phase model for **4**

	X-ray structure	Optimized model
Average Ce–N _{guanidine} (Å)	2.4812(14)	2.5125
Ce–N _{amide} (Å)	2.3677(14)	2.3721
Average N _{guanidine} –Ce–N _{guanidine} (°)	53.95(4)	53.50

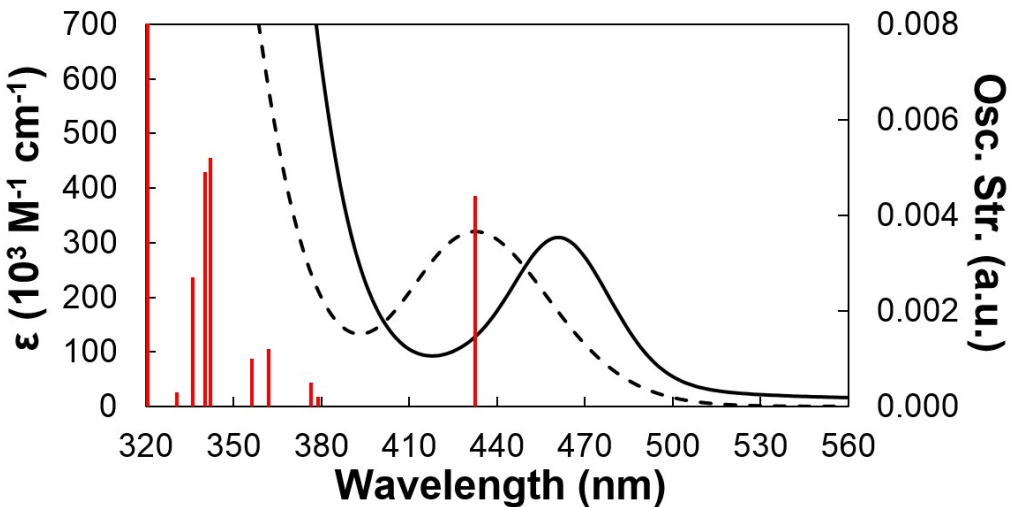


Figure S44. Experimental (black solid line) and TD-DFT predicted (black dashed line) absorption spectrum of **4**. The predicted spectra were rendered as Gaussian line shapes having a fwhm of 3000 cm^{-1} . Oscillator strengths for the electronic transitions are shown as red vertical lines.

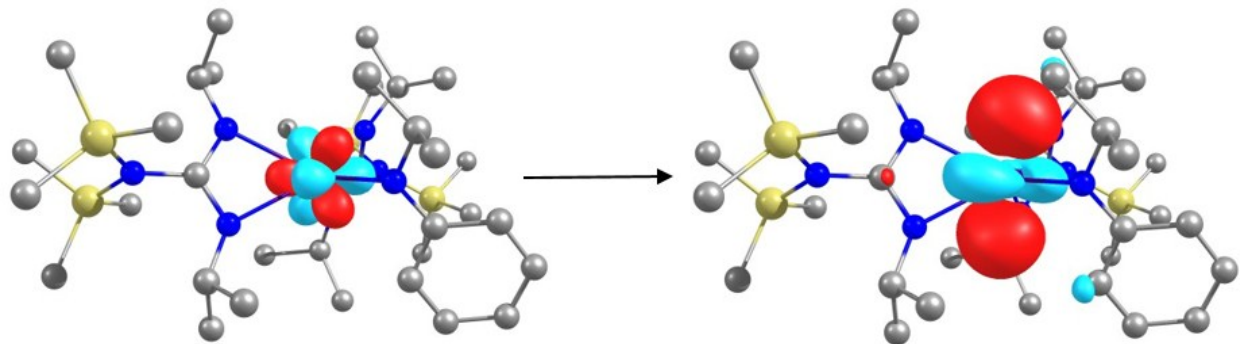


Figure S45. Calculated Natural Transition Orbitals (NTO) of λ_{abs}^1 of **4** in gas phase with contour value of 0.05. The calculated transition shown is centered at 433 nm (oscillator strength 0.0044).

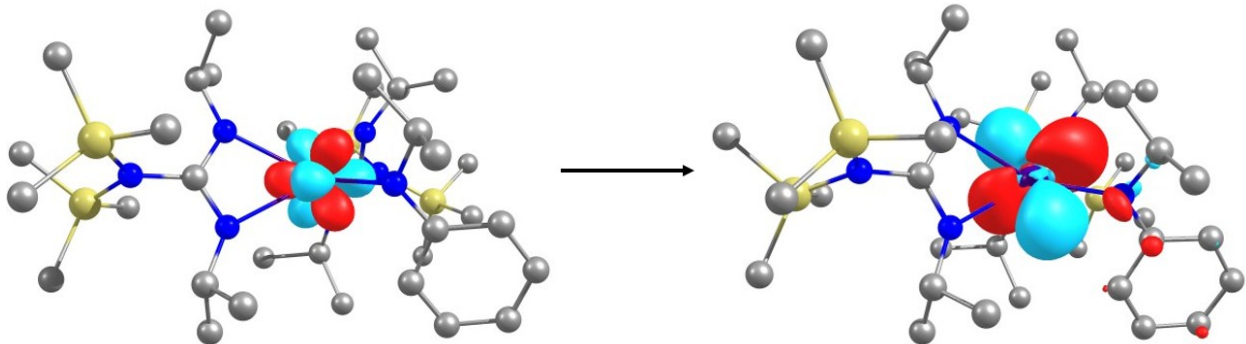


Figure S46. Calculated Natural Transition Orbitals (NTO) of λ_{abs}^2 of **4** in gas phase with contour value of 0.05. The calculated transition shown is centered at 340 nm (oscillator strength 0.0049).

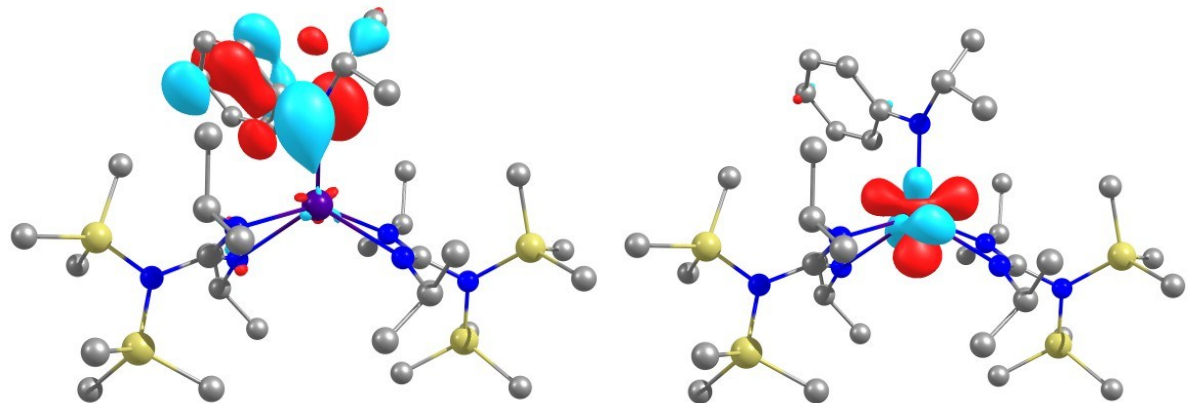


Figure S47. Calculated donor (left) and acceptor (right) orbitals for the LMCT transition of **4** at 342 nm (oscillator strength 0.0052).

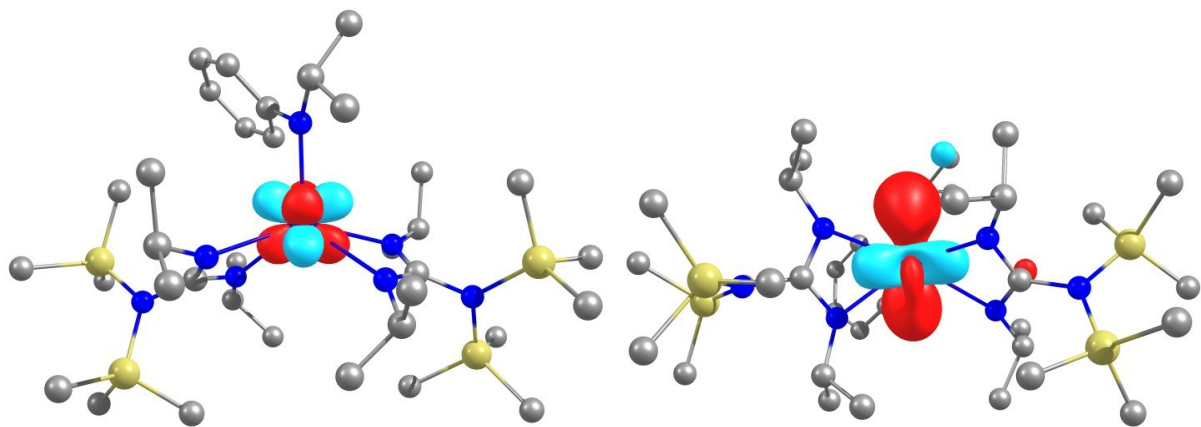


Figure S48. HOMO (left) and LUMO (right) of **4**.

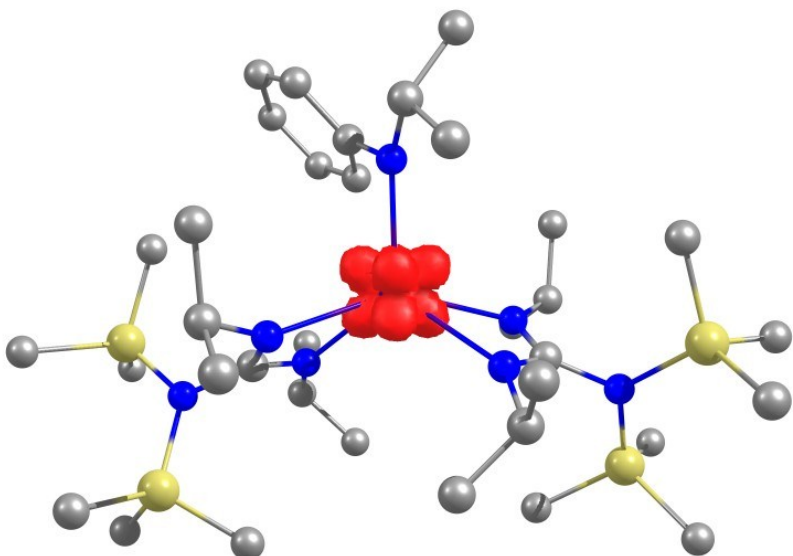


Figure S49. Spin density plot of **4**.

Table S9. Cartesian coordinates of optimized gas phase structure for **5**

Ce	-0.01059	0.463388	0.028218	H	3.317586	2.02547	-3.52493
Si	-5.36516	-0.37419	-0.49206	H	3.166114	2.242334	-1.76761
Si	-4.26225	-2.91785	0.974678	C	2.15834	-0.47723	-3.6923
Si	4.207851	-2.93608	-1.05683	H	1.115661	-0.16135	-3.82467
Si	5.327226	-0.42364	0.448787	H	2.165941	-1.56775	-3.59928
N	-1.91833	-0.81074	-0.91421	H	2.70672	-0.2058	-4.60281
N	-2.11292	-0.188	1.250825	C	2.24334	-1.6503	2.085148
N	-4.0195	-1.31437	0.221934	H	3.210335	-2.14157	1.923068
N	2.058645	-0.18864	-1.24484	C	2.365701	-0.73624	3.31706
N	1.885123	-0.87551	0.902143	H	1.400759	-0.26322	3.542249
N	3.973429	-1.34907	-0.26875	H	3.095871	0.062376	3.155547
N	0.002379	2.838268	0.033887	H	2.667723	-1.30957	4.202232
C	-2.68647	-0.77022	0.188232	C	1.191173	-2.74038	2.352326
C	-2.26758	-1.55492	-2.11975	H	0.213566	-2.28762	2.557816
H	-3.23913	-2.04349	-1.97953	H	1.468465	-3.35002	3.22136
C	-2.37174	-0.61024	-3.33002	H	1.078175	-3.40263	1.488632
H	-2.66533	-1.15985	-4.23287	C	2.543597	-3.81084	-1.23487
H	-1.40233	-0.13616	-3.53242	H	2.152636	-4.14235	-0.26742
H	-3.10174	0.186567	-3.1579	H	2.669804	-4.70226	-1.86231
C	-1.22008	-2.64544	-2.40248	H	1.784284	-3.17848	-1.70458
H	-1.12136	-3.32926	-1.55394	C	5.010062	-2.82275	-2.77062
H	-0.23739	-2.19512	-2.58674	H	5.145734	-3.83595	-3.17208
H	-1.49292	-3.23191	-3.28872	H	5.996705	-2.34925	-2.7396
C	-2.8413	0.166098	2.465983	H	4.395949	-2.26663	-3.48574
H	-3.88448	-0.16242	2.380032	C	5.332017	-4.02866	0.008446
C	-2.83924	1.690854	2.676939	H	4.932894	-4.15934	1.020676
H	-3.27046	2.214223	1.818877	H	6.353655	-3.64283	0.096434
H	-1.81803	2.068305	2.811542	H	5.402553	-5.02334	-0.45077
H	-3.41464	1.959805	3.571512	C	4.812142	1.372479	0.700185
C	-2.21809	-0.52723	3.689301	H	4.711268	1.901663	-0.25283
H	-2.76832	-0.27737	4.604809	H	5.586101	1.890585	1.280504

H	-1.17788	-0.20482	3.827191	H	3.868552	1.484973	1.243128
H	-2.21591	-1.61601	3.576504	C	6.814272	-0.45291	-0.7272
C	-4.84915	1.427326	-0.70334	H	6.559573	-0.06085	-1.71836
H	-5.61441	1.953908	-1.28768	H	7.243523	-1.45244	-0.85893
H	-3.89602	1.551409	-1.22679	H	7.606299	0.18474	-0.31336
H	-4.76636	1.939812	0.260513	C	5.928422	-1.12334	2.10611
C	-5.94865	-1.04124	-2.16913	H	5.164159	-1.07155	2.887711
H	-6.27144	-2.08622	-2.11484	H	6.789516	-0.53523	2.450836
H	-5.17882	-0.96965	-2.94371	H	6.255909	-2.16534	2.027697
H	-6.81012	-0.45047	-2.50828	C	-0.84183	3.604373	-0.77495
C	-6.86497	-0.42702	0.666677	C	-1.3765	4.850777	-0.37286
H	-7.65375	0.216407	0.255646	H	-1.07577	5.268037	0.58348
H	-6.62235	-0.0524	1.667511	C	-2.28267	5.535523	-1.17705
H	-7.29346	-1.42967	0.775517	H	-2.67478	6.491583	-0.83719
C	-2.6004	-3.7984	1.147493	C	-2.70314	5.00722	-2.40263
H	-2.73115	-4.69807	1.762098	H	-3.41235	5.546827	-3.02368
H	-1.8427	-3.17361	1.62988	C	-2.18585	3.779375	-2.81714
H	-2.20487	-4.11739	0.177667	H	-2.48331	3.35558	-3.77354
C	-5.38024	-3.98716	-0.12038	C	-1.26161	3.09691	-2.02518
H	-5.45533	-4.99	0.320048	H	-0.83219	2.167369	-2.39742
H	-4.97371	-4.10027	-1.13177	C	0.943185	3.459574	0.862485
H	-6.40087	-3.59875	-0.20884	C	1.736363	4.555663	0.446289
C	-5.07541	-2.83872	2.685424	H	1.561748	4.985207	-0.53577
H	-6.05613	-2.35267	2.660305	C	2.727993	5.075833	1.270979
H	-4.45952	-2.30853	3.41864	H	3.320105	5.918943	0.922161
H	-5.22581	-3.86008	3.05994	C	2.981529	4.521992	2.53244
C	2.641531	-0.80482	-0.20622	H	3.7596	4.933075	3.169231
C	2.775234	0.199987	-2.45671	C	2.208566	3.444458	2.962392
H	3.823886	-0.1142	-2.38211	H	2.3711	3.01307	3.947284
C	2.745816	1.728469	-2.6369	C	1.19533	2.931752	2.148275
H	1.717908	2.089716	-2.76739	H	0.551533	2.142787	2.53581

Table S10. Comparison of parameters between X-ray structure and optimized gas phase model

for 4

	X-ray structure	Optimized model
Average Ce–N _{guanidine} (Å)	2.4594(15)	2.4983
Ce–N _{amide} (Å)	2.3975(15)	2.3749
Average N _{guanidine} –Ce–N _{guanidine} (°)	54.33(5)	53.80

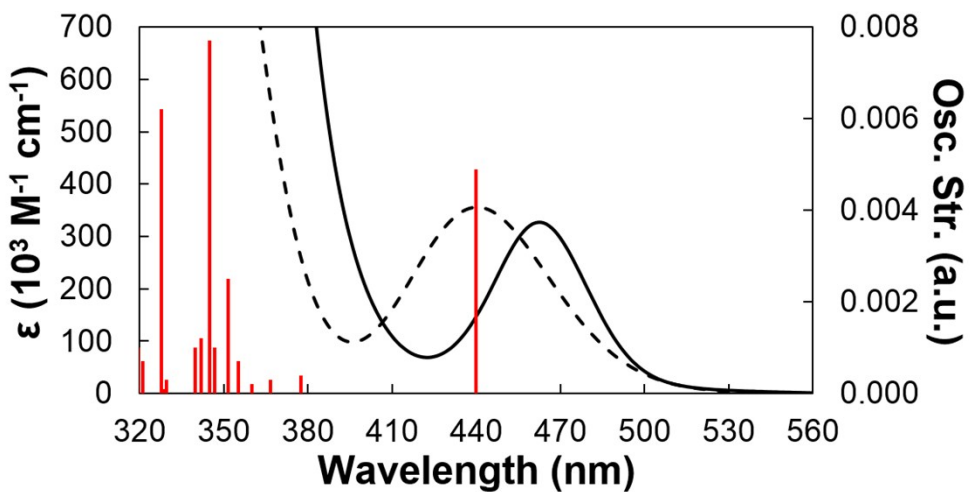


Figure S50. Experimental (black solid line) and TD-DFT predicted (black dashed line) absorption spectrum of **5**. The predicted spectra were rendered as Gaussian line shapes having a fwhm of 3000 cm^{-1} . Oscillator strengths for the electronic transitions are shown as red vertical lines.

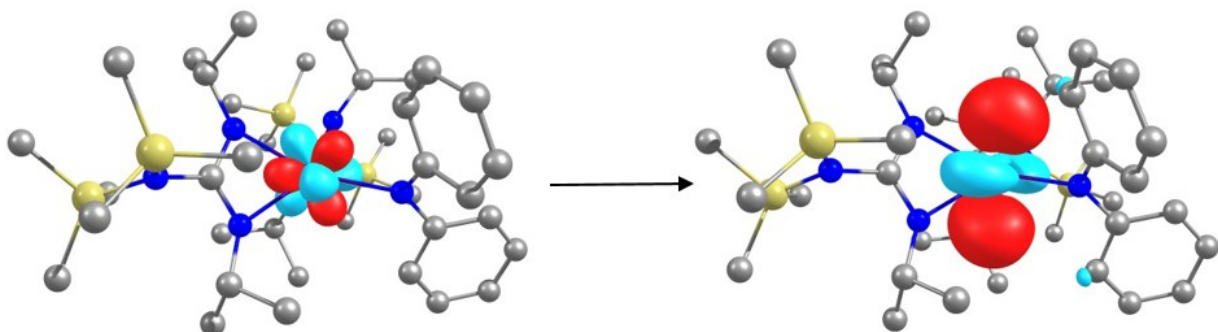


Figure S51. Calculated Natural Transition Orbitals (NTO) of $\lambda_{\text{abs}}^{-1}$ of **5** in gas phase with contour value of 0.05. The calculated transition shown is centered at 440 nm (oscillator strength 0.0049).

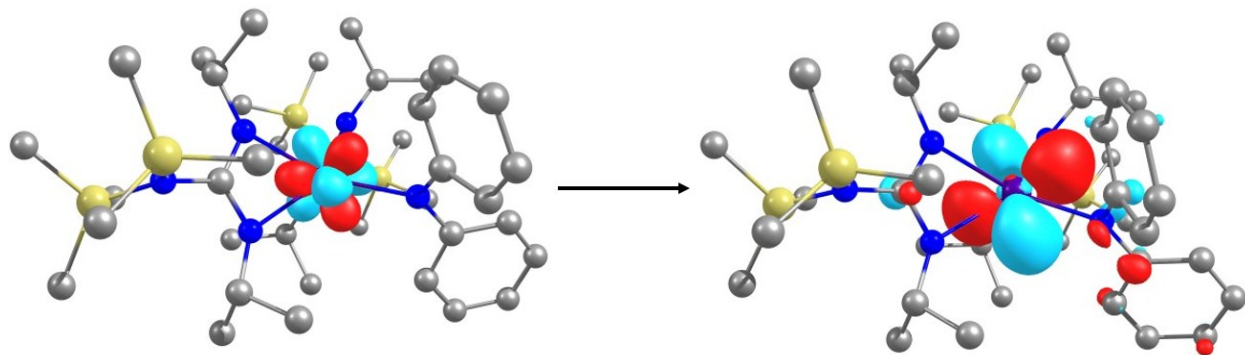


Figure S52. Calculated Natural Transition Orbitals (NTO) of λ_{abs}^2 of **5** in gas phase with contour value of 0.05. The calculated transition shown is centered at 342 nm (oscillator strength 0.0012).

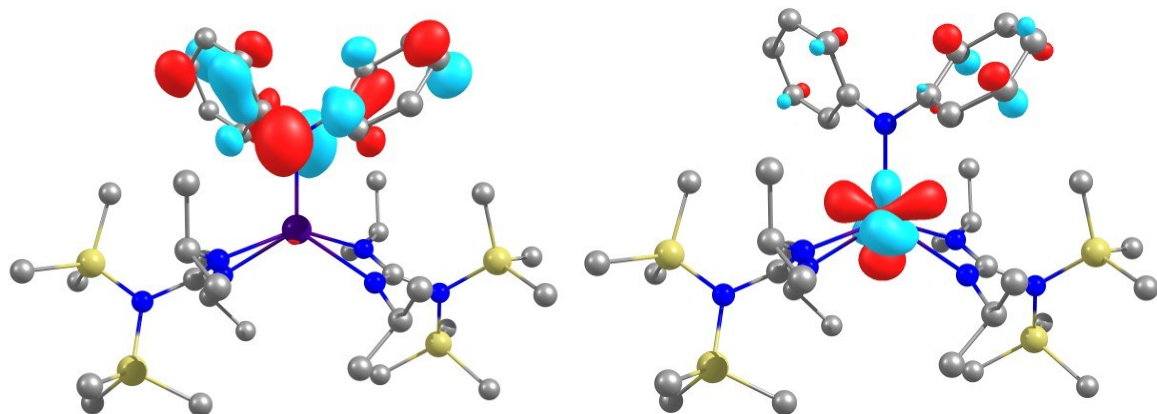


Figure S53. Calculated donor (left) and acceptor (right) orbitals for the LMCT transition of **5** at 345 nm (oscillator strength 0.0077).

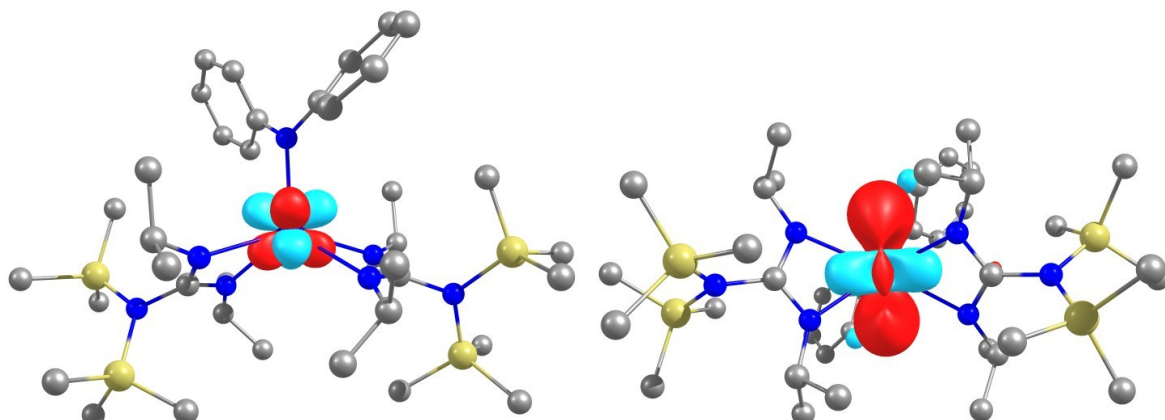


Figure S54. HOMO (left) and LUMO (right) of **5**.

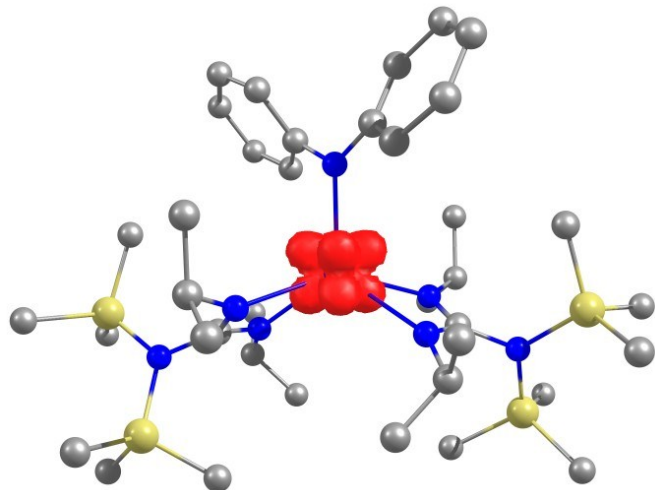


Figure S55. Spin density plot of **5**.

Table S11. HOMO and LUMO energies of complexes **1-5**.

	1	2	3	4	5
HOMO (eV)	-5.03	-4.86	-4.76	-4.52	-4.54
LUMO (eV)	-0.3	-0.12	-0.25	-0.26	-0.4

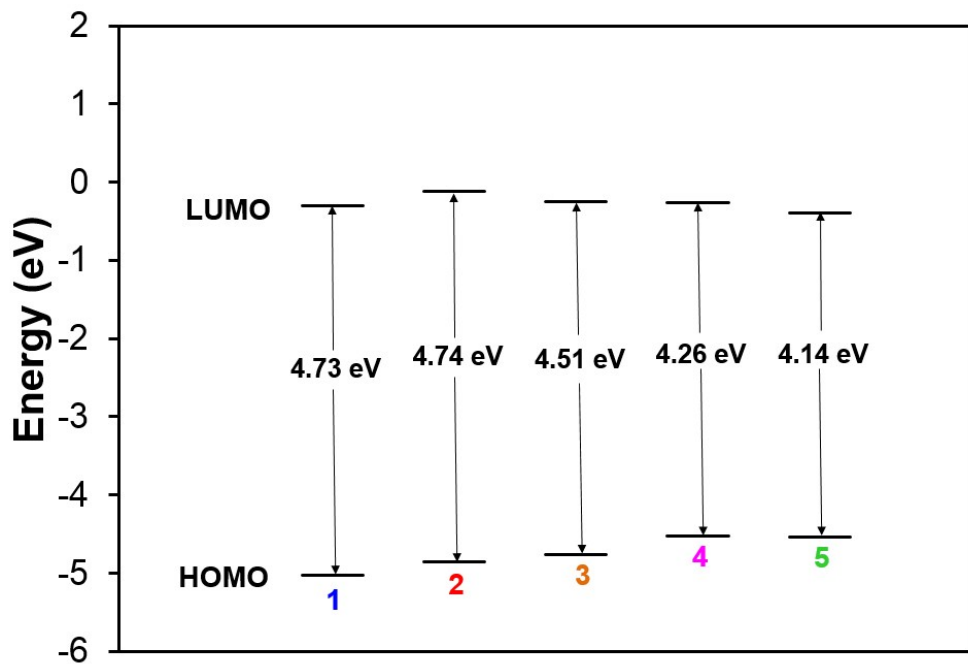


Figure S56. HOMO-LUMO energy gaps for complexes **1-5**.

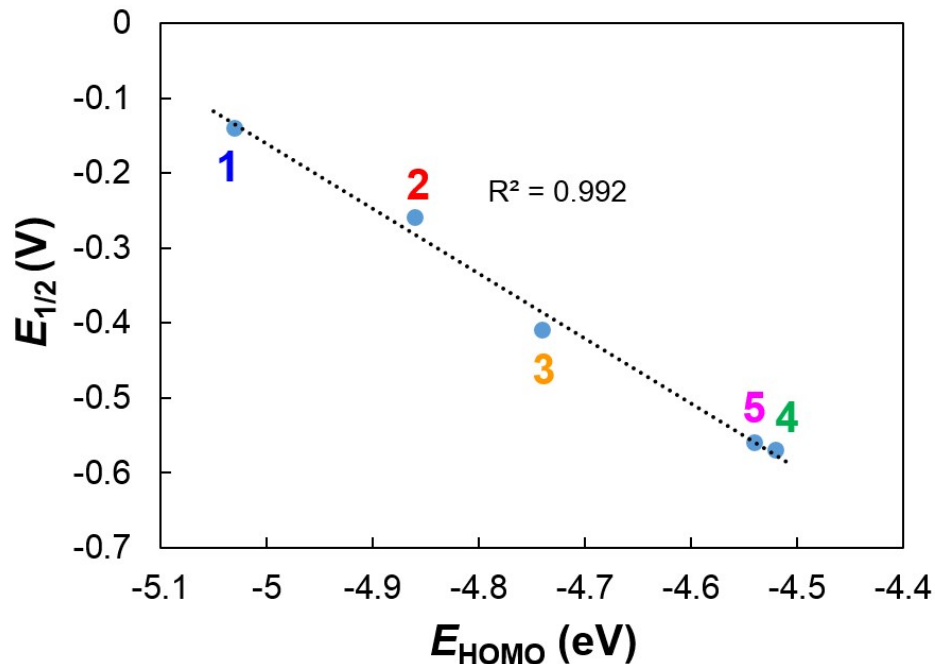


Figure S57. Correlation between the HOMO energies and reduction potentials for **1–5**

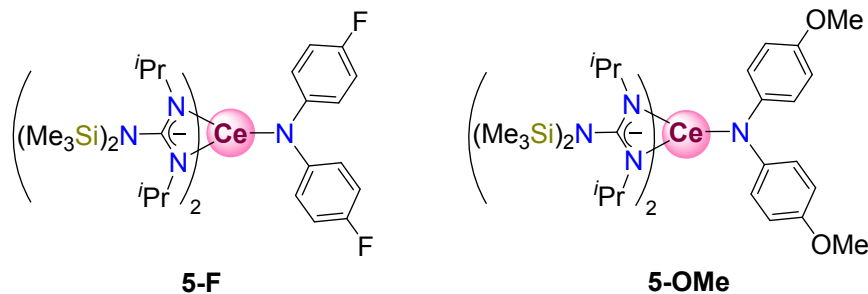


Figure S58. The putative complexes **5-F** and **5-OMe**.

Table S12. Cartesian coordinates of optimized structure in dichloromethane solvent field for **5-F**.

Sum of electronic and thermal Free Energies = –3706.91 Hartrees.

Ce	-0.00369	0.22759	0.032894	H	-3.08677	1.475342	3.917276
Si	5.373521	-0.56275	0.198981	H	-3.00364	1.874281	2.188166
Si	4.248272	-3.17124	-1.13049	C	-2.06836	-1.08166	3.764677
Si	-4.30098	-3.18804	1.021388	H	-1.00538	-0.83505	3.879834
Si	-5.37601	-0.50543	-0.19297	H	-2.14199	-2.15453	3.56107
N	1.969515	-1.07565	0.834938	H	-2.56685	-0.87908	4.721006
N	2.03692	-0.46251	-1.3357	C	-2.4169	-1.67888	-2.07468
N	4.01596	-1.55332	-0.40838	H	-3.41904	-2.10154	-1.93428

N	-2.04526	-0.5339	1.357309	C	-2.48366	-0.64823	-3.21515
N	-1.97433	-1.04359	-0.83912	H	-1.49052	-0.21981	-3.4033
N	-4.03671	-1.54525	0.369427	H	-3.16071	0.17649	-2.96974
N	-0.00968	2.700032	0.022816	H	-2.82975	-1.1137	-4.14639
C	2.674816	-1.03202	-0.30609	C	-1.47383	-2.82898	-2.47172
C	2.409826	-1.76817	2.03997	H	-0.46004	-2.45332	-2.65371
H	3.404129	-2.20074	1.875636	H	-1.82241	-3.31843	-3.38986
C	2.500769	-0.7855	3.220842	H	-1.41638	-3.58533	-1.68288
H	2.844496	-1.29403	4.130234	C	-2.65651	-4.1172	1.101259
H	1.516636	-0.34744	3.432817	H	-2.29638	-4.39694	0.106032
H	3.191162	0.036251	3.004393	H	-2.7993	-5.04234	1.673764
C	1.451284	-2.91859	2.39702	H	-1.87053	-3.53683	1.59504
H	1.379316	-3.64319	1.579967	C	-5.06763	-3.19845	2.756178
H	0.443824	-2.53585	2.598496	H	-5.18013	-4.2383	3.090953
H	1.796832	-3.44824	3.293745	H	-6.06116	-2.73894	2.775435
C	2.682601	-0.13624	-2.60204	H	-4.44548	-2.67983	3.49272
H	3.746719	-0.40257	-2.55744	C	-5.47473	-4.15272	-0.1113
C	2.5831	1.373294	-2.88734	H	-5.09495	-4.20868	-1.13797
H	3.020682	1.962719	-2.0757	H	-6.48336	-3.72549	-0.14746
H	1.534592	1.678922	-2.99632	H	-5.57176	-5.17962	0.26466
H	3.104291	1.628826	-3.81839	C	-4.79951	1.290688	-0.27722
C	2.042107	-0.9164	-3.76338	H	-4.63693	1.712399	0.720091
H	2.537759	-0.68109	-4.71367	H	-5.57693	1.89075	-0.76703
H	0.98153	-0.65321	-3.86218	H	-3.87581	1.414497	-0.85198
H	2.104625	-1.99731	-3.60352	C	-6.82752	-0.60488	1.020662
C	4.820705	1.235472	0.365389	H	-6.52658	-0.34157	2.040893
H	5.603152	1.80332	0.884569	H	-7.29678	-1.5947	1.049996
H	3.895616	1.344372	0.941064	H	-7.59932	0.10937	0.705381
H	4.667647	1.703082	-0.61288	C	-6.05348	-0.98877	-1.89766
C	6.049206	-1.13592	1.876261	H	-5.32004	-0.84429	-2.6974
H	6.363139	-2.18523	1.862556	H	-6.92114	-0.35587	-2.12725
H	5.322988	-1.01418	2.686236	H	-6.38774	-2.03122	-1.93345
H	6.930468	-0.53141	2.129436	C	0.975389	3.40791	0.728386

C	6.819835	-0.62679	-1.02307	C	1.688873	4.48581	0.144289
H	7.60413	0.058774	-0.67643	H	1.423578	4.806868	-0.85876
H	6.520089	-0.30953	-2.02821	C	2.72167	5.133348	0.816069
H	7.272785	-1.62148	-1.1018	H	3.264071	5.954159	0.356084
C	2.586997	-4.06572	-1.24981	C	3.072387	4.705029	2.09383
H	2.716629	-4.97399	-1.85185	C	2.402063	3.661282	2.714171
H	1.814381	-3.45576	-1.72864	H	2.679899	3.362477	3.720391
H	2.215164	-4.37207	-0.2668	C	1.351908	3.032038	2.038158
C	5.402129	-4.20907	-0.04326	H	0.792799	2.255925	2.553808
H	5.481506	-5.21822	-0.46825	C	-0.95761	3.456068	-0.68013
H	5.019408	-4.30751	0.979123	C	-1.54997	4.62135	-0.12759
H	6.41806	-3.8022	0.014249	H	-1.22134	4.963495	0.849317
C	5.01492	-3.12067	-2.86422	C	-2.54452	5.330294	-0.79555
H	6.014925	-2.67497	-2.8651	H	-2.99152	6.217994	-0.35761
H	4.399935	-2.56315	-3.57791	C	-2.98051	4.879372	-2.03813
H	5.112455	-4.14712	-3.24227	C	-2.43167	3.749177	-2.62613
C	-2.68635	-1.04271	0.298431	H	-2.77394	3.429535	-3.60583
C	-2.69303	-0.24812	2.632132	C	-1.41947	3.055907	-1.9561
H	-3.76059	-0.49744	2.573056	H	-0.96403	2.204312	-2.45363
C	-2.57253	1.247808	2.975195	F	4.08678	5.331178	2.748805
H	-1.51912	1.533297	3.091782	F	-3.95634	5.56708	-2.69115

Table S13. Cartesian coordinates of optimized structure in dichloromethane solvent field for **[5-F]⁺**. Sum of electronic and thermal Free Energies = -3706.75 Hartrees.

Ce	5.34E-05	0.139636	-6.2E-05	H	-3.15498	1.869479	3.65806
Si	5.340386	-0.52987	0.304193	H	-3.10207	2.111207	1.899845
Si	4.20154	-3.07004	-1.17325	C	-1.97829	-0.62547	3.737198
Si	-4.2012	-3.07023	1.173481	H	-0.93181	-0.30858	3.820375
Si	-5.34014	-0.53029	-0.30434	H	-1.99446	-1.71464	3.632126
N	1.886207	-1.04664	0.818118	H	-2.48512	-0.36436	4.673444
N	2.014097	-0.31285	-1.28843	C	-2.27667	-1.77064	-2.02964
N	3.964416	-1.46805	-0.38398	H	-3.24743	-2.24651	-1.85406
N	-2.01401	-0.31277	1.288445	C	-2.40986	-0.80375	-3.21777

N	-1.88605	-1.04665	-0.81806	H	-1.44607	-0.32873	-3.43782
N	-3.96416	-1.46833	0.384081	H	-3.13568	-0.01088	-3.01394
N	-0.00031	2.429096	0.00015	H	-2.73206	-1.34301	-4.11607
C	2.647978	-0.94849	-0.28986	C	-1.25235	-2.86933	-2.35251
C	2.276962	-1.77032	2.029842	H	-0.27108	-2.43089	-2.56655
H	3.247726	-2.24621	1.854287	H	-1.56752	-3.43726	-3.2354
C	2.410253	-0.80315	3.217733	H	-1.1395	-3.5673	-1.5175
H	2.732541	-1.3422	4.11612	C	-2.53882	-3.95662	1.290278
H	1.446473	-0.32811	3.437759	H	-2.16868	-4.26576	0.307382
H	3.136035	-0.01033	3.013632	H	-2.66941	-4.86389	1.893346
C	1.252706	-2.86895	2.35307	H	-1.76377	-3.35139	1.770509
H	1.139814	-3.56714	1.51825	C	-4.9379	-2.93277	2.910318
H	0.271445	-2.43048	2.567074	H	-5.08398	-3.94412	3.312042
H	1.567959	-3.43665	3.236083	H	-5.91251	-2.43448	2.912956
C	2.659926	0.068235	-2.54764	H	-4.28347	-2.39535	3.604008
H	3.70835	-0.24893	-2.51298	C	-5.36809	-4.12796	0.128003
C	2.627828	1.592859	-2.73757	H	-4.99812	-4.25386	-0.89572
H	3.101966	2.111261	-1.8996	H	-6.38667	-3.72866	0.07525
H	1.596592	1.955307	-2.81707	H	-5.43516	-5.12472	0.582822
H	3.155072	1.869647	-3.65783	C	-4.80022	1.259317	-0.56016
C	1.978506	-0.62537	-3.7372	H	-4.67919	1.783205	0.39357
H	2.485333	-0.36415	-4.67342	H	-5.58118	1.783178	-1.12545
H	0.932003	-0.30856	-3.82038	H	-3.86609	1.358818	-1.12242
H	1.994748	-1.71455	-3.63223	C	-6.78528	-0.54901	0.914082
C	4.800409	1.259735	0.559857	H	-6.4965	-0.15588	1.895298
H	5.581403	1.78373	1.124967	H	-7.2173	-1.545	1.059121
H	3.866357	1.359222	1.122265	H	-7.58204	0.094214	0.518715
H	4.679168	1.783508	-0.39391	C	-5.96362	-1.22511	-1.95074
C	5.964037	-1.22444	1.950647	H	-5.2128	-1.1717	-2.74535
H	6.293474	-2.26515	1.868536	H	-6.82832	-0.6315	-2.27575
H	5.213147	-1.17128	2.745196	H	-6.2927	-2.26593	-1.8686
H	6.828511	-0.63053	2.275716	C	0.978043	3.182418	0.699408
C	6.785398	-0.5487	-0.91437	C	1.692315	4.216463	0.053787

H	7.582217	0.094488	-0.51907	H	1.461898	4.452644	-0.98023
H	6.496562	-0.15557	-1.89556	C	2.683484	4.931631	0.717679
H	7.21737	-1.54471	-1.05944	H	3.23326	5.725666	0.222538
C	2.539235	-3.95655	-1.29003	C	2.976647	4.609354	2.041035
H	2.669976	-4.86384	-1.89304	C	2.295467	3.606384	2.715493
H	1.764173	-3.35143	-1.77038	H	2.531007	3.395186	3.75346
H	2.169009	-4.26568	-0.30716	C	1.289835	2.905122	2.044333
C	5.368546	-4.12758	-0.12772	H	0.720935	2.158121	2.588925
H	5.435692	-5.12439	-0.58242	C	-0.97879	3.182077	-0.69939
H	4.998629	-4.25338	0.896031	C	-1.69367	4.215693	-0.05376
H	6.387087	-3.72818	-0.07505	H	-1.46363	4.451748	0.980368
C	4.93812	-2.93264	-2.91014	C	-2.68492	4.9306	-0.7178
H	5.912645	-2.4342	-2.91296	H	-3.23518	5.724325	-0.2227
H	4.28353	-2.39542	-3.60384	C	-2.97755	4.60844	-2.04132
H	5.084312	-3.94402	-3.31175	C	-2.29579	3.605868	-2.71576
C	-2.64781	-0.94853	0.289935	H	-2.53096	3.394769	-3.75383
C	-2.6598	0.068187	2.547714	C	-1.29006	2.904886	-2.04443
H	-3.7082	-0.24904	2.513086	H	-0.72074	2.158175	-2.58897
C	-2.62779	1.592804	2.737739	F	3.943292	5.302104	2.6868
H	-1.59658	1.955333	2.817129	F	-3.94427	5.300952	-2.68723

Table S14. Cartesian coordinates of optimized structure in dichloromethane solvent field for **5-OMe**. Sum of electronic and thermal Free Energies = -3737.42 Hartrees.

Ce	-0.01422	-0.00034	0.019837	H	1.956737	-2.17867	-3.6897
Si	-5.40193	-0.72155	0.005868	H	2.342337	-0.86131	-4.8164
Si	-4.28053	-3.40394	1.174222	C	2.481394	-2.00975	1.919089
Si	4.220406	-3.35904	-1.31787	H	3.467977	-2.44146	1.710897
Si	5.370397	-0.7476	-0.01839	C	2.621416	-1.03713	3.103708
N	-2.02352	-1.26054	-0.76732	H	1.647188	-0.59954	3.3577
N	-2.02096	-0.73846	1.428706	H	3.303856	-0.2143	2.867331
N	-4.04178	-1.76188	0.513441	H	3.00002	-1.55397	3.994434
N	1.988365	-0.6502	-1.42043	C	1.536878	-3.16215	2.306912
N	1.991209	-1.30907	0.738452	H	0.540379	-2.77933	2.5574

N	4.000901	-1.74871	-0.57731	H	1.920476	-3.70133	3.182216
N	-0.0338	2.452618	0.031784	H	1.42596	-3.87827	1.486727
C	-2.69525	-1.2549	0.395366	C	2.566415	-4.27388	-1.36816
C	-2.51101	-1.89742	-1.98485	H	2.249891	-4.60371	-0.37347
H	-3.50296	-2.32906	-1.80489	H	2.675325	-5.16857	-1.99416
C	-2.63347	-0.86693	-3.12112	H	1.762857	-3.66488	-1.79453
H	-3.01004	-1.33564	-4.03886	C	4.906011	-3.29281	-3.08479
H	-1.65306	-0.42747	-3.34666	H	5.023477	-4.31812	-3.46032
H	-3.30983	-0.05013	-2.84892	H	5.887978	-2.81113	-3.13451
C	-1.57372	-3.03828	-2.42133	H	4.238906	-2.76382	-3.77301
H	-1.47374	-3.79302	-1.63519	C	5.436881	-4.38489	-0.28913
H	-0.57266	-2.65188	-2.64691	H	5.107695	-4.48228	0.751788
H	-1.95558	-3.53239	-3.32366	H	6.450668	-3.96851	-0.28493
C	-2.6156	-0.47628	2.733307	H	5.503603	-5.39479	-0.7144
H	-3.67746	-0.75442	2.724269	C	4.804026	1.041522	0.194255
C	-2.51994	1.019998	3.082424	H	4.604281	1.520102	-0.77009
H	-3.00396	1.639613	2.321199	H	5.601417	1.611647	0.687644
H	-1.47085	1.334346	3.152569	H	3.903268	1.132278	0.810164
H	-2.99664	1.226539	4.048826	C	6.763295	-0.77829	-1.30202
C	-1.91309	-1.30011	3.82688	H	6.418201	-0.43935	-2.28537
H	-2.36618	-1.11715	4.809411	H	7.214655	-1.76929	-1.42409
H	-0.85217	-1.02662	3.88792	H	7.560361	-0.09793	-0.97501
H	-1.96909	-2.37329	3.618566	C	6.122396	-1.32984	1.623144
C	-4.82729	1.072662	-0.12166	H	5.425791	-1.23112	2.461901
H	-5.62422	1.66766	-0.58572	H	7.001312	-0.71146	1.849489
H	-3.92841	1.189231	-0.73578	H	6.455069	-2.37268	1.584767
H	-4.62338	1.506127	0.862856	C	-0.98603	3.239502	-0.63619
C	-6.15607	-1.21543	-1.66341	C	-1.52107	4.423491	-0.07871
H	-6.49856	-2.25559	-1.67726	H	-1.14907	4.763702	0.883749
H	-5.45664	-1.08161	-2.49499	C	-2.51365	5.170571	-0.71605
H	-7.02855	-0.57824	-1.8606	H	-2.88255	6.070478	-0.23511
C	-6.79604	-0.80777	1.286033	C	-3.02847	4.750098	-1.94902
H	-7.58833	-0.10627	0.994025	C	-2.51675	3.582419	-2.5273

H	-6.4498	-0.52233	2.285867	H	-2.90088	3.266427	-3.49362
H	-7.25391	-1.80082	1.3566	C	-1.51141	2.855082	-1.89415
C	-2.64152	-4.34635	1.159026	H	-1.1095	1.983653	-2.4047
H	-2.7539	-5.26362	1.75068	C	0.981864	3.137763	0.726555
H	-1.8205	-3.76724	1.593562	C	1.729346	4.182448	0.137628
H	-2.34973	-4.64015	0.145623	H	1.472649	4.50617	-0.86747
C	-5.52167	-4.35732	0.105644	C	2.786337	4.808893	0.798969
H	-5.5973	-5.38713	0.478465	H	3.324552	5.604566	0.294892
H	-5.20297	-4.40497	-0.94194	C	3.150583	4.398287	2.089423
H	-6.53022	-3.9293	0.132923	C	2.424789	3.369464	2.700073
C	-4.94926	-3.42041	2.94928	H	2.693421	3.067162	3.708678
H	-5.92043	-2.92188	3.034033	C	1.355549	2.766596	2.038776
H	-4.26606	-2.94443	3.660164	H	0.778368	2.008438	2.562802
H	-5.08541	-4.4625	3.267945	O	4.17669	4.938092	2.825916
C	2.660077	-1.23738	-0.42292	O	-4.00645	5.404412	-2.66067
C	2.581125	-0.32019	-2.71099	C	4.934712	5.987104	2.240436
H	3.646041	-0.58712	-2.71287	H	5.686355	6.266424	2.981275
C	2.470216	1.18989	-2.98907	H	5.437635	5.658747	1.321433
H	1.418304	1.496591	-3.052	H	4.309467	6.860453	2.012939
H	2.951159	1.446106	-3.94138	C	-4.53306	6.603205	-2.11197
H	2.943208	1.777793	-2.19643	H	-5.27726	6.962005	-2.82574
C	1.889496	-1.09736	-3.84512	H	-5.01816	6.426838	-1.14275
H	0.825962	-0.83217	-3.89513	H	-3.75436	7.367321	-1.98669

Table S15. Cartesian coordinates of optimized structure in dichloromethane solvent field for **[5-OMe]⁺**. Sum of electronic and thermal Free Energies = -3737.25 Hartrees.

Ce	0.000133	-0.05394	0.000161	H	1.833374	-1.95478	-3.68646
Si	-5.35122	-0.73439	-0.07696	H	2.282368	-0.61826	-4.76451
Si	-4.15253	-3.2892	1.318868	C	2.368642	-1.96355	1.950833
Si	4.152803	-3.28916	-1.3186	H	3.333807	-2.4366	1.738869
Si	5.351484	-0.73407	0.07666	C	2.549019	-0.98695	3.124593
N	-1.92206	-1.25139	-0.75203	H	1.593858	-0.51423	3.383665
N	-1.96341	-0.52938	1.362941	H	3.260845	-0.19242	2.881228

N	-3.94777	-1.68267	0.533607	H	2.913874	-1.51708	4.012052
N	1.963462	-0.52961	-1.36278	C	1.364943	-3.06484	2.326054
N	1.922499	-1.25117	0.752345	H	0.38723	-2.63044	2.563116
N	3.948023	-1.68256	-0.53349	H	1.713036	-3.61493	3.207956
N	-0.00018	2.216185	0.000075	H	1.231237	-3.77832	1.507383
C	-2.63534	-1.16048	0.386977	C	2.494026	-4.19123	-1.3402
C	-2.36805	-1.96393	-1.95049	H	2.189689	-4.51735	-0.34032
H	-3.3333	-2.43686	-1.73862	H	2.594313	-5.08886	-1.96319
C	-2.54812	-0.98749	-3.12443	H	1.684662	-3.58717	-1.76198
H	-2.91293	-1.5177	-4.01186	C	4.791155	-3.16778	-3.09585
H	-1.59286	-0.51496	-3.38343	H	4.941151	-4.18307	-3.48614
H	-3.25985	-0.19281	-2.88129	H	5.750844	-2.64554	-3.16293
C	-1.36444	-3.06542	-2.32538	H	4.085676	-2.66133	-3.76235
H	-1.23108	-3.77888	-1.50664	C	5.38452	-4.32687	-0.32821
H	-0.38659	-2.63121	-2.56222	H	5.071382	-4.44522	0.715189
H	-1.71241	-3.6155	-3.20734	H	6.400333	-3.91702	-0.33403
C	-2.55386	-0.16275	2.652411	H	5.437182	-5.32766	-0.77597
H	-3.60282	-0.48045	2.662922	C	4.824698	1.059298	0.33539
C	-2.51387	1.359869	2.858159	H	4.669218	1.574903	-0.61788
H	-3.02054	1.887857	2.0456	H	5.6271	1.586492	0.866647
H	-1.47999	1.721147	2.899629	H	3.912335	1.165775	0.93133
H	-3.00303	1.62681	3.802156	C	6.737426	-0.76711	-1.20859
C	-1.81823	-0.86653	3.803343	H	6.401952	-0.37632	-2.17582
H	-2.28296	-0.61793	4.76462	H	7.155916	-1.76607	-1.3716
H	-0.77028	-0.5459	3.842143	H	7.556441	-0.12684	-0.85638
H	-1.83403	-1.95454	3.686664	C	6.05046	-1.40493	1.702988
C	-4.82466	1.05905	-0.33548	H	5.34217	-1.32085	2.533406
H	-5.62699	1.586114	-0.86697	H	6.940421	-0.81985	1.970171
H	-3.91212	1.165751	-0.93111	H	6.357031	-2.4531	1.627389
H	-4.6696	1.574632	0.617872	C	-1.0036	2.967396	-0.6692
C	-6.04963	-1.40538	-1.70348	C	-1.70215	3.997981	-0.01052
H	-6.35589	-2.45365	-1.62801	H	-1.44315	4.237542	1.016497
H	-5.34118	-1.32102	-2.53373	C	-2.71506	4.716915	-0.64206

H	-6.93971	-0.82056	-1.97084	H	-3.22317	5.502805	-0.09486
C	-6.73755	-0.76769	1.20786	C	-3.06923	4.413962	-1.96621
H	-7.55646	-0.12735	0.855525	C	-2.38145	3.395692	-2.64012
H	-6.4024	-0.37714	2.175295	H	-2.64303	3.182141	-3.67214
H	-7.15609	-1.7667	1.370474	C	-1.35977	2.694143	-2.00609
C	-2.49346	-4.19069	1.341856	H	-0.8104	1.946627	-2.5713
H	-2.59423	-5.0888	1.964074	C	1.003116	2.967794	0.669114
H	-1.68487	-3.58662	1.765111	C	1.701554	3.998248	0.010098
H	-2.18771	-4.51598	0.342149	H	1.442597	4.237369	-1.01703
C	-5.38325	-4.32747	0.327808	C	2.714271	4.717584	0.641465
H	-5.436	-5.3282	0.775699	H	3.222291	5.503357	0.094017
H	-5.06935	-4.44592	-0.71536	C	3.06837	4.415204	1.965782
H	-6.39916	-3.91785	0.332825	C	2.380759	3.397019	2.639974
C	-4.79215	-3.16767	3.095649	H	2.642281	3.183887	3.672099
H	-5.75245	-2.64645	3.161855	C	1.35927	2.695026	2.006101
H	-4.08765	-2.66012	3.762353	H	0.810004	1.94757	2.571498
H	-4.94129	-4.18293	3.48633	O	4.043592	5.052614	2.675256
C	2.635589	-1.16045	-0.38678	O	-4.04471	5.050856	-2.67582
C	2.55372	-0.16309	-2.65237	C	4.758469	6.10908	2.040944
H	3.602633	-0.48096	-2.66309	H	5.472181	6.473216	2.781401
C	2.513918	1.35953	-2.85815	H	5.301499	5.751514	1.157527
H	1.480081	1.720982	-2.89926	H	4.088438	6.926849	1.748432
H	3.002778	1.626385	-3.80232	C	-4.75975	6.107421	-2.04185
H	3.020967	1.887448	-2.04579	H	-5.47371	6.471016	-2.78234
C	1.817762	-0.86677	-3.80315	H	-5.30251	5.750114	-1.15816
H	0.769869	-0.54595	-3.84178	H	-4.08988	6.925506	-1.74985

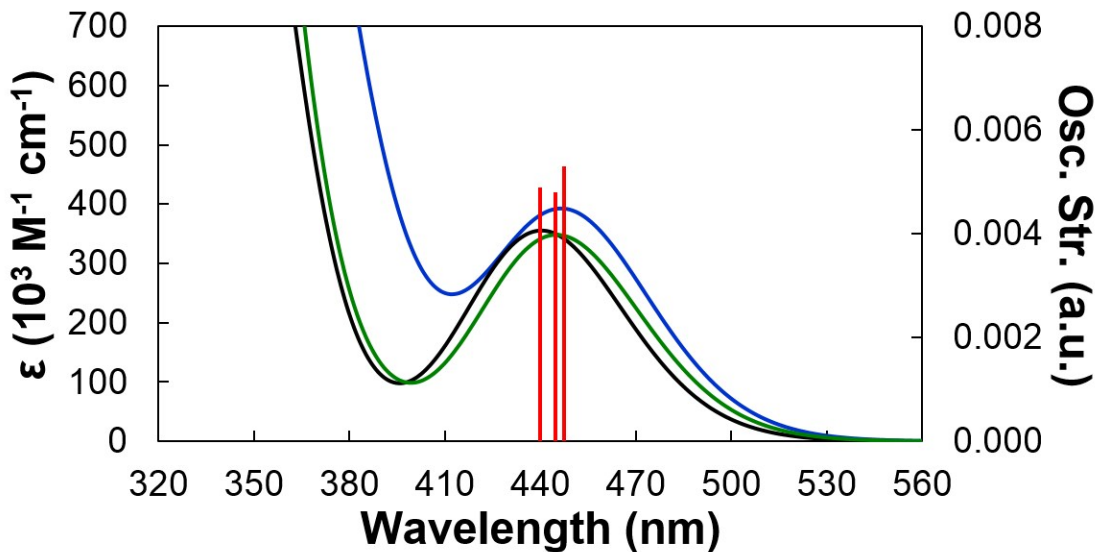


Figure S59. TD-DFT predicted absorption spectra of **5** (black), **5-F** (green), and **5-OMe** (blue). The predicted spectra were rendered as Gaussian line shapes having a fwhm of 3000 cm^{-1} . Oscillator strengths for the $4f \rightarrow 5d_z^2$ transitions of all complexes are shown as red vertical lines. Energies of the $4f \rightarrow 5d_z^2$ transitions are 440 nm, 445 nm, and 448 nm for **5**, **5-F**, and **5-OMe**, respectively.

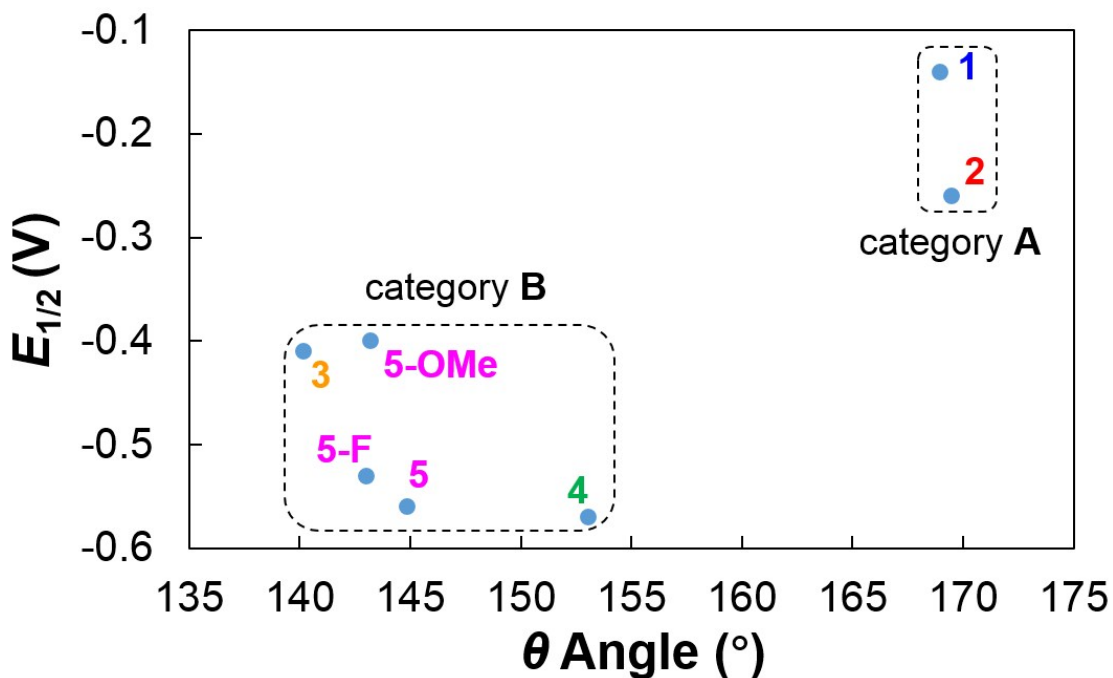


Figure S60. A plot of the calculated cone angles (θ), the experimental reduction potentials ($E_{1/2}$) for complexes **1–5**, and predicted $E_{1/2}$ for complexes **5-F** and **5-OMe**. The dashed box is used to

indicate two categories of compounds.

10. Determination of the Cone Angle and Cone Angle-Property Correlations.

The cone angle (θ) of the amide group was computed by a Mathematica package FindConeAngle.^{19,20} Hydrogens are not considered. The results are shown in Table S13.

Table S16. Summary of the cone angles for 1–5.

	1	2	3	4	5
θ angle/ °	173.87	173.56	147.41	155.78	146.68

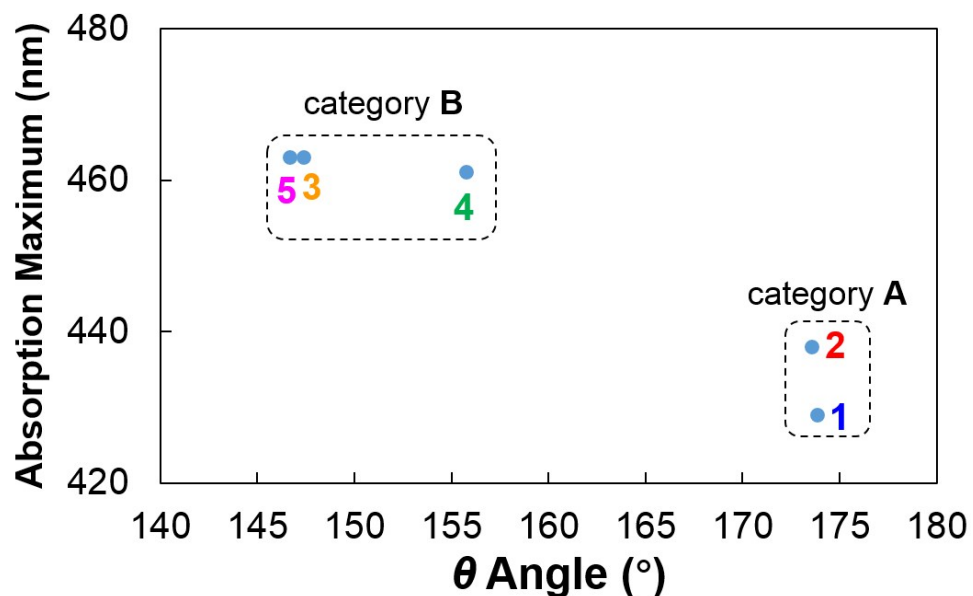


Figure S61. A plot of the cone angles (θ) and the absorption maxima ($\lambda_{\text{abs}}^{-1}$) for complexes 1–5.

The dashed box is used to indicate two categories of compounds.

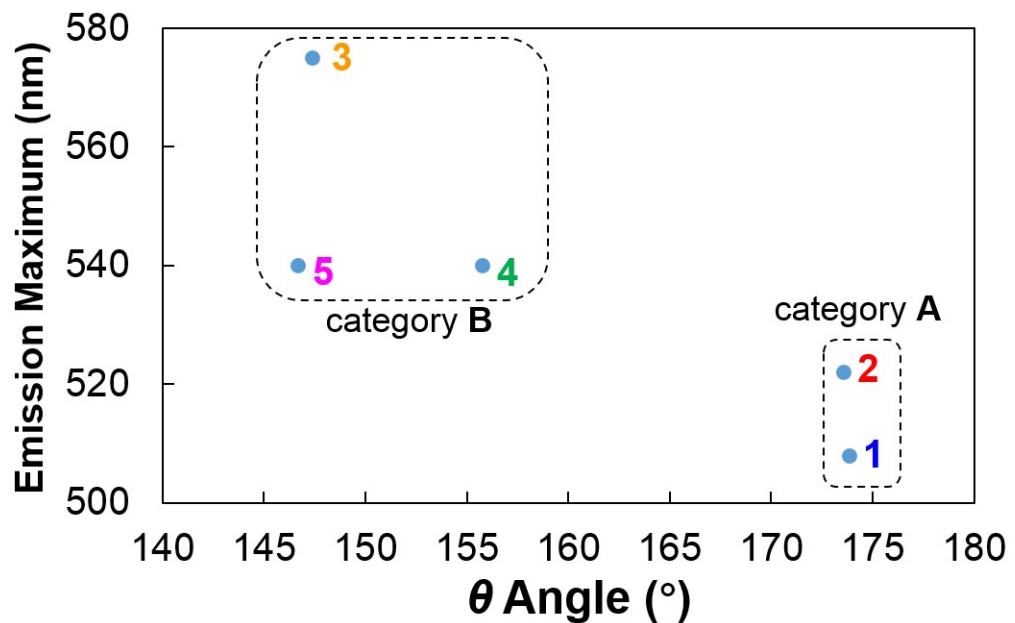


Figure S62. A plot of the cone angles (θ) and the emission maxima for complexes 1–5. The dashed box is used to indicate two categories of compounds.

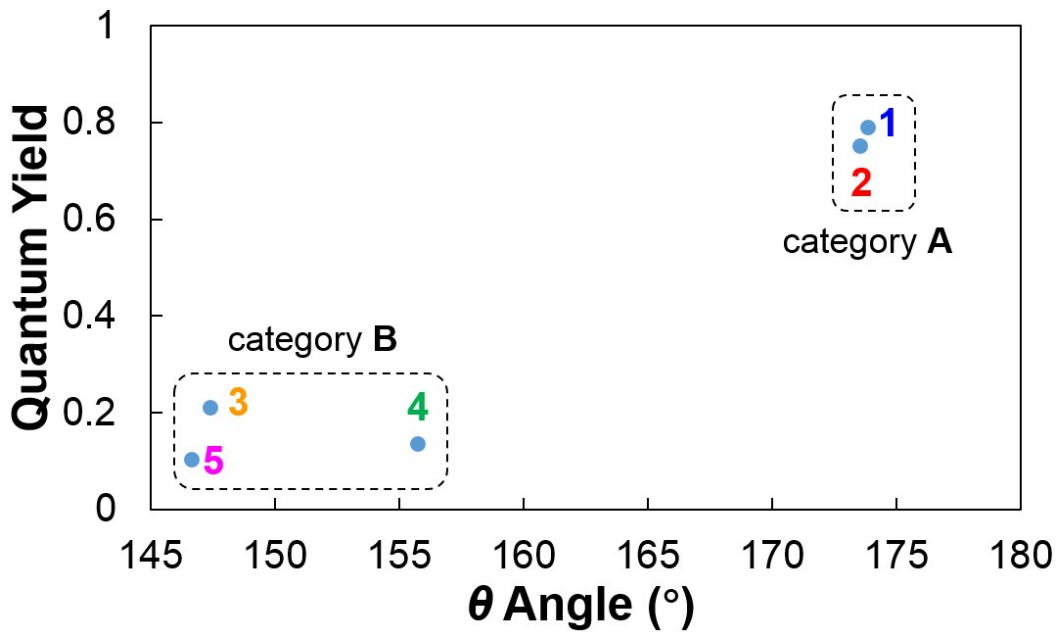


Figure S63. A plot of the cone angles (θ) and the quantum yields for complexes 1–5. The dashed box is used to indicate two categories of compounds.

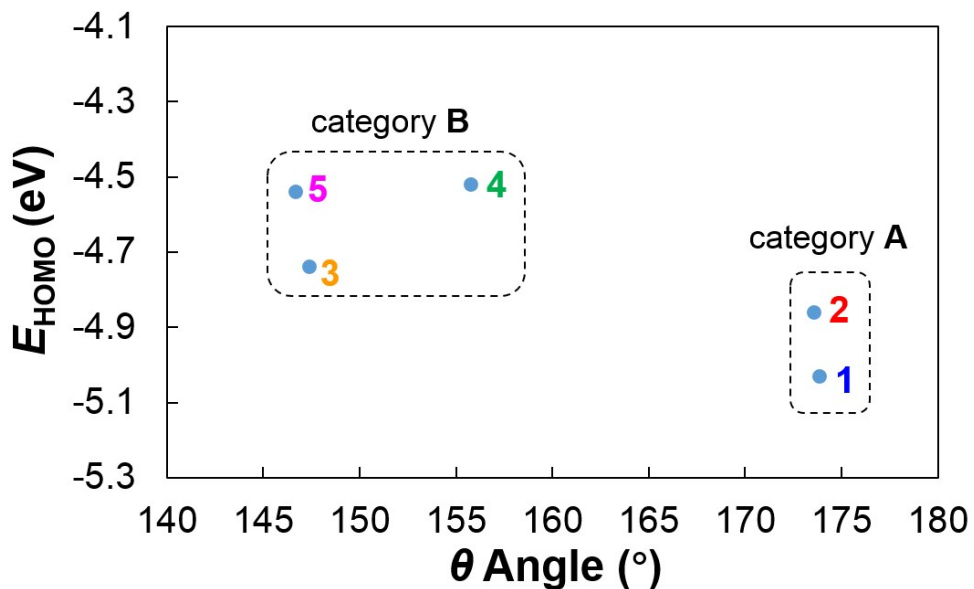


Figure S64. A plot of the cone angles (θ) and the HOMO energies for complexes 1–5. The dashed box is used to indicate two categories of compounds.

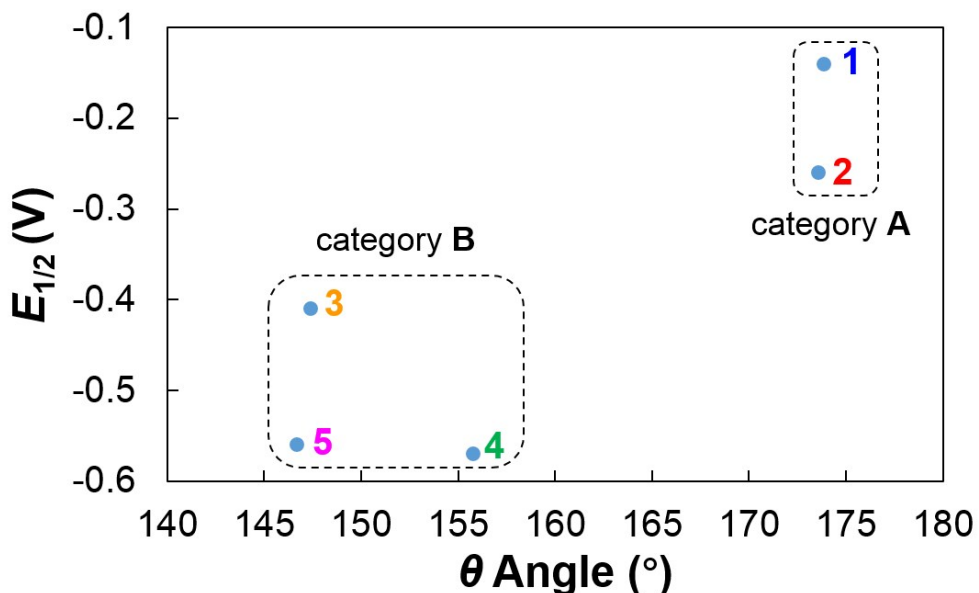


Figure S65. A plot of the cone angles (θ) and the reduction potentials ($E_{1/2}$) for complexes 1–5. The dashed box is used to indicate two categories of compounds.

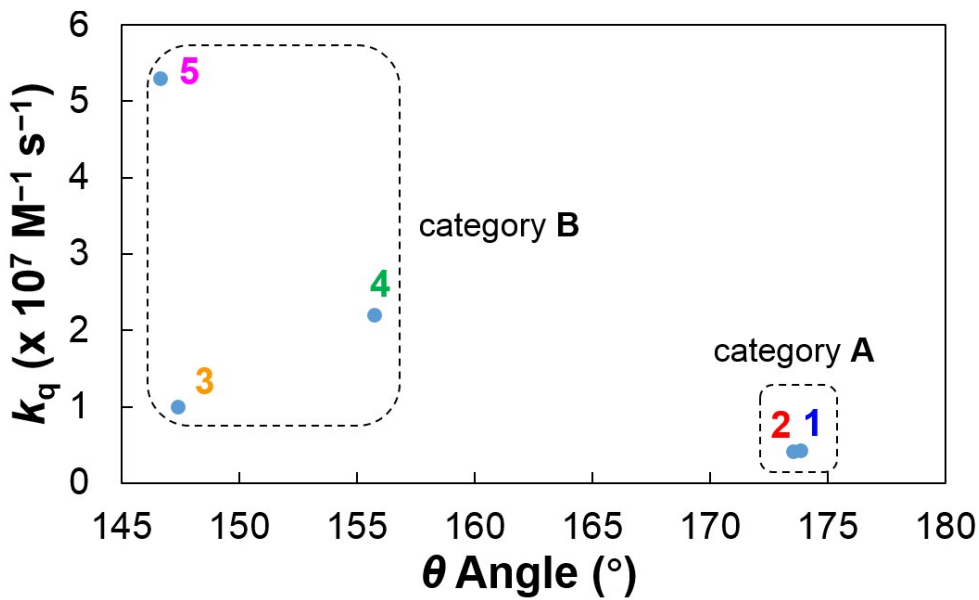


Figure S66. A plot of the cone angles (θ) and the quenching rates (k_q) for complexes **1–5**. The dashed box is used to indicate two categories of compounds.

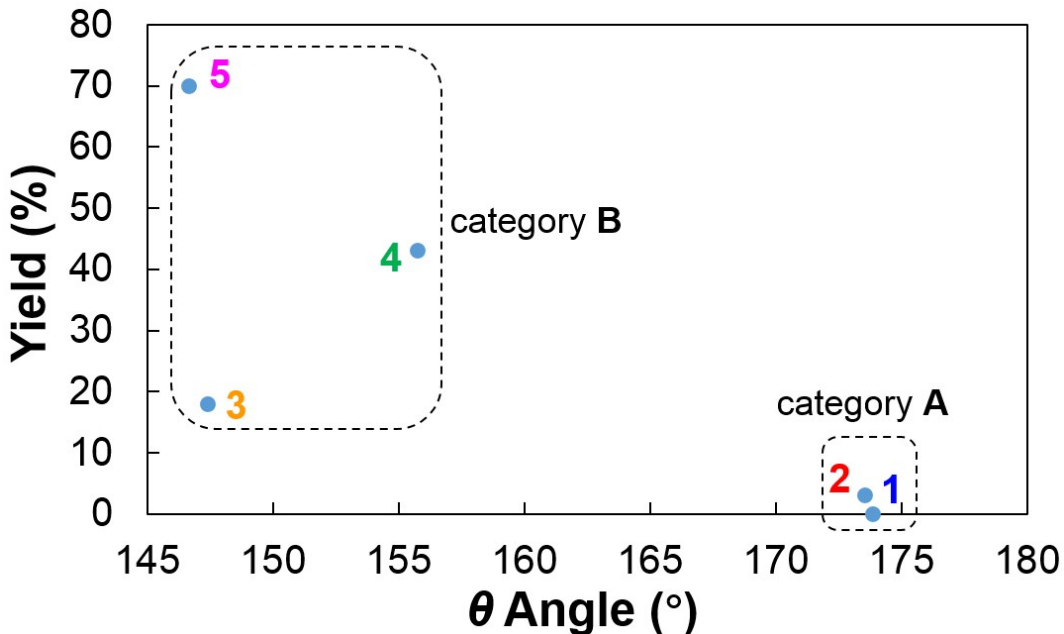
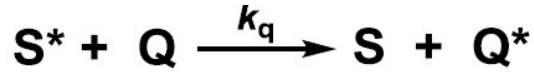


Figure S67. A plot of the cone angles (θ) and the product yields of phenylation of 4-bromofluorobenzene for complexes **1–5**. The dashed box is used to indicate two categories of compounds.

11. Stern-Volmer experiments.

The quenching of excited-state photosensitizer (S^*) with externally added quencher (Q) follows Stern-Volmer relationship:



$$\frac{I^0}{I} - 1 = k_q \tau^0 [Q] = K_{SV}[Q]$$

where I^0 is the intensity at emission maximum in the absence of quencher; I is the intensity at the emission maximum in the presence of quencher at a concentration of $[Q]$; τ^0 is the lifetime of the photosensitizer in the absence of quencher; k_q is the rate constant for the quenching process by the quencher; K_{SV} ($= k_q \tau_0$) is directly obtained from Stern-Volmer plots as the slope.

The ratio of excited-state photosensitizer involved in energy transfer process with the quencher (Φ_q) is given by:

$$\Phi_q = \frac{k_q[Q]}{k_d + k_q[Q]} = \frac{1}{1 + \frac{k_d}{k_q}[Q]}$$

k_d is the decay rate (including radiative and non-radiative decay rates) and $k_d = 1/\tau_0$. Therefore, larger k_q/k_d ratio implies larger Φ_q .

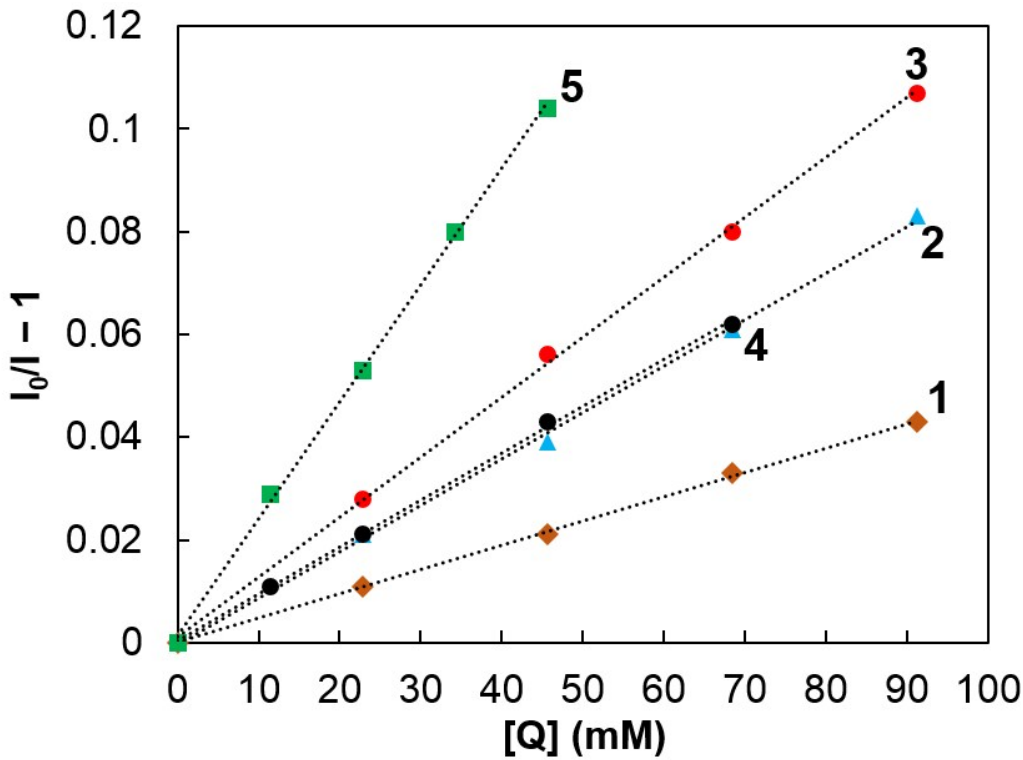
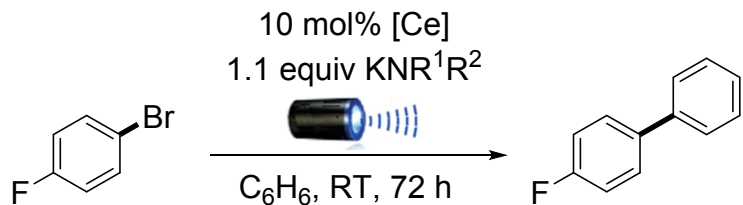


Figure S68. Overlay of Stern-Volmer plots for **1–5** in toluene solution using 1-bromo-4-fluorobenzene as the quencher.

Table S17. Summary of quenching rates. Standard deviations are given in parentheses.

compound	K_{SV} (M^{-1})	$k_q \times 10^7 M^{-1}s^{-1}$
1	0.5(1)	0.43(1)
2	0.9(1)	0.41(1)
3	1.5(1)	1.0(1)
4	0.9(1)	2.2(1)
5	2.3(1)	5.3(1)

12. Procedure for Ce-catalyzed phenylation reaction.



To an 8 mL vial containing a stir bar, cerium(III) catalyst (**1–5**, 0.020 mmol, 0.10 equiv), potassium amide salt (0.220 mmol, 1.10 equiv), and 2 mL benzene were added. After addition of 4-bromofluorobenzene (0.035 g, 0.200 mmol, 1.00 equiv), the vial was sealed and irradiated with a 34 W blue LED lamp (placed 4 cm away). After irradiation (with stirring and fan cooling) for 72 h, two drops of DI water were added, and the solvent was evacuated. The mixture was extracted by diethyl ether and evacuated to leave a crude residue, which was purified by silica gel column chromatography (100% hexanes) to afford 4-fluorobiphenyl as a white solid (for **3**, 4.1 mg, 12%; for **4**, 12.4 mg, 36%; for **5**, 22.8 mg, 66%). ¹H NMR (500 MHz, CDCl₃) δ 7.57–7.55 (m, 4H), 7.46–7.43 (m, 2H), 7.37–7.34 (m, 1H), 7.16–7.12 (m, 2H). ¹⁹F NMR (282 MHz, CDCl₃) δ -116.01 (s). ¹³C NMR (126 MHz, CDCl₃) δ 162.63 (d, *J* = 245 Hz), 140.42 (s), 137.48 (s), 128.95 (s), 128.83 (d, *J* = 8 Hz), 127.39 (s), 127.16 (s), 115.75 (d, *J* = 21 Hz). 4-fluorobiphenyl was characterized previously; the NMR data matched the reported data.²²

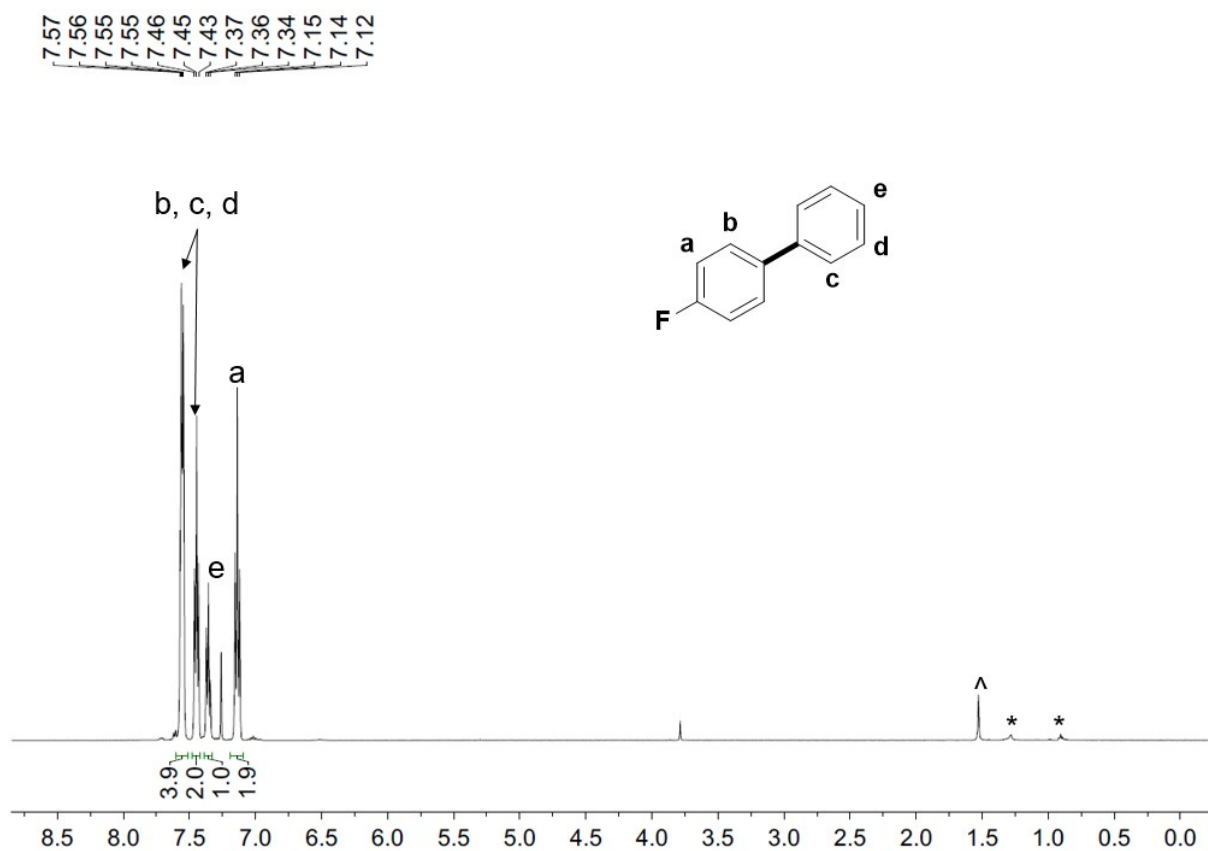


Figure S69. ^1H NMR of 4-fluorophenylbenzene in CDCl_3 . Residue hexanes is noted by *. Moisture in NMR solvent is noted by ^.

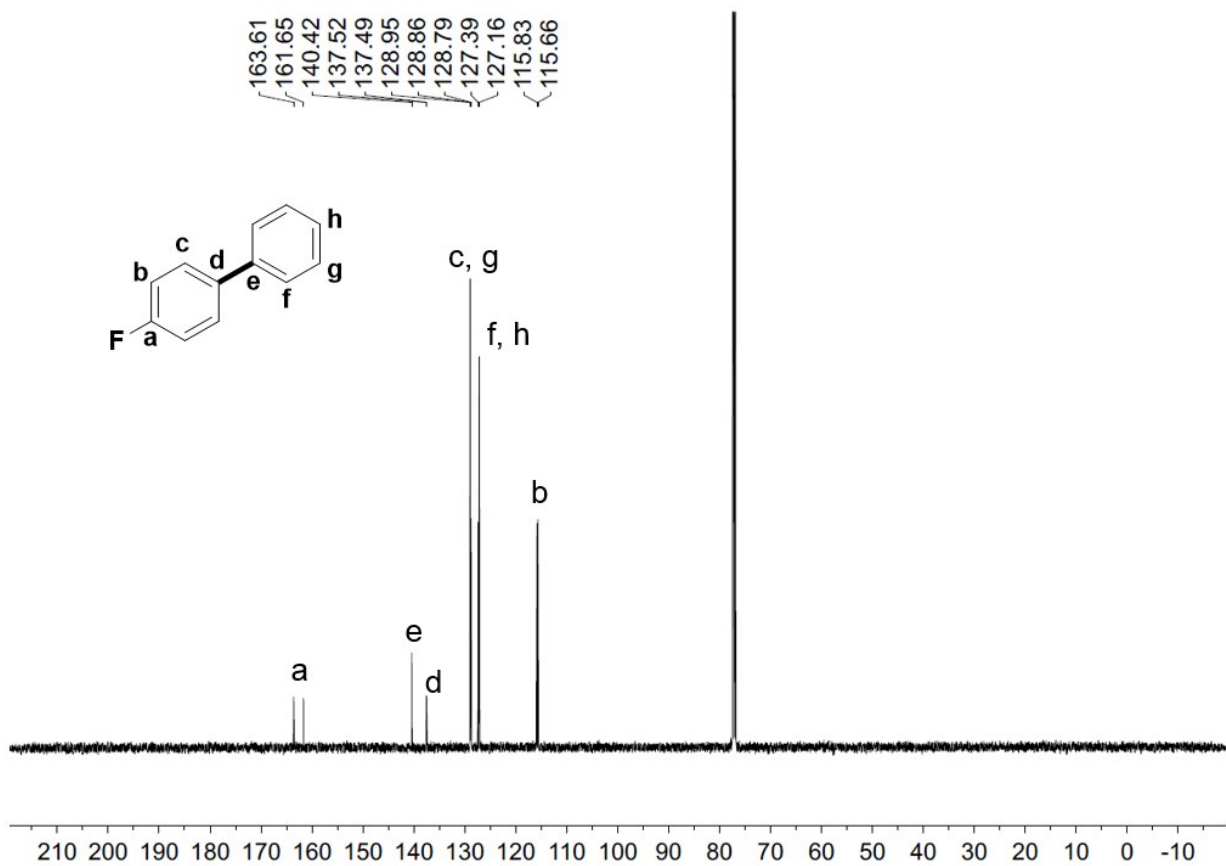


Figure S70. $^{13}\text{C}\{^1\text{H}\}$ NMR of 4-fluorophenylbenzene in CDCl_3 .

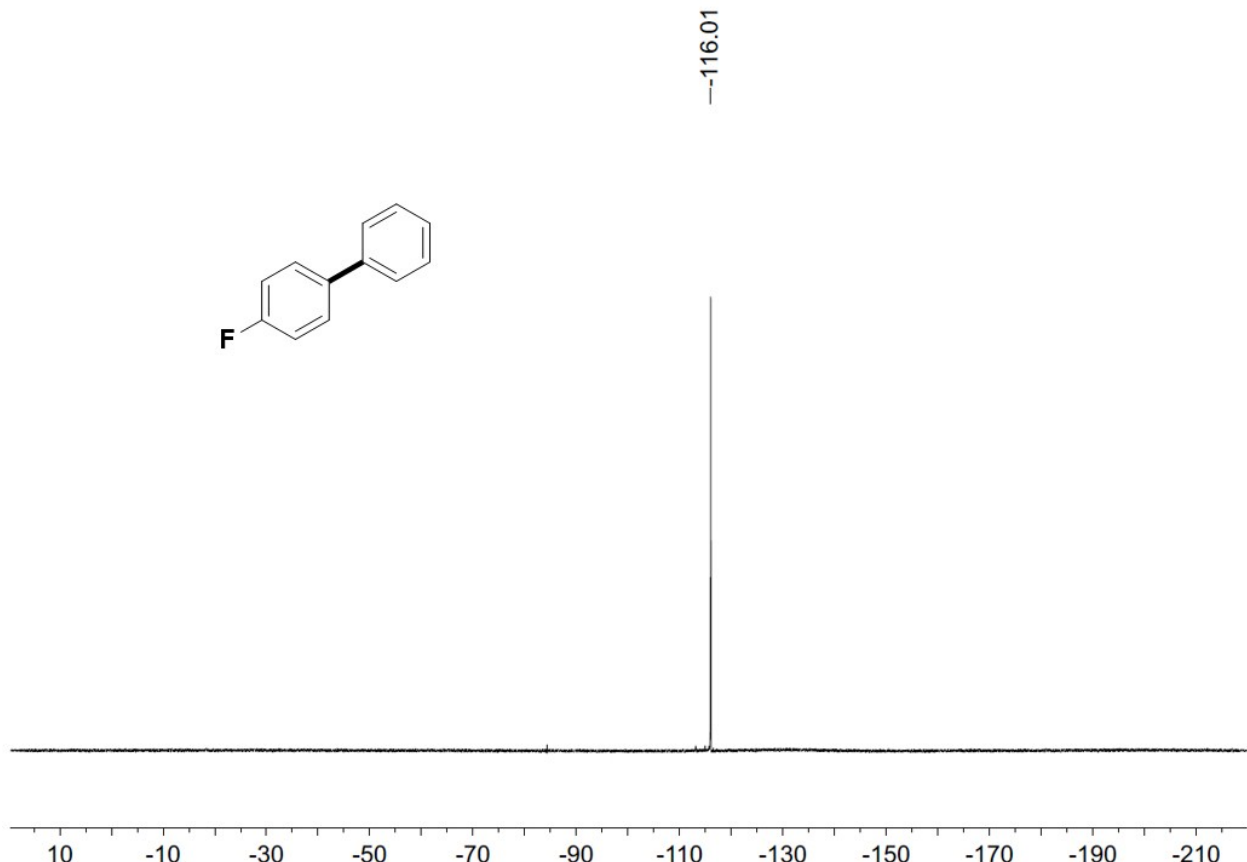


Figure S71. ${}^{19}\text{F}$ NMR of 4-fluorophenylbenzene in CDCl_3 .

13. References

1. Antolini, P. B.; Hitchcock, A. V.; Lappert, M. F.; *Eur. J. Inorg. Chem.* **2003**, 3391.
2. Yin, H.; Carroll, P. J.; Manor, B. C.; Anna, J. M.; Schelter, E. J. *J. Am. Chem. Soc.* **2016**, 138, 5984.
3. Thomson, R. K.; Scott, B. L.; Morris, D. E.; Kiplinger, J. L. *C. R. Chim.* **2010**, 13, 790-802.
4. Wojdyr, M. *J. Appl. Crystallogr.*, **2010**, 43, 1126.
5. Lakowicz, J. R. *Principles of Fluorescence Spectroscopy*, 3rd Ed.; Springer: New York, **2006**.
6. <http://www.horiba.com/fileadmin/uploads/Scientific/Documents/Fluorescence/quantumyieldstrad.pdf>
7. Suzuki, K.; Kobayashi, A.; Kaneko, S.; Takehira, K.; Yoshihara, T.; Ishida, H.; Shiina, Y.; Oishi, S.; Tobita, S., *Phys. Chem. Chem. Phys.* **2009**, 11, 9850.
8. Bruker, SAINT, Bruker AXS, Inc., Madison, WI, USA, **2009**.
9. Bruker, SHELXTL, Bruker AXS, Inc., Madison, WI, USA, **2009**.
10. Sheldrick, G. M. SADABS, University of Gottingen, Germany, **2007**.
11. Sheldrick, G. M. TWINABS, University of Gottingen, Germany, **2008**.
12. Sheldrick, G. M. *Acta Crystallogr. Sect. A* **2008**, 64, 112-122.
13. Sheldrick, G. M. SHELXL 2014/7; University of Gottingen, Germany, 2014.
14. Frisch, M. J.; Trucks, G. W.; Schlegel, H. B.; Scuseria, G. E.; Robb, M. A.; Cheeseman, J. R.; Scalmani, G.; Barone, V.; Mennucci, B.; Petersson, G. A.; Nakatsuji, H.; Caricato, M.; Li, X.; Hratchian, H. P.; Izmaylov, A. F.; Bloino, J.; Zheng, G.; Sonnenberg, J. L.; Hada, M.; Ehara, M.; Toyota, K.; Fukuda, R.; Hasegawa, J.; Ishida, M.; Nakajima, T.; Honda, Y.; Kitao, O.; Nakai, H.; Vreven, T.; Montgomery, Jr., J. A.; Peralta, J. E.; Ogliaro, F.; Bearpark, M.; Heyd, J. J.; Brothers, E.; Kudin, K. N.; Staroverov, V. N.; Kobayashi, R.; Normand, J.; Raghavachari, K.; Rendell, A.; Burant, J. C.; Iyengar, S. S.; Tomasi, J.; Cossi, M.; Rega, N.; Millam, J. M.; Klene, M.; Knox, J. E.; Cross, J. B.; Bakken, V.; Adamo, C.; Jaramillo, J.; Gomperts, R.; Stratmann, R. E.; Yazyev, O.; Austin, A. J.; Cammi, R.; Pomelli, C.; Ochterski, J. W.; Martin, R. L.; Morokuma, K.; Zakrzewski, V. G.; Voth, G. A.; Salvador, P.; Dannenberg, J. J.; Dapprich, S.; Daniels, A. D.; Farkas, Ö.; Foresman, J. B.; Ortiz, J. V.; Cioslowski, J.; Fox, D. J. Gaussian 09, Revision A.02, Gaussian, Inc., Wallingford CT, **2009**.
15. Dolg, M.; Stoll, H.; Preuss, H. *J. Chem. Phys.* **1989**, 90, 1730-1734; Cao, X.; Dolg, M.; Stoll, H. *J. Chem. Phys.* **2003**, 118, 487-496.
16. Grigoriy, D. A. Z.; Zhurko, A. <http://chemcraftprog.com/>.
17. (a) Martin, R. L. *J. Chem. Phys.* **2003**, 118, 4775. (b) Tretiak, S.; Saxena, A.; Martin, R. L.; Bishop, A. R., *Chem. Phys. Lett.* **2000**, 331, 561.
18. Levin, J. R.; Dorfner, W. L.; Dai, A. X.; Carroll, P. J.; Schelter, E. J. *Inorg. Chem.*, **2016**, 55,

- 12651.
19. <https://www.molnac.unisa.it/OMtools/sambvca2.0/index.html>.
 20. Mathematica 8.0; Wolfram Research, Inc.: Champaign, IL, **2010**.
 21. Bilbrey, J. A.; Kazez, A. H.; Locklin, J.; Allen, W. D. *J. Comput. Chem.* **2013**, *34*, 1189.
 22. Lee, H. G.; Milner, P. J.; Buchwald, S. L. *J. Am. Chem. Soc.* **2014**, *136*, 3792.